• U C •

FCTUC FACULDADE DE CIÊNCIAS E TECNOLOGIA
UNIVERSIDADE DE COIMBRA

DEPARTAMENTO DE ENGENHARIA MECÂNICA

Mechanisms for Active Protection of People and Infrastructures against Forest Fires

Submitted in Partial Fulfilment of the Requirements for the Degree of Master in Mechanical Engineering in the speciality of Energy and Environment

Mecanismos de Proteção Ativa de Pessoas e Infraestruturas Contra Incêndios Florestais

Author

Rui Marcelo Batista

Advisors

Professor Doutor Domingos Xavier Filomeno Carlos Viegas

Professor Doutor Carlos Xavier Pais Viegas

Jury

President	**Professor Doutor José Manuel Baranda Moreira da Silva Ribeiro** **Professor Auxiliar da Universidade de Coimbra**
Vowels	**Professor Doutor Miguel Rosa Oliveira Panão** **Professor Auxiliar da Universidade de Coimbra**
Advisor	**Professor Doutor Carlos Xavier Pais Viegas** **Professor Auxiliar da Universidade de Coimbra**

Institutional Collaboration

Associação para o Desenvolvimento da Aerodinâmica Industrial

Centro de Estudos sobre Incêndios Florestais

Coimbra, September, 2018

Não sou nada.

Nunca serei nada.

Não posso querer ser nada.

Á parte isso, tenho em mim todos os sonhos do Mundo.

Álvaro de Campos, 1928.

À minha família e amigos.

ACKNOWLEDGEMENTS

First of all I would like to thank my family in general, for their presence and support given over the years. I leave a special word to my father for his support, words and advice that are so useful to me. At last a big thank you to my mother, for being everything to me, a true heroine, thank you for your love, affection, dedication, patience and understanding.

My second word goes to my friends, thank you for your fellowship, for your continued presence and for your friendship.

Finally I leave a word of thanks to my advisor Prof. Dr. Domingos Xavier Filomeno Carlos Viegas for his knowledge transmitted, useful advices and the availability of resources and a helpful team. To my co-advisor Prof. Dr. Carlos Xavier Pais Viegas thank you for your guidance, accompaniment and help provided throughout the work. To the CEIF/ADAI team, thank you for the help made available in all my tasks. Finally to the teachers who were somehow involved in this work thank you for your help and encouragement to work and search for knowledge.

Abstract

Wild fires (WF) have proven to be one of the biggest problems in Portugal in recent years, representing not only a severe environmental threat, but also bearing a significant economic impact in the whole country, with the loss of assets and, above all, the loss of human lives.

Most of these problems occur when WF reach the so-called wildland urban interface (WUI). This is the area where vegetation and human made structures coexist, making them highly susceptible to the impact of a wildfire prone environment. In Portugal the WUI is spread throughout the whole country, being the north and the central regions the ones with the highest risk associated with WF. This work aims at finding and developing solutions which can be used in these interfaces, with the purpose of protecting people and goods from the high levels of heat and radiation from WF, in addition to aid in the firefighting and fire line suppression.

This work is framed in the project Fireprotect that aims to develop, test and validate several solutions for wild fire protection, with the ultimate goal of placing them in the market.

The mechanism developed is a simple but effective fire barrier that can have multiple uses, as a fixed perimeter protection, or as mobile and fast setup protection mechanism to be easily used in any place.

This mechanism comprises two main structures, fences which contain water sprinkling systems for active humidification of the barriers and the vegetation in their vicinity, but also for direct flame and fire-front suppression; barriers which are large fire resistant fabrics, whose purpose is to sustain the advance of the fire front, while protecting everything inside their protection perimeter.

The whole process of solution development included several steps. First, a state-of-the-art study was carried out to investigate different types of barriers, fire protection solutions and standards and procedures for testing and certification of fire structures. After this, both a theoretical and a practical experimentation of different types of fire resistant fabrics with the propose of accessing their resistance limit to the fire, was carried out,

including a study on the effect of a water cooling. Once the best fabric was selected, the flows and pressures necessary for the correct operation of the sprinkling system for the barrier were studied. The water reservoirs and feed pumps were also dimensioned. Finally, field trials were carried out in the Castanheira de Pera area to overcome the scale limitations found in the laboratory tests.

These tests serve to constantly improve the final solution, by accessing the real behavior of the mechanism and its systems when exposed to the extreme conditions of a WF, including the advantage of using a water spray system, the best fire fabric to use and also the height of the barrier required for a similar fire verified in an wildland urban interface area. In the end, one concludes that this solution can be used in the field, despite more testing and improvement is required prior to place it on the market.

Keywords Wild fires, Wildland urban interface, Fences, Barriers, Fire resistant fabrics, Water sprinkling.

Resumo

Os incêndios florestais provaram ser um dos maiores problemas em Portugal nos últimos anos, representando não só uma grave ameaça ambiental, mas também um impacto económico significativo em todo o país, com a perda de bens e, acima de tudo, a perda de vidas humanas.

A maioria desses problemas ocorre quando incêndios florestais atingem a chamada interface urbano florestal. Esta é a área onde coexiste vegetação e estruturas humanas, tornando as últimas altamente suscetíveis ao impacto de um ambiente propenso a incêndios florestais. Em Portugal, a interface urbano florestal está espalhada por todo o país, sendo as regiões norte e centro as que apresentam maior risco associado a incêndios florestais. Este trabalho visa encontrar e desenvolver soluções que possam ser utilizadas nestas interfaces, com o objetivo de proteger pessoas e bens dos altos níveis de calor e radiação de incêndios florestais, além de auxiliar no combate a incêndios e supressão da frente de fogo.

Este trabalho está enquadrado no projeto Fireprotect que visa desenvolver, testar e validar diversas soluções para proteção contra incêndios florestais, com o objetivo final de colocá-las no mercado.

O mecanismo desenvolvido é uma barreira contra incêndios que se intende simples, mas eficaz, que pode ter múltiplos usos, como a proteção de um perímetro fixo ou como mecanismo de proteção de configuração rápida e móvel para ser facilmente usado em qualquer lugar.

Este mecanismo compreende duas estruturas principais, cercas que contêm sistemas de aspersão de água para a humidificação ativa das barreiras e da vegetação em seu redor, mas também para a supressão direta de chamas e frentes de fogo; barreiras que são grandes tecidos feitos de telas ignífugas, cuja finalidade é sustentar o avanço da frente de incêndio, protegendo tudo no interior do seu perímetro de proteção.

Todo o processo de desenvolvimento de soluções incluiu várias etapas. Primeiro, um estudo do estado-de-arte foi realizado para investigar diferentes tipos de barreiras, soluções de proteção contra incêndios e normas e procedimentos para testes e certificação de estruturas de incêndio. Em seguida, realizou-se uma experimentação teórica e prática de

diferentes tipos de telas ignífugas com a proposta de alcançar o limite de resistência ao fogo, incluindo um estudo sobre o efeito do arrefecimento a água. Uma vez selecionada a melhor tela, foram estudados os fluxos e pressões necessários para o correto funcionamento do sistema de aspersão da tela. Os reservatórios de água e as bombas de alimentação também foram dimensionados. Por fim, foram realizados ensaios de campo na área de Castanheira de Pera para superar as limitações de escala encontradas nos testes de laboratório.

Estes testes servem para melhorar constantemente a solução final, descobrindo o comportamento real do mecanismo e seus sistemas quando expostos às condições extremas de um incêndio florestal, incluindo a vantagem de usar um sistema de aspersão de água, a melhor tela ignífuga para usar e também a altura da barreira necessária para um fogo similar ao verificado numa área de interface urbano florestal. No final, conclui-se que esta solução pode ser usada no campo, apesar de mais testes e melhorias serem necessárias antes de colocá-la no mercado.

Palavras-chave: Incêndios florestais, Interface urbano florestal, Cercas, Barreiras, Telas ignífugas, Aspersão de água.

Contents

LIST OF FIGURES

LIST OF TABLES

SIMBOLOGY AND ACRONYMS

Symbology

I – Fire Line Intensity

R – Propagation Speed

H_c – Fuel Calorific Power

C – Fuel Load

φ – Flow Values

T_1 – Under Fire Part Temperature

T_2 – Protected Part Temperature

L – Thickness

k – Conductivity

T_{disk} – Disk Temperature

T_{flame} – Flame Temperature

T_∞ – Room Temperature

m_{copper} – Copper Mass

c_p – Cooper Specific Heat

A – Copper Disk Area

h – Heat Transfer Coefficient

t – Time

E – Energy of the Campingaz

$\dot{m}$ – Mass Flow

PCI – Calorific Value of the Fuel

Q – Flow Rate

q – Water Flow per Minute

p – Perimeter

Q' – Reduced Flow Rate

p' – Reduced Perimeter

C – Capacity

C_{final} – New Capacity

n – Safety Coefficient

RE – Relative Error

$Value_{exact}$ – Exact Value

$Value_{approximate}$ – Approximate Value

ARE – Average Relative Error

Acronyms

CEIF – Centro de Estudos sobre Incêndios Florestais

ADAI – Associação para o Desenvolvimento da Aerodinâmica Industrial

WF – Wild Fires

WUI – Wildland Urban Interface

IR - Infrared

1. INTRODUCTION

1.1. Motivation

Taking a brief study of the recent history of our country, it is easy to see that wildfires are one of the problems that most haunt Portugal. It is well known the serious environmental, social and economical problems caused by the fires.

In addition to the environmental consequences associated with deforestation, soil degradation, wildlife and biodiversity losses, as well as the release of enormous amounts of carbon dioxide into the atmosphere, the destruction of property such as vehicles, housing or infrastructures, most tragic outcome from the WF is the loss of human lives. According to the Report from the Working Group of the Assembly of the Republic for the analysis of the wild fires problem[1], from 2006 to 2013, the average tangible damage from WF is 123M€/year, and the average operational costs are 70M€/year. The last year of 2017 was especially tragic in this matter, about 550 thousand hectares were burned registering a record number of human lives lost (114 lives). In that year, Portugal registered the highest average maximum temperatures and the fourth lowest precipitation records since 1931, with the period from April to December being the driest of the last 87 years. In fact, the five years with the highest temperatures occurred in the last 30 years[2], showing that these record high temperatures and low precipitation are becoming a worrisome trend. Most of these disasters occur when these fires hit areas of WUI, places where fires tend to coexist, with increasing frequency and severity, with the human presence in housing or urban agglomerations[3], and where there are insufficient human or resources to fight them.

In the case of Portugal, more specifically in the interior regions, it is possible to note that the settlements are quite dispersed in what is a dense forest area, combining it with the topography of our territory (mainly composed of steep mountains and valleys), the climatic changes (characterized by the consecutive increase of the maximum temperatures and decrease of the levels of precipitation) and the reduction and aging of the population in these areas, the conditions necessary for the occurrence of catastrophic events are gathered, such as those we have witnessed especially in the last year.

It is therefore clear that in the event of a WF, the protection of people and property is the absolute priority. Currently there is much research into effective means for

wild fire suppression to be used by firefighters, but few work is being done into developing means for wild fire protection of population. Thus, the desire arises to employ the technical knowledge to achieve this goal, aiming at the development of a simple but effective solution, that one day could save peoples goods, infrastructures, or even human lives.

1.2. Objectives

This work addresses a current theme and a real problem of our country. Its goal to develop an effective solution that can be implemented in a short time in the market. This solution can be divided into two structures that will work together: fences and barriers.

The fences have mechanisms, such as sprinklers for water projection. This is used for several purposes in prevention and active combat to the flames, by increasing the moisture content of the vegetation near the fence, in order to reduce the fire line intensity and the speed of propagation of the fire as well as the height of flame, so that when it reaches the barriers the fire can be easily extinguished. The purpose of this system is also to allow the barrier to last longer when directly exposed to flames, by having a thin water film flowing in its surface, thus maintaining the material cool and below a certain threshold temperature. For this, it makes use of a very common element in the fight against WF, the water, which is an efficient suppression medium due to its high latent heat of vaporization, allowing it to absorb great amounts of heat energy before evaporating.

The barriers consist of a fire resistant fabric that is capable of withstanding high temperature and radiation levels. These barriers can be permanently fixed in a protection perimeter or mobile and fast assembled on any site.

In order to develop this solution several steps have been taken, namely:

1. A state-of-the-art study, where several topics were investigated, such as: types of fabrics used to protect against high temperatures (fire, welding, among others); fire-fighting solutions similar to those to be developed; standards and procedures for testing and certification of structures and materials against fire;
2. A modeling of the heat transfer phenomena occurring on the fabric (where various fabrics have been tested for their fire resistance), including the effect of water cooling;

3. Calculation of the flows and pressures required for the operation of the water sprinkler system on the barrier;
4. The dimensioning of water reservoirs and feed pumps, depending on the requirements of the water sprinkler system;
5. The testing of the various components of the system in the laboratory and in field trials.

This work is part of the Fireprotect project, whose logo is shown in Figure 1.1, co-financed by the European Regional Development Fund. This project is dedicated to the development of several mechanisms for protection of people and infrastructures against wild fires. This thermal barrier is one of the mechanisms conceived in this project. The present thesis details some parts of this development, while another, master thesis from the student Miguel Coelho Costa is dedicated to the design and implementation of the structures which support the thermal barrier.

Figure 1.1. Fireprotect logo

1.3. State-of-the-Art

The solution sought in this work for protection against wildfires was challenging as there were only a few similar products in the market.

To develop some of the aspects of this solution, several patents were studied, to compare their characteristics, strong points and opportunities for improvement and novelty.

Of the several patents studied, three types of protection mechanisms emerged: the first involving water spray systems, the second involving fireproof panels and the third one, which most closely resembles the solution to be developed, involves fireproof fabrics.

The system developed by Timothy Orrange & Gary J. Sweeton[4], consists of a set of rotating plastic sprinklers, that can be seen in Figure 1.2. These sprinklers should be installed, for example, on the roof of the infrastructure to be protected, its purpose is not only to humidify the roofs of these infrastructures but also to humidify the entire environment, including trees and bush.

It is a simple, effective and low-cost solution, as well as being a small dimension solution that will reduce its visual impact.

Despite these strong points, this solution has some limitations, such as the fact that because it only uses water sprinkling, it needs high flow rates to perform its function, and also involves a large investment in auxiliary equipment, namely high capacity water pumps. Having only a single protection mechanism is highly susceptible to failures, making it useless in the absence or failure in the water supply.

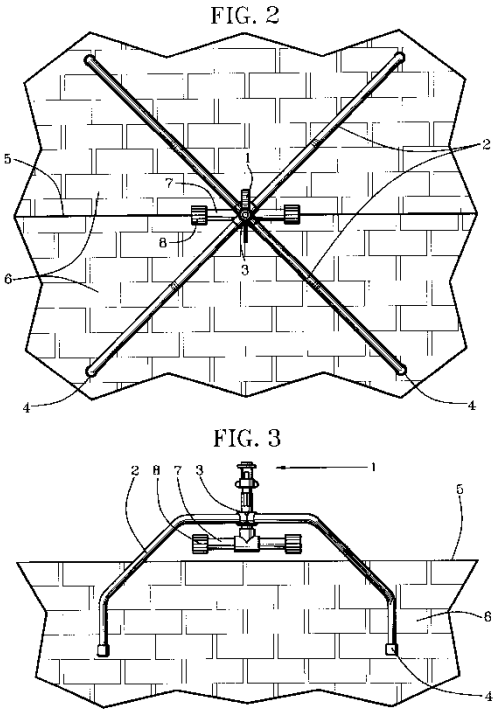

Figure 1.2. Timothy Orrange & Gary J. Sweeton's solutions

The system, conceived by Terry M. Smith & Hugh W. Smith[5], consists of a fireproof panel that should preferably be mounted next to the walls of an infrastructure, shown in Figure 1.3. This panel is composed of one or more layers of ceramic fiber that can be aligned in different orientations. In turn, these layers must be contained in a metal structure that can be cold rolled steel or high temperature stainless steel. It is therefore such a sturdy structure that it does not need to resort to water sprinkling.

However, this system also presents some inconveniences because it is composed of ceramic fibers and a steel structure, it becomes a heavy solution that implies that it is permanently mounted in a site. In addition to this, it is an expensive solution with great visual impact.

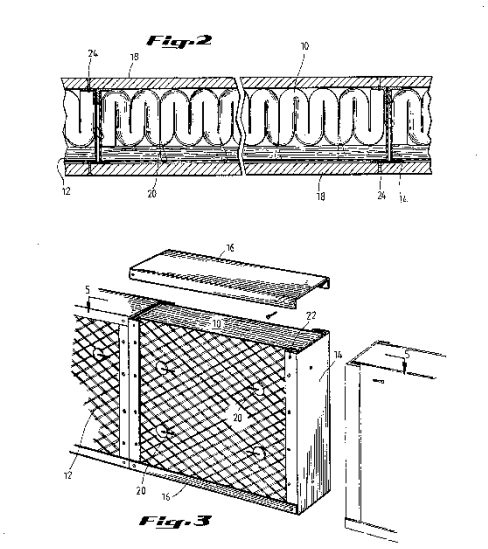

Figure 1.3. Terry M. Smith & Hugh W. Smith's solutions

Valentin Ortiz Teruel[6], proposes several uses for a fire resistant fabric, as shown in Figure 1.4, which can be applied to wildland urban interface areas. According to the author, in his work were developed multi-layered fabrics capable of acting in WF and protecting people and goods. For this, these fabrics must be composed of a layer of reflective metal (capable of reflecting the radiation) and other layers that give it mechanical resistance and resistance to high temperatures, composed by artificial mineral fibers (silica, carbon or glass fibers). In addition to the composition of the fabrics, the author mentions the need for

these fabrics to be malleable, adaptable to the terrain, and capable of being used permanently or temporarily in fixed or mobile installations.

However, this solution does not include an active mechanism for barrier cooling, as well as fire fighting, in the form of water sprinklers. This means that the resistance of the barrier is directly dependent of the resistance of the fabric and its operating temperature ratings, which are usually not suitable for conditions with continuous exposure to high intensity fire.

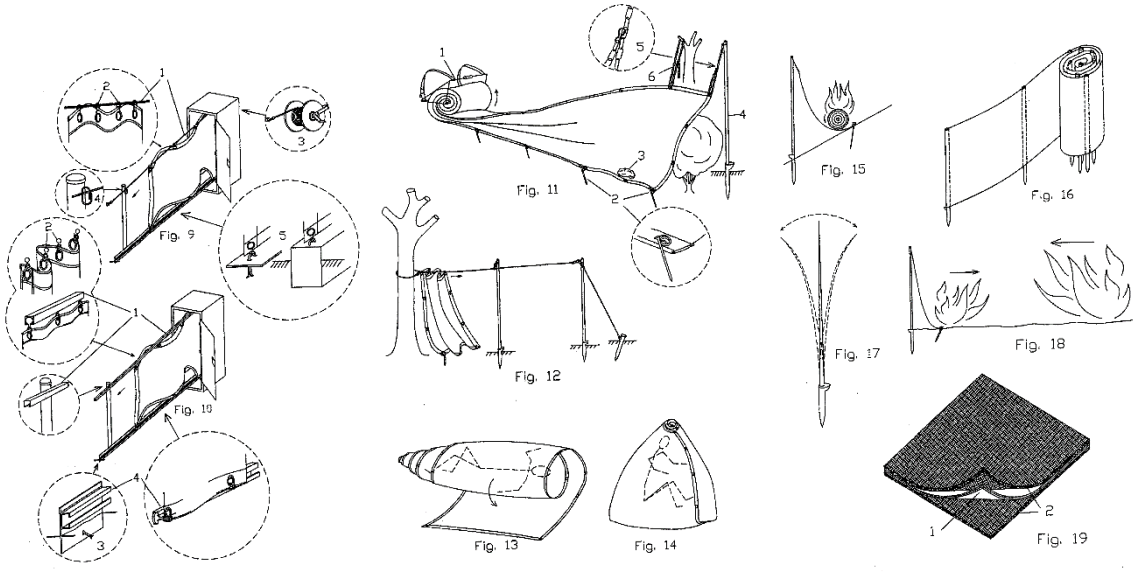

Figure 1.4. Valentin Ortiz Teruel 's solutions

Thus, in order to overcome the limitations of the existing solutions, our approach was developed, which, in addition to the use of fireproof fabrics, makes use of a water sprinkler system.

1.4. Standards and procedures

To develop products for fire protection it is important to know the standards and procedures which regulate such equipments, so that the final solution can be directly comparable to what is available on the market. These standards include the procedure for testing and certification of these equipments. Even if the exact same procedures are not

adopted in this work, one can say that a similar and directly comparable methodology was done, taking into account laboratorial equipment and time limitations.

The standards related to our solution include both building materials standards and fire proof materials standards[7].

For the resistance of the structural elements, one should consider:

- The EN 1363 stablishes the rules, requests and procedures connected to fire resistance tests[8];
- The EN 1364 to EN 1366 include the tests for the fire resistance of different kind of building materials;
- The EN 1634 is applicable to fire doors, shutters and their closing devices and it classifies these products according to their resistance to fire[9].

For the fireproof barriers and their performance regarding the resistance to fire, one should consider:

- EN 13501 that classifies these products according to their resistance to fire. It is applicable to fire protection panels[9];
- EN 13381 includes the test procedures for accessing the fire resistance of vertical protective membranes[10].

Taking all these standards into consideration, there is a recommended procedure that should be followed. In this procedure a sample/prototype is exposed to a specified regime of heating/fire and its performance is monitored using the criteria described in the standards mentioned before. The duration of each test should be the one that is specified in the correspondent standard.

1.5. Outline

This dissertation is divided in six chapters.

This first chapter is dedicated to the research work motivation and objectives. It also includes the state-of-the-art regarding similar fire protection systems.

The second chapter details the conceptual development of the novel barrier against fire propagation, including also a description of its several components and mathematical model of heat transfer phenomena which occur in it.

The third chapter describes the laboratorial testing stages of the fire resistant barrier which ultimately led to the selection of the most effective fabric to be adopted in the final prototype.

The fourth chapter is devoted to the active water cooling system proposed and the laboratorial experiments conducted during its development.

The fifth chapter discusses the final prototype with its several components integrated and the field tests which were conducted with it.

The last chapter concludes the work, presenting an extended discussion on the results obtained, this dissertation contribution and possible future developments.

2. NOVEL BARRIER FOR FIRE PROPAGATION

2.1. Conceptual design

The proposed solution, represented in Figure 2.1, uses two complementary mechanisms, the water sprinkler system and the fire resistant fabrics which constitute a physical barrier to the progression of the fire.

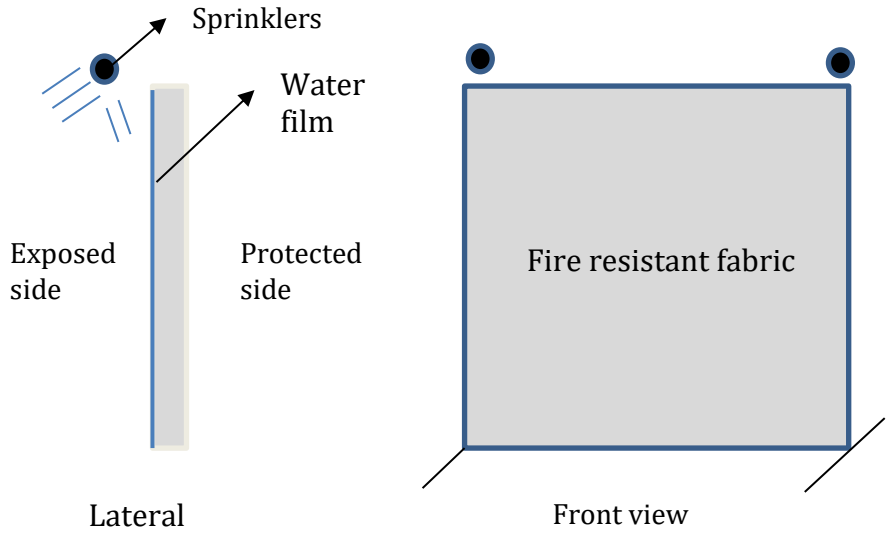

Figure 2.1. Proposed solution

The sprinkler system aims at keeping the barrier, vegetation and surrounding environment humid, reducing the intensity of fire propagation and maintaining the temperatures of the barrier below a certain threshold, thus ensuring its structural integrity and efficiency. The barrier goal is to prevent the progression of the fire front beyond that safe perimeter, and protect people or goods inside said perimeter from the high levels of heat and radiation.

In addition to the advantages mentioned so far, others may be highlighted, namely the fact that they are safe solutions in the absence of firefighters, since they do not require the presence of people in the site, as opposed to more traditional solutions like the

use of hoses or buckets of water by the population. Furthermore, they require little care or maintenance. This solution can be applied to small structures, like poles of electricity or antennas, or large perimeters of dwellings, warehouses, factories, among others. They can also be used for the protection of vehicles or even people.

2.2. Heat transfer modeling

The fire line intensity (I) [kW/m] is a property which translates the amount of energy carried by the fire front, and depends on the fire propagation speed (R) [m/s], the fuel calorific power (H_c) [kJ/kg] and the fuel load (C) [kg/m^2]:

$$I = R * H_c * C. \tag{2.1}$$

Some part of this energy from the fireline is directed to the fabric, and it is important to understand which are the mechanisms involved in the heat transfer and dissipation, through mathematical modelling. This ultimately allows to see which kind of fabric is theoretical superior, as well as the role played by the metal coating and the water on the fabric surface.

When exposed to the convective and radiative heat from the flames, the fabric absorbs part of this heat, while the rest is reflected, as depicted in Figure 2.2.

The heat flow absorbed, φ,is responsible for the heating of the fabric and should be minimized by employing the metal coating or the water film on the surface of the fabric.

The metal coating purpose is to reflect part of the radiative heat, having a mirrored appearance the surface of the coating allows reflecting part of the incident radiation, decreasing the temperature and degradation of the fabric.

The water film aims at absorbing a great amount of radiative and convective heat, due to the high specific heat and the high latent heat of vaporization of the water. In spite of the high thermal conductivity of the water, which in a first phase increases the temperature of the fabric, it is later verified that the temperature does not reach such high levels as those reached in the absence of water. This is due to the high specific heat of the water which allows it to absorb large amounts of heat without raising its temperature too much. Also the latent heat of vaporization plays an important role in maintaining the

temperature of the water and consequently of the fabric. Once the phase change temperature is reached this temperature is kept constant until the end of the process, absorbing during this phase change a high amount of energy.

To estimate the heat flow absorbed, φ [W/m^2],by the fabric, one can use the expression (2.2), which relates this with the surface temperatures in both the surface exposed to the fire (T_1) [ºC] and the protected surface (T_2) [ºC], as well as the fabric thickness (L) [m] and its conductivity, k [W/(m.ºC)].

$$\varphi = -k * \frac{T_2 - T_1}{L}. \tag{2.2}$$

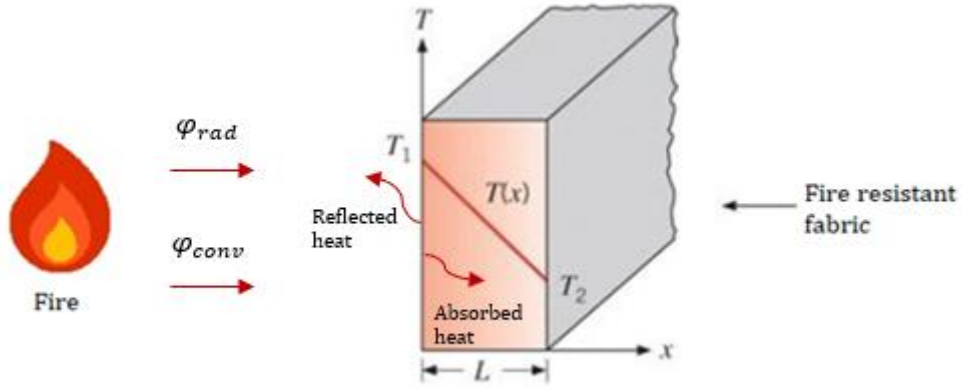

Figure 2.2. Radiative and convective heat flow

Another analytical alternative to estimate the heat flow is once again proposed by Figueiredo, A. R. & Costa, J. J.[11]. This solution relies on a well characterized cooper disk that is directly exposed to the heat source.

For the calculation of the heat flow, the following expression will be used, in which A [m^2] represents the area of the copper disk (used for the calculation of the heat transfer coefficients), h [W/(m^2.ºC)] represents the heat transfer coefficient, T_{flame} [ºC] represents the flame temperature, T_{disk} [ºC] represents the disk temperature and φ [W/m^2] represents the heat flow.

$$\varphi = A * h * (T_{flame} - T_{disk}), \tag{2.3}$$

In the previous expression, the only property that is difficult to obtain is the heat transfer coefficient, which can be estimated using the characteristic curve of the ambient temperature graphs as a function of time. This curve is obtained by using properties such as:

- T_{disk} [ºC] – disk temperature;
- T_{flame} [ºC] – flame temperature;
- T_{∞} [ºC] – room temperature;
- m_{copper} [kg] – copper mass;
- c_p [kJ/(kg.ºC)]– cooper specific heat;
- A [m^2] – copper disk area;
- h [W/(m^2.ºC)] – heat transfer coefficient;
- t [s] – time.

$$\frac{T_{disk} - T_{flame}}{T_{\infty} - T_{flame}} = e^{-\frac{A*h}{m_{copper}*c_p}*t}. \quad (2.4)$$

Once this coefficient is determined the heat flow can be easily obtained.

This method is particularly effective in cases where one needs to know the heat flow from a strong punctual heat source, such as a butane blowtorch. In such cases, a flowmeter cannot be used as it risks being damaged in the process. In this dissertation work, this method is proposed to access the heat flow from a campingaz torch used in the water cooling system tests. The heat flow can be calculated for different flame distances, so that it is possible, in addition to the temperature values, to characterize the intensity of the fire with one more metric.

In addition to the study referred to in the previous paragraph, and because it is a dimensionless calculation, it is possible to obtain, for example, the heat flow that will have to be counterbalanced depending on the temperature at which it is desired to maintain the barrier.

It is also important to mention that the heat flow to be used results from the joining of the radiative heat flow with the convective heat flow.

Also, if water is used for cooling the fabric, it will be necessary to take into account its possible evaporation, during which a large amount of thermal energy will be absorbed.

Finally, the radiation emitted by the fabric itself on heating must also be taken into account, which may influence the flow values obtained.

3. FABRIC SELECTION

3.1. Introduction

3.1.1. Framework

A fireproof barrier is a structure, whose purpose is to protect something from the fire, or constitute a barrier against the progression of the fire.

Typically they are made from fire resistant mineral or composite fabrics, and depending on the application we can find different types of fabrics, made up of different types of materials.

The most common material in the manufacture of such fabrics is fiberglass, namely type E glass, this material can be coated, or not, with an aluminium film as shown in Figure 3.1, or with silicone[12] or even PVC[13] (these coatings have as objectives to increase the resistance to fire, also increasing the mechanical resistance).

Figure 3.1. Fiberglass fabrics (with and without aluminium film)

In addition to fiberglass, other materials are employed, such as polyethylene[14] or polyester[15], which constitute cheaper but less effective solutions. KEVLAR[12] is another material that can be used, but works exclusively as a fire retardant.

The fiberglass based fabrics have as main characteristics: their thickness, that can vary between 0.2 and 3mm;their service temperature, which can vary between 400 and 1100°C; and their coating (with[16] or without[17] coating).

These fabrics are typically capable of withstand rain, dust, wind and solar light exposure without losing their properties. They are however susceptible to tears and rupture, and characteristics such as the fabric weaving density or the fabric coating plays a major role in the mechanical resistance of the barrier.

3.1.2. Fabric samples analysed

There are very few studies regarding the applicability of these fabrics in the exterior environment, for wild fire protection. To better access and evaluate their behaviour, five different fabrics from four different suppliers (whose names are not disclosed in this thesis), whose characteristics are present in Table 3.1, were tested. Some further characteristics of the fabrics from manufacturer B can be found in ANNEX A. The aim was to learn how their characteristics impact their resistance to fire, water or exterior elements, being the ultimate goal to find the best fabric to integrate the final solution.

Table 3.1. Five fabric barriers tested

Reference	Manufacturer Reference	Thickness [mm]	Density [g/m^2]	Service Temperature [ºC]	Alum. Coating	Supplier	Price [€/m^2]
Tela1	Liztherm 500	0.45	500	550	Yes	A	11.60
Tela2	TVL 126	0.5	520	600	Yes	B	5.45
Tela3	TSI 291	0.7	650	950	No	B	13.20
Tela4	Liztherm 500	0.75	650	550	No	C	6.65
Tela5	Type E	0.3	300	550	No	D	1.80

Each of these characteristics may have a positive or negative contribution on the applicability of the fabric for the proposed solution. Material thickness and density, for

starters, is an indication of the robustness of the fabric. Higher thickness means a denser mesh, with increased interlacing of the fiberglass threads, thus making it more resistant to not only the flames but also mechanical abrasion, tears and ruptures. It does, however, decrease its maneuverability and increases its weight, which may have a negative impact on its applicability. The aluminium coating is another aspect which may be beneficial, as it might reflect a large part of the radiative heat, preventing its absorption by the barrier. However, it is also impermeable to the water, having less capacity to retain water than the exposed fiberglass weaving. This might mean that higher flows of water might be necessary to cool the surface of the barrier. Service temperatures are the temperatures for which the material was tested and is certified, under the European norms and regulations. However, this does not mean that the fabric cannot withstand higher temperatures, nor can be used to directly compare the performance of the fabrics. Finally, the price of the fabrics also plays an important role, as the proposed solutions rely on large amounts of fabric. Making them affordable and accessible to the general population is also one of the goals of this development work.

3.1.3. Experimental tests overview

The laboratorial tests of the five fabrics, for their characterization and selection, was performed in two phases. In the 1st Phase – Fabric selection tests, five fabrics presented in Table 3.1 were tested in a scale simulation of a real wildfire, in order to choose the two best, one with aluminium coating and the other with no coating. This selection was made taking into account not only the visible damage to the fabrics after the experiments, but also from the data from the sensors in the experimental setup.

After this first phase, a 2nd Phase – Resistance limit tests in the same wildfire scale simulation setting was done, to access the fire line resistance limit of the two barriers previously selected.

3.2. Methodology

3.2.1. 1st Phase – Fabric selection tests

In this first phase, the goal was to evaluate the performance of five different fireproof barriers in a scale simulation of a real wildfire, in order to find the two best, one

with aluminium coating and the other with no coating, to be tested in later phases. For this, a fixed experimental setup mounted inside a combustion wind tunnel was adopted, as shown in Figure 3.2.

In this tunnel, different wind speeds can be generated (0m/s, 1m/s and 2m/s speeds used in the experiments). A fuel bed made of shrubs, with the dimensions of 1.8 by 3 meters and fuel density of 1kg/m^2 was placed inside the tunnel. A fireproof barrier section with a length of 2meters and 1 meters high was placed at the end of the fuel bed, while the fire ignition was done in a line at the beginning of the fuel bed, as shown in Figure 3.3.

Several sensors were used in this experimental setup. Six K type thermocouples (K PTFE twin twist fine thermocouple wire) were installed in both faces of the barrier and at three different heights, 0.15m, 0.50m and 0.85m, Figure 3.4 represents the front view of the barrier, where the front thermocouples of the top (FT), middle (FM) and bottom (FB) can be identified. A water-cooled flowmeter (Vatell Corp, Thermogage 9000-9) was installed above the barrier, at an height of 1.25m as can also be seen in Figure 3.4. Two video cameras mounted in front and laterally to the setup were used to record the experiments and access the flame height, and an Infra-red camera (Flir Systems, ThermaCAM S Series) was installed behind the barrier to record the temperature distribution in the barrier.

The experimental procedure applied to this test phase can be found in APPENDIX A.

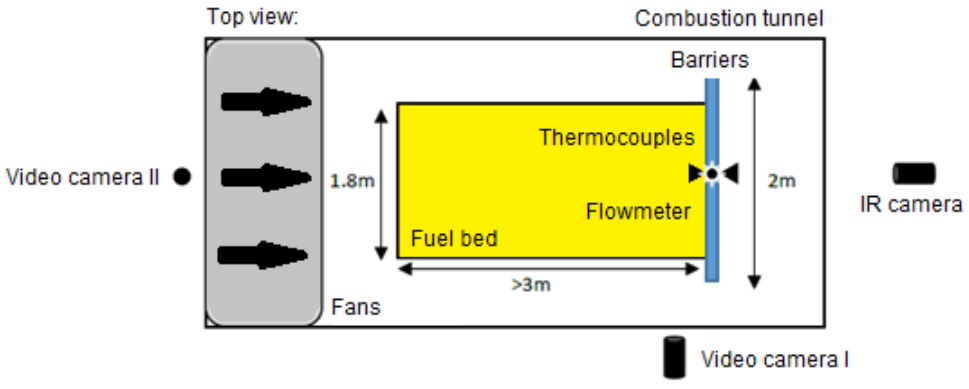

Figure 3.2. Schematics of the experimental setup for 1st and 2nd testing phases

Figure 3.3. Photo of the experimental setup

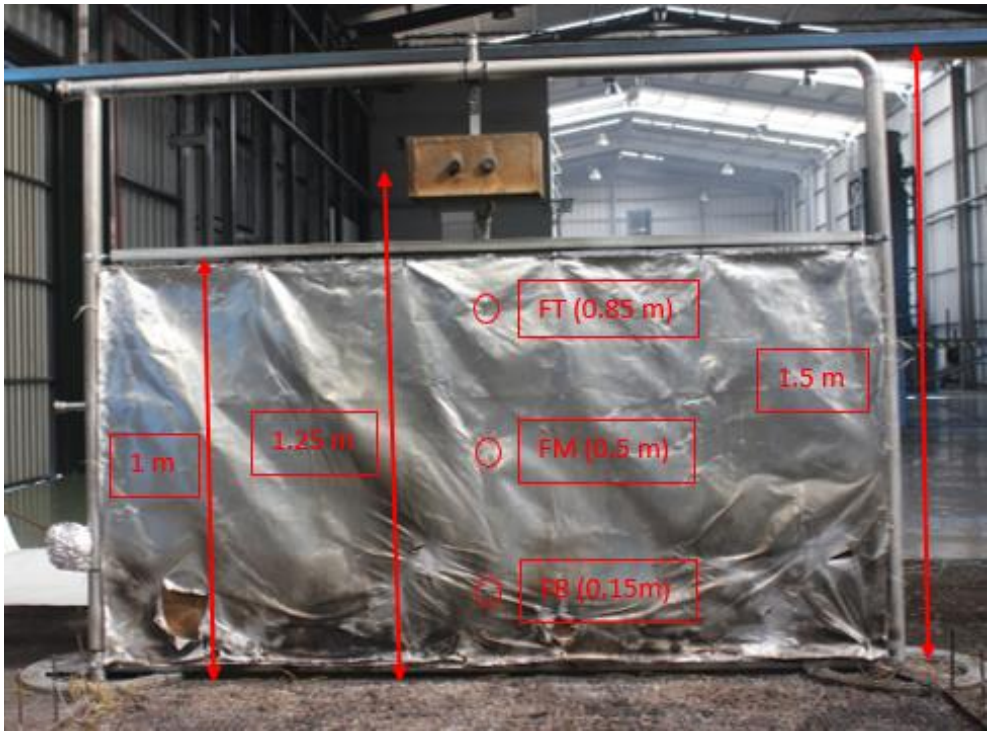

Figure 3.4. Barrier dimensions

3.2.2. 2nd Phase – Resistance limit tests

After accessing the two best fireproof barriers, the goal of the next testing phase was to find their resistance limit. The same procedure and experimental setup from 1st Phase was used, except this time, the fuel mass and wind speeds were gradually increased, with the purpose of generating higher fire intensities.

3.3. Results

3.3.1. 1st Phase – Fabric selection tests

Once the considerations in section 2.2 are worked out, the results will be presented in this section. However, only the summarized results will be shown, the complete results, can be consulted in APPENDIX B.

In the study of the conductivity was used the data obtained during this phase. The characteristic in question was calculated by an average performed using the heat flow values for the two extremes situations, i.e. for windless tests (U = 0m/s) and for tests with a wind speed of two meters per second (U = 2m/s). In addition to the heat flow values (q''_x), the respective temperatures were used, made in both the part under fire (T_1) and in the protected part (T_2), as well as the thickness (L) of the tested fabrics.

The thicknesses used are those shown in Table 3.1, and the temperatures that should be used to perform these calculations should be those obtained by the top-of-the-barrier thermocouples (closest to the flowmeter), however due to their malfunction, other temperatures have sometimes been used.

In the case of Tela1 it was necessary to use the temperatures obtained by the thermocouples of the barrier medium.

In the case of Tela3 it was only possible to use the values referring to U = 2m/s, since for the test without wind the values of temperatures were higher in the back of the barrier (sign that the fire passed under the barrier and that directly reached the thermocouples).

For Tela4 it was necessary to use the temperatures obtained by the thermocouples of the barrier medium.

For Tela5 it was necessary to use the temperatures obtained by the thermocouples of the barrier bottom.

Table 3.2. Tela1 to Tela5 (Conductivity)

		φ [W/m^2]	T_1 [ºC]	T_2 [ºC]	K [W/m.ºC]
Tela1	U = 0 m/s	21615	269.05	70.03	0.049
	U = 2 m/s	45939	385.70	78.70	0.067
	Average	-	-	-	0.058
Tela2	U = 0 m/s	17460	89.22	63.24	0.336
	U = 2 m/s	44398	239.70	33.99	0.108
	Average	-	-	-	0.222
Tela3	U = 0 m/s	26295	-	-	-
	U = 2 m/s	49640	317.30	282.61	1.002
	Average	-	-	-	-
Tela4	U = 0 m/s	38823	346.38	162.39	0.158
	U = 2 m/s	56287	434.94	132.81	0.130
	Average	-	-	-	0.144
Tela5	U = 0 m/s	44641	136.13	46.43	0.149
	U = 2 m/s	42941	177.21	112.71	0.200
	Average	-	-	-	0.175

Tela1

Table 3.3. Tela1

Wind speed [m/s]	0	1	2
Propagation speed [cm/s]	0.81	2.92	6.65
Max. temperature [ºC]	451.7	459.5	632.6
Max. heat flow [kW/m^2]	21.6	26.2	45.9
Fire line intensity [kW/m]	182.6	656.6	1495.5
Flame height [m]	0.98	1.20	1.05
Max. temperature at the rear of the barrier [ºC]	169.4	152.3	95.0

Tela2

Table 3.4. Tela2

Wind speed [m/s]	0	1	2
Propagation speed [cm/s]	1.0	3.0	6.0
Max. temperature [ºC]	477.4	459.9	394.8
Max. heat flow [kW/m^2]	17.5	37.7	44.4
Fire line intensity [kW/m]	268.3	752.2	1237.8
Flame height [m]	0.88	1.28	1.20
Max. temperature at the rear of the barrier [ºC]	261.3	191.2	199.13

Tela3

Table 3.5. Tela3

Wind speed [m/s]	0	1	2
Propagation speed [cm/s]	1.0	3.0	6.0
Max. temperature [ºC]	272.2	580.2	627.4
Max. heat flow [kW/m^2]	26.3	38.7	49.6
Fire line intensity [kW/m]	312.0	678.4	1372.7
Flame height [m]	0.88	1.30	1.20
Max. temperature at the rear of the barrier [ºC]	251.80	325.67	395.40

Tela4

Table 3.6. Tela4

Wind speed [m/s]	0	1	2
Propagation speed [cm/s]	1.0	4.0	7.0
Max. temperature [ºC]	572.2	404.8	565.5
Max. heat flow [kW/m^2]	38.8	44.7	56.3
Fire line intensity [kW/m]	263.1	902.0	1607.0
Flame height [m]	0.95	1.28	1.23
Max. temperature at the rear of the barrier [ºC]	220.40	210.30	308.30

Tela5

Table 3.7. Tela5

Wind speed [m/s]	0	1	2
Propagation speed [cm/s]	1.41	3.24	6.42
Max. temperature [ºC]	594.7	400.2	478.00
Max. heat flow [kW/m^2]	44.6	46.8	42.9
Fire line intensity [kW/m]	317.8	729.8	1445.2
Flame height [m]	0.85	1.15	0.95
Max. temperature at the rear of the barrier [ºC]	111.64	141.99	329.56

In the following figures, the images of the IR camera are shown for the maximum recorded temperatures. Figure 3.5 refers to Tela1 and Tela2 (coated barriers) respectively and Figure 3.6, refers to Tela3 and Tela4 (uncoated barriers).

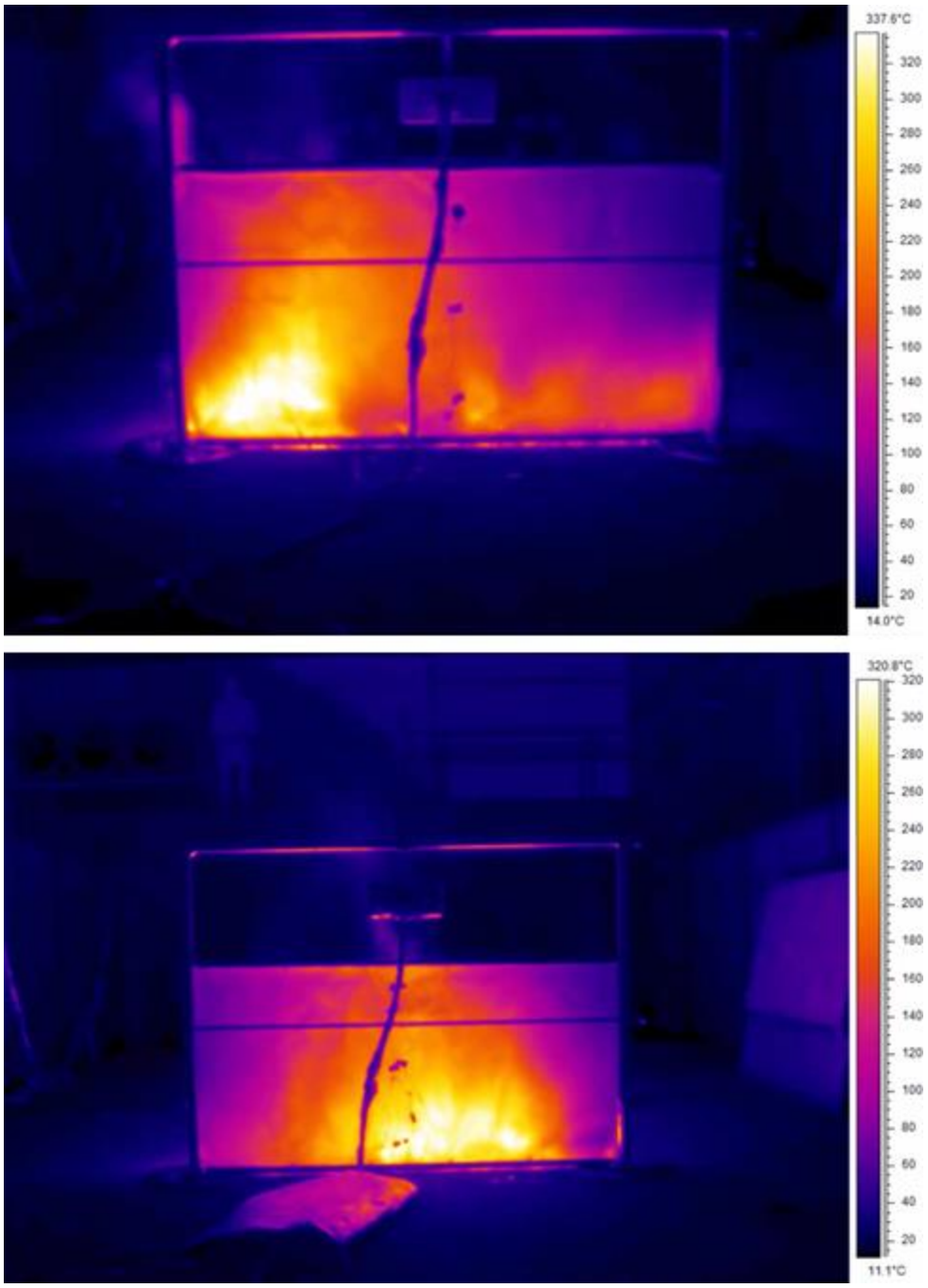

Figure 3.5. Maximum temperature recorded by the IR camera for wind speed U=2 m/s, for Tela1 and Tela2 respectively

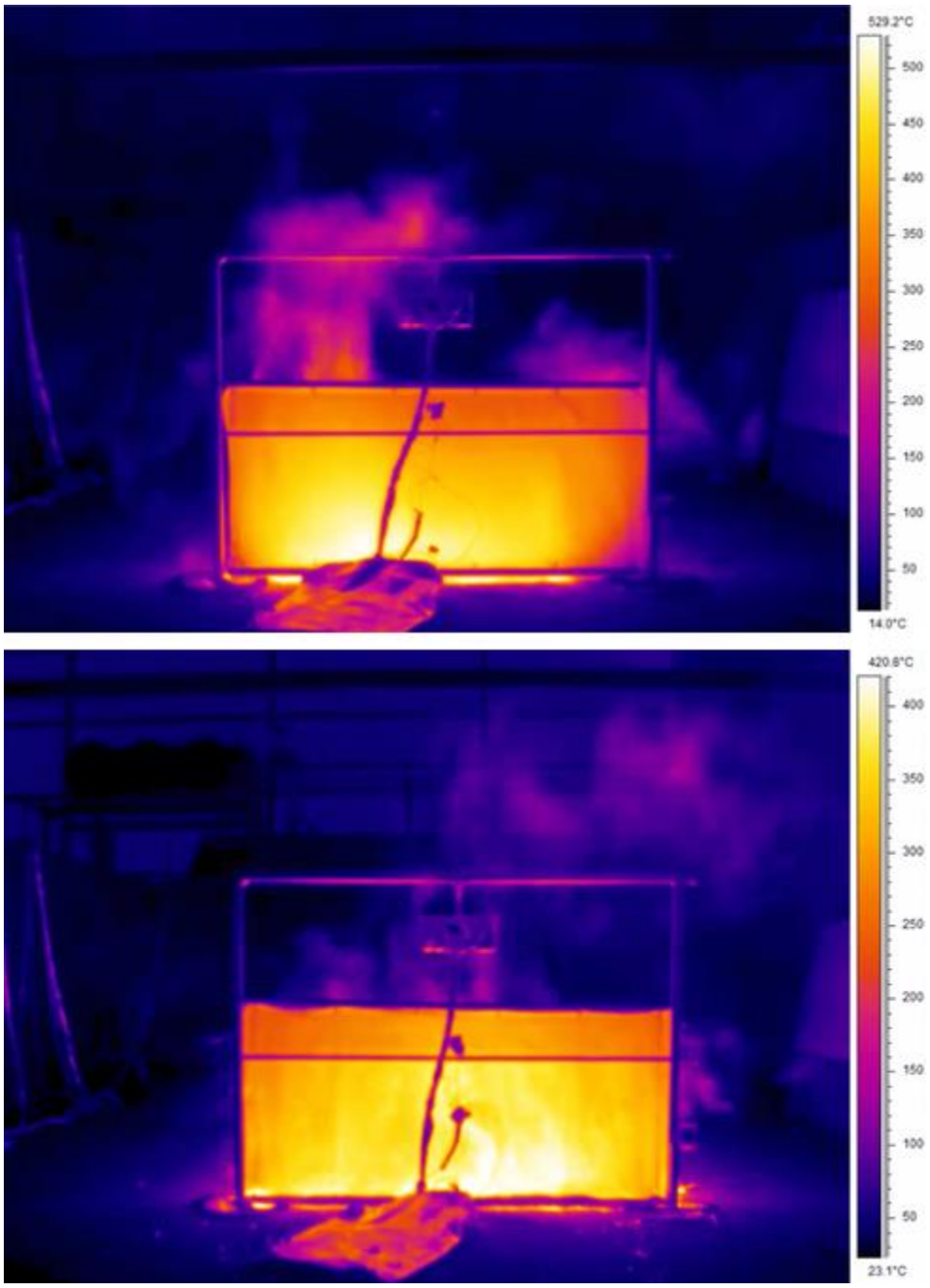

Figure 3.6. Maximum temperature recorded by the IR camera for wind speed U=2 m/s, for Tela3 and Tela4 respectively

To conclude this section two graphs were made that directly compares the five barriers, Figure 3.7 and Figure 3.8. These graphics show the evolution of the temperature of the front and back faces of the barriers, respectively, for a wind speed of 2m/s.

These temperatures are the average for the three thermocouples placed in each face. The front face is considered to be the face which is exposed to the fire.

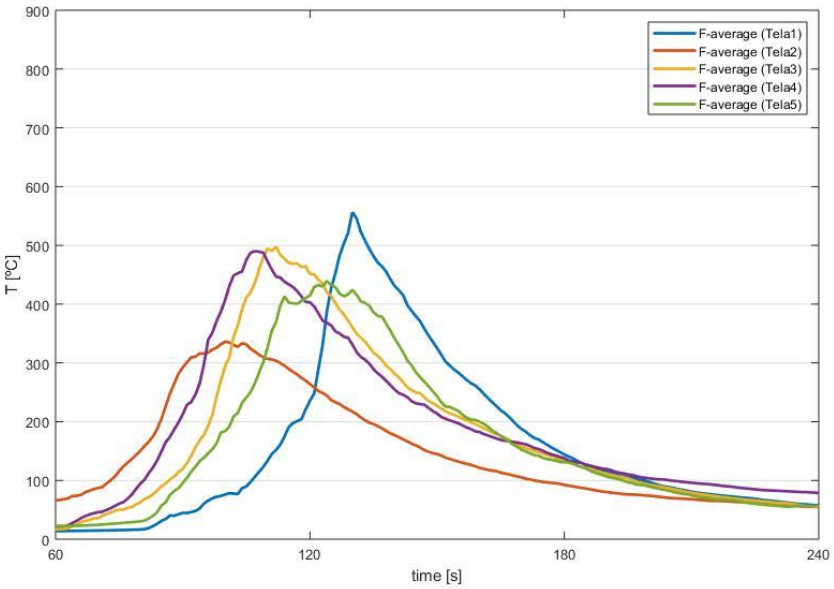

Figure 3.7. Front temperatures of the five barriers vs time

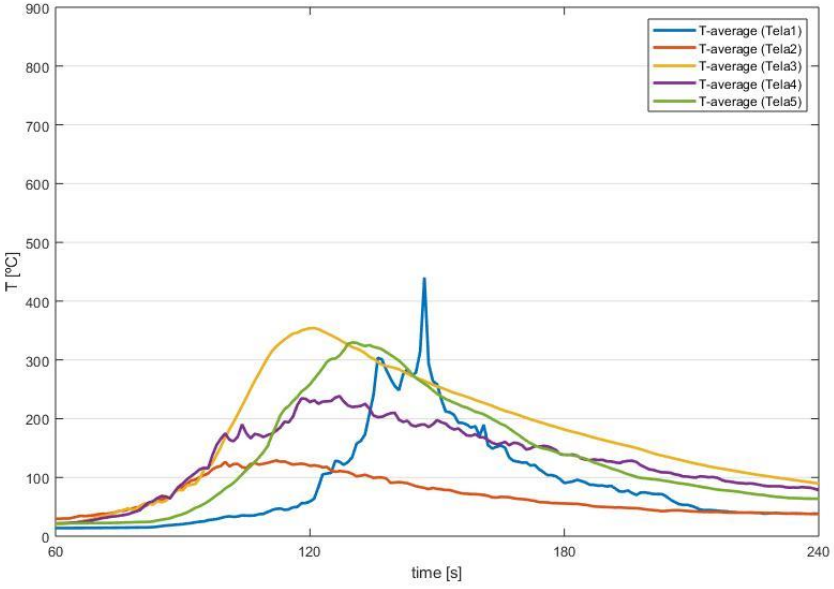

Figure 3.8. Back temperatures of the five barriers vs time

In addition to these last graphs, a study was carried out on the need to increase the height of the barrier, which resulted in Figure 3.9.

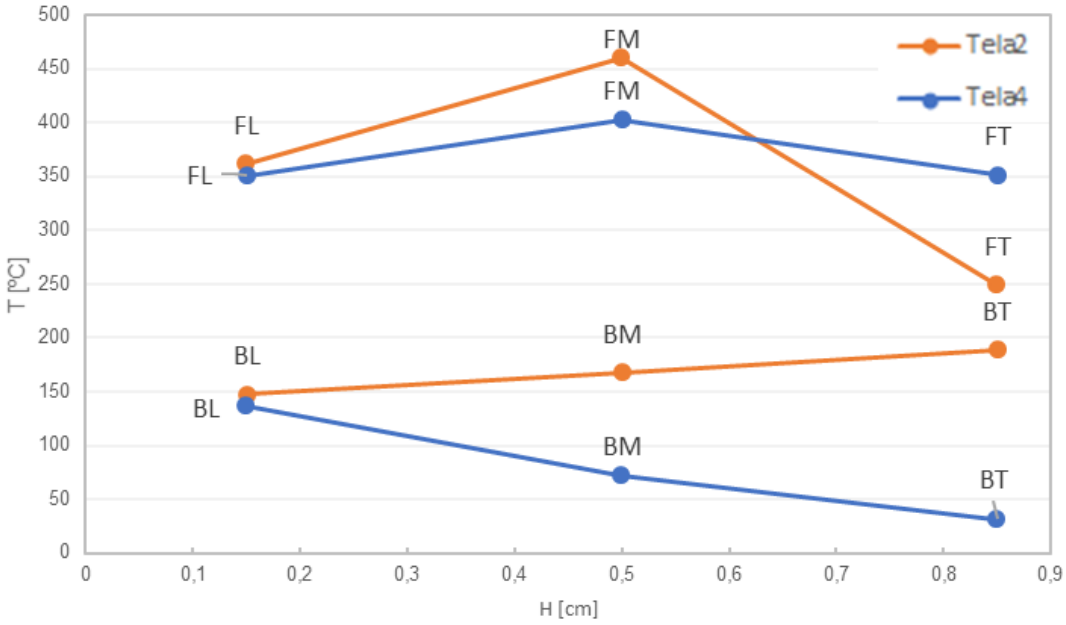

Figure 3.9. Temperatures of the barrier vs height (U= 1m/s) (Tela2 and Tela4, respectively

3.3.2. 2nd Phase – Resistance limit tests

In order to access the resistance limit of the best barrier, three tests were performed, using the previous experimental setup, but increasing the fuel mass density and the wind speed, to increase the fire intensity, as stated in Table 3.8.

To perform this test, the Tela2 was used, as it was the fabric which deemed the best results and the lower temperatures in the previous phase of tests.

Table 3.8. 2nd Phase tests to access the resistance limit of Tela2

	Exp1	Exp2	Exp3
Fuel load [kg/m2]	2.5	3.5	3.5
Wind speed U [m/s]	3	3	1
Average fuel bed height [cm]	22.75	35.50	27.25
Propagation speed [cm/s]	6.39	7.33	4.06
Max. temperature [ºC]	875.6	606.3	-
Max. heat flow [kW/m2]	111.0	43.1	-
Fire line intensity [kW/m]	3591.9	5770.4	3195.5
Flame height [m]	1.23	1.35	1.45
Max. temperature at the rear of the barrier [ºC]	383.1	490.6	-

Due to the malfunctioning of the data acquisition systems, it was not possible to retrieve some data from the last test.

Despite increasing the fire line intensity to almost three times the maximum intensity achieved in the previous stage of tests, the Tela2 was able to sustain the fire, suffering only visible damage on the aluminum coating, but maintaining full fabric integrity, as can be seen in Figure 3.10.

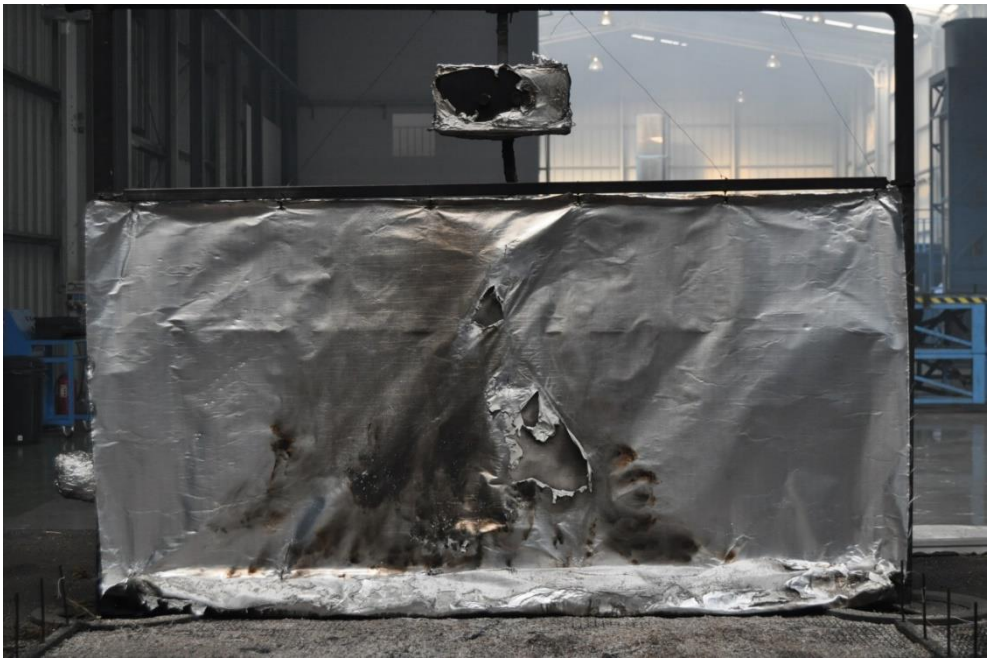

Figure 3.10. Tela2 at the end of the tests (wind speed, 1m/s; Fuel mass, 3.5 kg/m^2)

As in the previous section, this section only presents the summarized results. Graphics such as Thermocouple temperatures vs time or Heat flow vs time and representative images of flame height, state of the barrier at the end of the tests or the maximum temperature recorded by the IR camera can be found in APPENDIX B.

3.4. Discussion

3.4.1. 1st Phase – Fabric selection tests

The goal of the first phase of tests was select the two best fabrics, one with coating and one without coating.

Despite the barriers being all made from fiberglass, the coating, thickness, fiber density and weaving properties for each barrier varied significantly, leading to different results of fire resistance, as seen in Table 3.3 to Table 3.7. From these last tables, it can be also seen that the maximum flame heights are generally found for wind speed values of 1m/s (for wind speeds of 0m/s the flame develops but is not intensified by the wind, so its height is not significant. On the other hand, for wind speeds of 2m/s, the flame tends to incline in the direction of the ground, decreasing its height).

From Figure 3.7 and Figure 3.8 can be concluded that Tela2 is the barrier which reveals the lowest and more stable temperature in both faces. Tela4 is the barrier that deemed the lowest temperatures among the uncoated barriers.

Figure 3.5 and Figure 3.6 show the temperature distribution in the fireproof barriers, for coated and uncoated barriers, respectively. One can see that the higher temperatures occur at the base of the barrier, while on the top part temperatures tend to be lower. This remark is also backed up by the graph in Figure 3.9, where one can conclude that top thermocouple temperatures (at 0.85m height) are consistently lower than the low (0.15m height) and middle ones (0.50m height). One can also conclude that the barriers without aluminium coating (Tela3 and Tela4) have a better distribution of the heat throughout the whole surface, while barriers with aluminium coating tend to concentrate the heat in a spot.

Regarding the height of the barriers, given these conditions (type, moisture content and amount of fuel, wind speed, among others) we conclude that 1.5m is enough, as flame heights are always below 1.3m, as proved in Table 3.3 to Table 3.7 and temperatures

on the top part of barrier are relatively low when compared to the middle and lower parts, Figure 3.9.

Is also important to notice that the selected fabrics are those that have lower prices, with the exception of Tela5.

3.4.2. 2nd Phase – Resistance limit tests

Despite having increased the fire intensity from 1237.8 kW/m to 5770.4 kW/m and reaching temperatures in the order of 900ºC, 50% superior to the barrier rating, the ultimate objective of determining the resistance limit of the barrier was not achieved.

While the aluminium layer suffered visible damage, the fiberglass layer remained intact, as shown in Figure 3.10.

One can then conclude that the resistance of the fabric goes beyond their rating, and that these materials can be effectively used to contain a fire front. However, there is still a need to determine the maximum temperatures which these barriers can sustain before degrading, and how the water can be used to maintain the fabric below those temperatures. This mechanism is the subject of the next chapter.

4. ACTIVE WATER COOLING SYSTEM

4.1. Introduction

This chapter is devoted to development of the active water cooling system. This development once again included two laboratorial test phases: the first for accessing the effectiveness of the water cooling system in improving the temperature resistance limit of the fabrics; and the second, regarding the conception of the water cooling system and load losses along the tubing.

4.2. Experimental methodology

4.2.1. 3rd Phase - Water cooling tests

The purpose of these tests was to evaluate the effectiveness of the water cooling system to improve the temperature resistance limit of the fireproof barrier. For this, two sets of experiments were done for each barrier, one with water sprinkling and another without it.

In these tests, both the two best barriers selected previously in the fabric selection tests and a third barrier (the one with the lower cost) were tested. The goal was to see if, by eventually using more water, one could similar efficiency when compared to the more expensive and effective solutions. This can lead to a solution where initial costs are lower but running and maintenance costs are superior.

For this, in a first stage, a new experimental setup was conceived, in which a portion of the barrier was exposed to the high intensity flame from a Campingaz blow torch (whose flame reaches a maximum temperature around 1000ºC), Figure 4.1, and will be monitored using an IR camera which was installed behind the barrier to measure its temperature distribution.

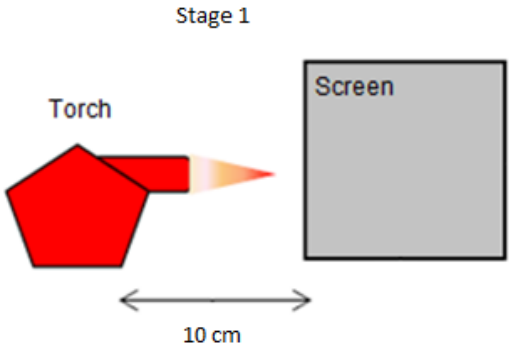

Figure 4.1. Stage 1

In this way a campingaz was installed in front of a piece of fabric (30x30cm, representative of the fabrics that are intended to be studied) fixed vertically through wires to a metallic structure, as can be seen in Figure 4.2, so that its flame strikes perpendicularly, the distance between the two was made to vary between 10 and 12.5cm (values for which it was verified the destruction of the fabric at an acceptable time). For accessing the gas consumption, the Campingaz blow torch mass was measured before and after each experiment.

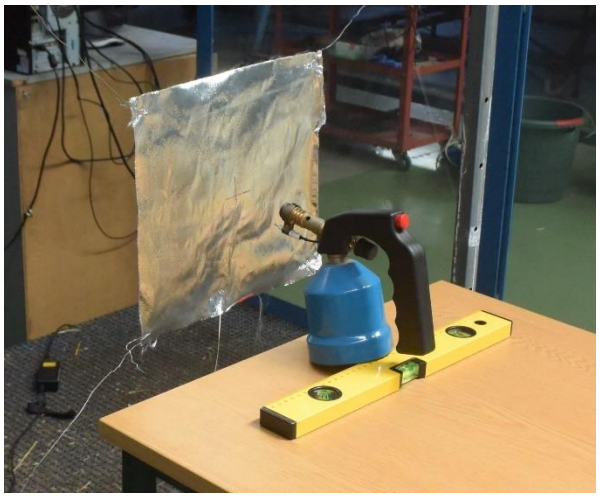

Figure 4.2. Experimental setup

The procedure adopted can be seen in APPENDIX A.

The second stage in turn is quite similar to the first one. This similarity was maintained so that both stages are directly comparable. In this way, the equipment used and

its positioning were maintained, as well as the test fabrics and their dimensions. The only difference is that the fabrics will be cooled using a water sprinkler system, in this case using a micro-sprinkler tube (with 1cm spacing between holes), as can be seen in Figure 4.3 and Figure 4.4. During these tests the water consumption was also measured, for which the container responsible for its collection was weighed before and after each test.

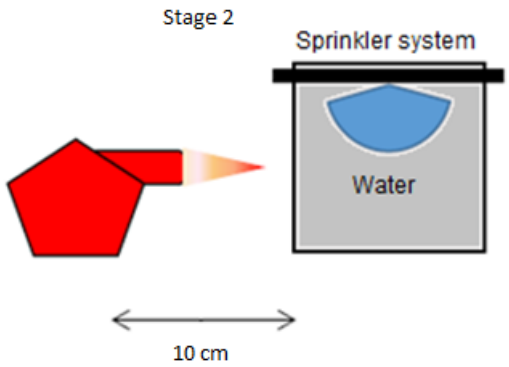

Figure 4.3. Stage 2

With the new changes, also the experimental procedure has undergone some variations, these variations can be found in APPENDIX A.

Figure 4.4. Sprinkler system

4.2.2. Micro-tube load losses

Despite having successfully tested the perforated micro-tube on a small scale, it was necessary to verify its performance on a real scale. The main concern regarding this solution is the pressure and water flow losses along the tubing, which may lead to short

maximum lengths for which this tube is effective and projects water. To access this, a test was designed to measure the load losses in a 10 meter long perforated micro-tube (with 1cm spacing between holes).

In this experiment, two trials were carried out. In the first trial, the micro-tube was fed by a water tap (pressure of approximately 1.5 bar) and in the second trial, a centrifugal pump providing a water pressure of approximately 8.5 bar, was used.

For the accomplishment of these tests a very simple experimental setup was adopted. This assembly consisted of passing the micro-tube inside a set of plastic jars (united two by two (section) until they reach 10m of tube). In order to avoid additional load losses, the tube was perfectly stretched, as shown in Figure 4.5.

The experimental procedure for these trials can be found in APPENDIX A.

Figure 4.5. Experimental setup

4.3. Results

4.3.1. 3rd Phase - Water cooling tests

Having reached the limits of 2nd Phase experimental setup, one proceeded to the third phase of experiments, using a small scale setup and superior heat flows, provided by the campingaz torch.

In the first stage the tissues will be studied taking into account their resistance to fire, this resistance in turn will be obtained by the average times and by the average

temperatures at the time of the rupture of the fabrics. Also in APPENDIX B will be presented images obtained through the IR camera of the fabrics that have supported the fire of the campingaz for the longest time. Finally, the consumption of gas will be calculated.

Table 4.1. Average rupture times for 3rd phase tests with no water, for two different distances

	Average rupture time [s]		
	Tela2	Tela4	Tela5
Dist. 10cm	9.9	8.0	2.5
Dist. 12.5cm	20.7	11.1	3.2

Table 4.2. Average fail temperature 3rd phase tests with no water, for two different distances

	Average fail temperature [ºC]		
	Tela2	Tela4	Tela5
Dist. 10cm	927.8	923.3	928.6
Dist. 12.5cm	888.3	888.7	902.5

For the calculation of gas consumption presented in Table 4.3, five trials were randomly chosen, and during its realization the campingaz was weighed at the beginning and at the end of each test. With the mass differences and the times of each test, the mass loss per unit of time was calculated for each test, then an average of these values was performed and the average gas consumption per unit of time was obtained.

Table 4.3. Gas consumption

Test	Initial mass [g]	Final mass [g]	Mass loss [g]	Time [s]	Mass loss / time [g/s]
1	732.4	729.1	3.3	92.20	0.036
2	729.1	728.7	0.4	37.03	0.012
3	728.7	728.1	0.6	19.80	0.03
4	728.1	727.7	0.4	6.67	0.06
5	727.7	723.7	4.0	97.68	0.041

Once the average of the obtained results was reached, it was concluded that there is an average consumption of 0.036 g/s.

To calculate the energy of the campingaz (E) [kJ] it is necessary to know the mass flow ($\dot{m}$) [kg/h], calorific value of the fuel (PCI) [kWh/kg]and the time of the test (t) [s]:

$$E = \dot{m} * PCI * t, \tag{4.1}$$

The cartridge used in the campingaz is a cartridge of 190g of butane gas, so the properties to use will have to be those of this gas.

- $\dot{m}$ = 0.036 g/s = 129.6 g/h = 0.1296 kg/h
- PCI = 12.68 kWh/kg

$$E = 0.1296 * 12.68 * t = 1.64\ kW * t \tag{4.2}$$

In this way, using the previous formula we can obtain the energy consumption of campingaz, taking into account its time of use.

In this stage, both the resistance of the fabrics and the water consumption will be determined. Notice that the water consumption measures do not take into account the evaporated water.

Again, five trials were made for each barrier where several water flows were tested until achieving the minimum water flow which ensured full barrier integrity after exposing it for 120s to the torch flame, at 10cm distance.

During this section will only be presented the main results as images obtained through the IR camera, this time the images will be representative of the fabrics that have not broken and that have registered lower temperatures (more efficient water sprinkler system) and other results are present in APPENDIX B.

Table 4.4. Average times, temperatures and water flows at the time of the rupture of the fabrics

Distance [10cm]	Average times [s]	Average temperatures [°C]	Average water flows [l]	Average water flows [l/min]
Tela2	84.32	883.35	0.96	0.48
Tela4	36.86	856.7	0.39	0.26
Tela5	32.11	845.35	0.85	0.52

4.3.2. Micro-tube load losses

In this section a study of the load losses will be made, as described in section 4.2.2. For this study, the decrease of the water volume with the length of the tube will be the main focus. These results can be seen in Figure 4.6.

In this section will be presented only the main results The complete results of this study are present in the APPENDIX B.

The following calculated volumes were obtained taking into account a water density of 999.1 g/l for an average water temperature of 15°C.

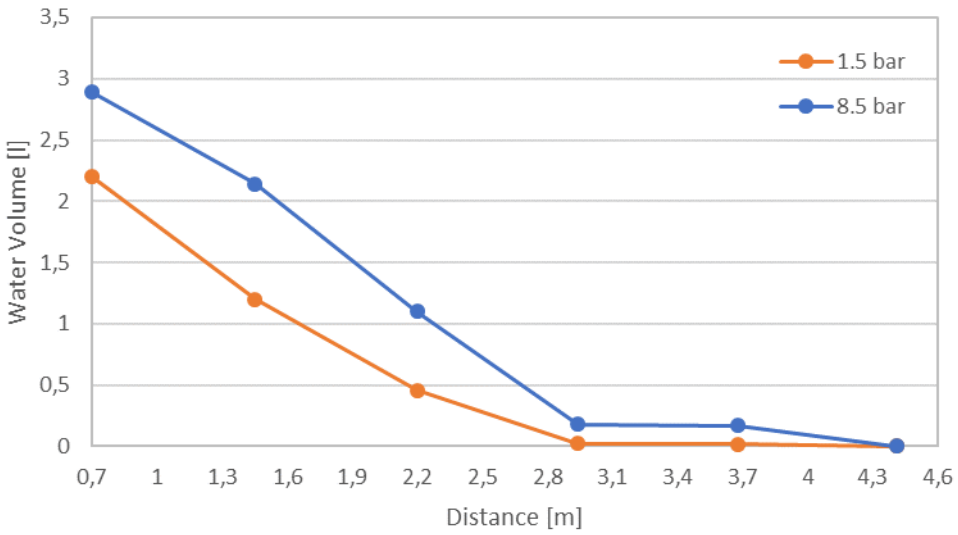

Figure 4.6. 1st and 2nd Tests

Since the tests performed lasted approximately one minute, it is reasonable to assume that the volume flow per minute is in this case equal to the volume.

4.4. Discussion

4.4.1. 3rd Phase - Water cooling tests

Tela2 is, once again, the barrier which deems the best results, in average, for both distances, lasting at least 4 times longer than the cheapest barrier, Tela5, even though both have similar ratings, this data can be verified in Table 4.1. In fact, using the IR camera images, one was able to determine the average temperature for which the barriers fail. The

results, present in Table 4.2, show that the three barriers fail at roughly the same temperature. However, the coating of Tela2 or the higher thickness of Tela4 ensure this temperature takes more time to be reached.

Again, in the second stage, five trials were made for each barrier, except this time the active water cooling system, consisting on a spray of water to the barrier surface, was employed. Several water flows were tested until achieving the minimum water flow which ensured full barrier integrity after exposing it for 120s to the torch flame, at 10cm distance. In five trials, Tela5 presented rupture four times, even with water flows superior to 5L/min per linear meter of barrier. Comparing the other two barriers, this time Tela4 showed to be slightly superior, with a minimum water flow of 2.6L/min per linear meter of barrier, against the 4.8L/min water flow for Tela2. This can be explained by the fact that because of not having any coating, the exposed fiberglass of barrier Tela4 is capable of holding more water than the aluminum surface in Tela2, thus allowing more absorption of the heat.

To conclude, it could be verified that the water tests are clearly better, since in these tests the barriers to the same conditions have not always broken and thus Tela4 was selected as the best solution.

4.4.2. Micro-tube load losses

From the load loss tests in the micro-tube, one can conclude that this solution cannot be used for long tubes, and that the input pressure and water flow bears little impact in the performance of this solution.

With this system it is only possible to humidify the barrier to a distance of 4.5m, which is clearly insufficient, on the other hand if this solution was chosen, it could only be guaranteed the safety of the barrier for a distance of 1.5m, where the flow rate is higher than the required 2.6 l/min.

Finally, the main conclusion that can be drawn from the results is that another solution will have to be adopted.

4.5. Water circuit dimensioning

Continuing the study of water sprinkling, in this section will be studied a particular case in which the sprinkling system will be designed for a 200m fence.

Figure 4.7. Example of the setup to be developed

As it could be seen in section, the minimum water flow per minute (q) [l/(minute.m)] for Tela4 (fabric to be used in the final solution) is 2.6 l/minute/m. So, for instance, to protect a perimeter (p) [m] of 200m, one will be need a flow rate of 520 l/minute (Q) [l/minute], this is therefore the first requirement to select the mechanisms of water supply and storage.

$$Q = q * p = 2.6 * 200 = 520\ l/minute\ , \tag{4.3}$$

Of course this value assumes that water is used for the whole perimeter at the same time. In reality, the water circuit can have ramifications and control valves which might enable the independent control of separate sections of the perimeter. This means that, for instance, only a small part of the perimeter which is located in the side of the fire front can be activated, thus requiring a much inferior water flow. We can safely assume that in the case of this 200m perimeter, only 50m would be under the threat of the fire front at a given time, meaning a water flow of 130 l/minute.

$$Q' = q * p' = 2.6 * 50 = 130\ l/minute\ , \tag{4.4}$$

As for the service pressure, the tests performed with the micro-tube revealed that this bears no significant impact on the performance of the system. However, one has to account for the load losses in the entire water circuit, which increases with its size, number of derivations and valves and other components, so this must be taken into account in each specific case, to ensure that a minimum water pressure reaches the water sprinklers.

Lastly, only the capacity of the water reservoir needs to be calculated, and in view of the satisfactory results of the field trials, with an average duration of 8 minutes, it was considered sufficient that the water sprinkling lasts for 10 minutes.

With the average duration of sprinkling (t) [minute], it is enough to multiply this time by the aforementioned reduced flow rate (Q') (130 l/minute), so the reservoir will have a capacity (C) [l] of 1300 l.

$$C = t * Q' = 10 * 130 = 1300\ l, \tag{4.5}$$

However it was decided to use a safety coefficient (n) of 2.5 and thus the new capacity (C_{final}) of the tank should be 3250 l.

$$C_{final} = n * C = 2.5 * 1300 = 3250\ l, \tag{4.6}$$

4.6. IR camera calibration

4.6.1. Methodology

Once with the tests with and without water sprinkling performed, the question arose whether or not the camera was calibrated.

To check this question, a calibration process was performed on the IR camera.

This method involved performing a calibration curve, which was obtained, by measuring the heating/cooling temperatures of the fabrics. These curves were simultaneously obtained by a thermocouple connected to the material and by the camera to be calibrated.

To perform this calibration some equipment were used, among which, the IR camera used during the tests, a thermocouple, a campingaz, auxiliary equipment as a support for fabrics and wires and the fabrics to be tested.

Due to logistical issues the fabrics tested were only four, leaving Tela1 untested.

In order to carry out this calibration the infrared camera was mounted on its support at the medium height of the fabric to be tested and at a distance from its rear part equal to that used in the tests already mentioned.

Once the fabric was fixed to the structure by means of wires, an instrumented thermocouple was installed on the back.

In turn, at the front of the fabric and situated at a distance of 15cm was a campingaz whose flame was made to point to the center of the fabric, as demonstrated in Figure 4.8.

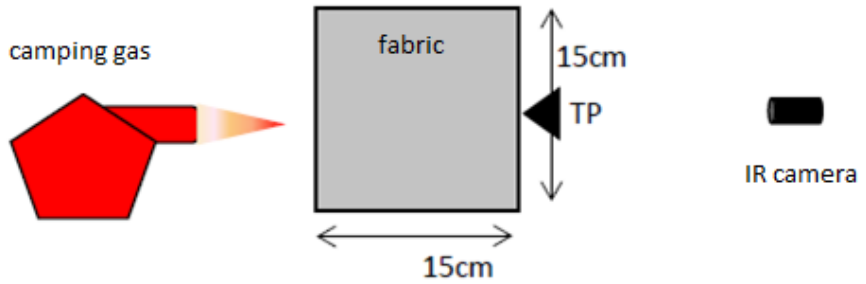

Figure 4.8. IR camera calibration setup

Finally, a very simple methodology was used. In this process the flame of a campingaz (typically around 1000 ° C) was used to heat a 15x15 cm piece of fabric. A thermocouple was placed on the back of the fabric, and the test was shot with the IR camera also placed on the back of the fabric. Four tests of this type were done (one for each of the fabrics), and the decay of the temperature on the fabric was recorded using the two methods.

4.6.2. Results

With these tests it was possible to obtain the heating/cooling curves of the barriers tested that can be consulted since Figure 4.9 to Figure 4.12. In addition to these results, it was also possible to obtain representative IR camera's images of these tests, that

can be found in APPENDIX B, and also the relative error values between the two readings (this error was calculated taking into account the maximum values reached in each of the readings).

The relative error, RE, will be calculated using the following expression:

$$RE = \frac{|Value_{exact} - Value_{approximate}|}{Value_{exact}} \%, \tag{4.7}$$

Tela2

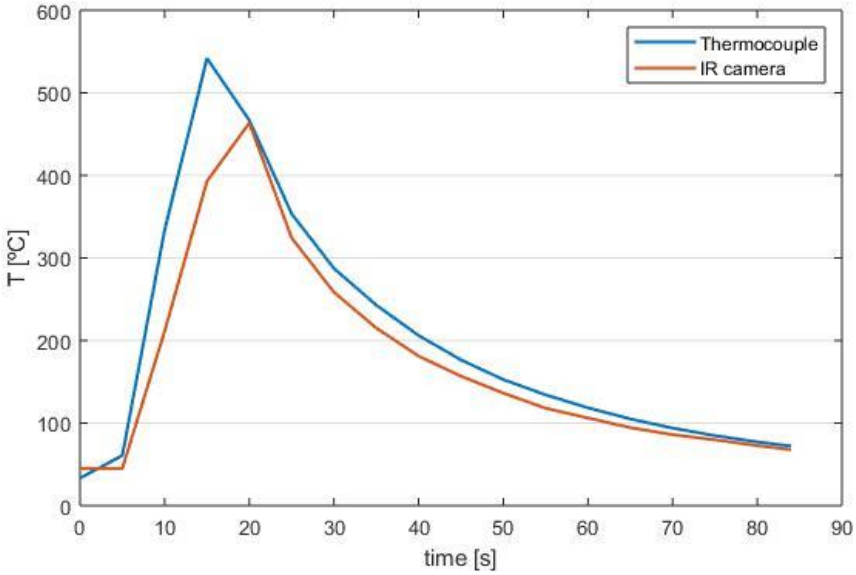

Figure 4.9. Heating/cooling curves (Tela2)

$$RE = 14.43\%. \tag{4.8}$$

Tela3

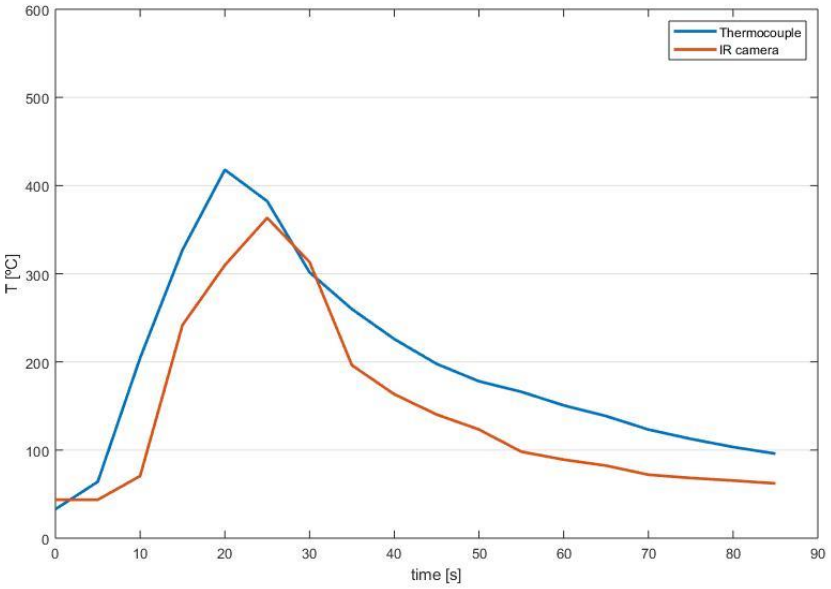

Figure 4.10. Heating/cooling curves (Tela3)

$$RE = 13.06\%. \tag{4.9}$$

Tela4

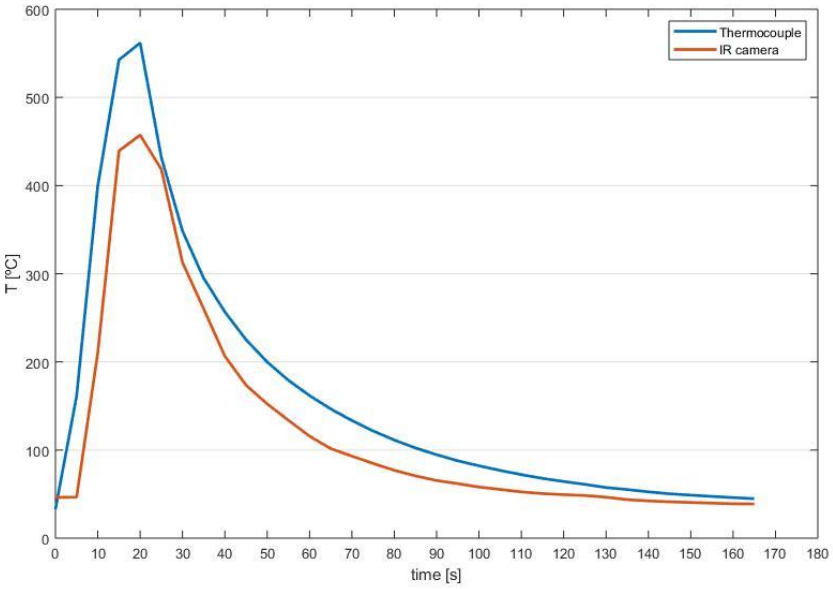

Figure 4.11. Heating/cooling curves (Tela4)

$$RE = 18.61\%. \tag{4.10}$$

Tela5

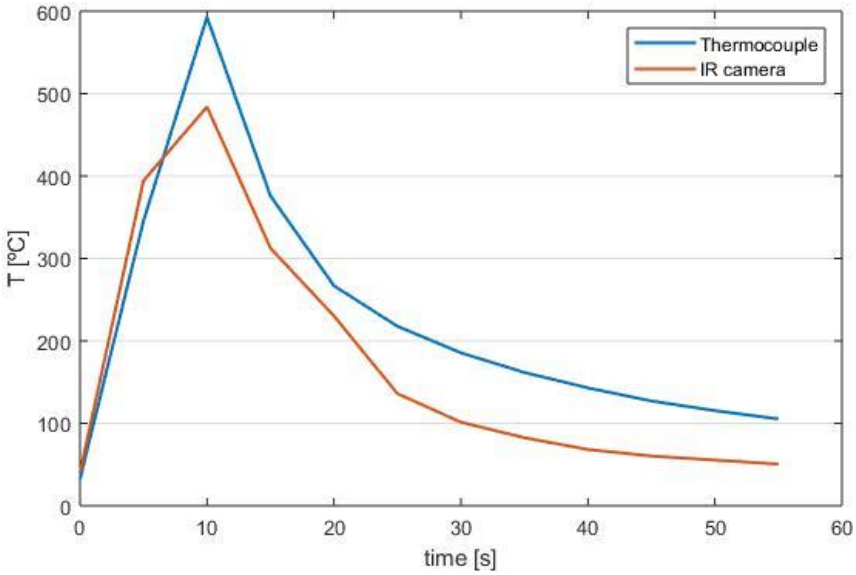

Figure 4.12. Heating/cooling curves (Tela5)

$$RE = 18.38\%. \tag{4.11}$$

4.6.3. Discussion

Once the calibration of the IR camera was performed, some descriptions were verified in relation to the values obtained by the thermocouple. These differences are verified in the reaction time, where the IR camera presents an approximate delay of 5s in relation to the reaction time of the thermocouple, and in the values of the read temperatures, where the IR camera presents an average relative error, ARE, of 16.12% that should be taken into account in all the values registered by the IR camera, which should be increased by the said percentage.

5. FIELD DEMONSTRATION AND VALIDATION

5.1. Methodology

In order to overcome the limitations inherent in the laboratory tests (in particular the scale of these tests) Gestosa field trials were carried out in the Coentral area, Castanheira de Pera. A map of the site and the schematics of the field plots can be found in ANNEX B.

At this site two experimental plots were tested, each with an area of 400m^2 (20x20m) and with a slope of 30º, this site was composed by vegetation of the bush type with approximately 0.5m height.

At the top of these plots was placed the barrier to be tested, the barrier in question was 1.5m height and 18m long and also had five diffusers of curtain with an angle of sprinkling of 180º as shown in Figure 5.2.

Two tests were performed. In the first, only the fence or support structure with the water sprinklers was tested. In the second, shown in Figure 5.1, was tested the fireproof barrier fitted with the Tela4 and using a water sprinkling system.

Figure 5.1. Second field test

As in the laboratory tests, a previously defined procedure was also used, that can be consulted in APPENDIX A.

5.2. Results

1st Test

The barrier was positioned 16m from the start of the experimental field, leaving 4m behind. In this way it is possible to see if the fire can propagate past the structure, causing an ignition in the inside of the protected perimeter.

Unlike the laboratory tests, in the Gestosa trials, the fuel bed consisted of several species of vegetation, namely Erica umbellate, Erica australis, Baccharis trímera and Ulex. Knowing the different species present in the field, the humidity of each one of them was obtained, which in the end allowed to obtain an average fuel moisture content.

In this first test, the intention was to test the fence effectiveness in suppressing the fire front, not relying on the fireproof barrier. Thus, only the metal structure and the sprinklers to project water to the terrain were used, as can be seen in Figure 5.2 and Figure 5.3.

Figure 5.2. Fence and sprinklers (during first field test)

Figure 5.3. Fence and sprinklers (at the end of first field test)

2nd Test.

As in the first test also in the second test the fuel bed was composed of several species of vegetation, of all the species already mentioned, in this second plot only the presence of Erica australis was not verified. So it is natural that the moisture content of the fuel is different.

With this test, and once studied the performance of the fence, it was intended to study the performance of the barrier. As a result, the active combat sprinklers were rotated so that they faced the back of the barrier and had no effect on the fire front and the thermal barrier fitted with a micro-tube similar to that tested in section 4.2.2 was installed, as can be seen Figure 5.4.

Figure 5.4. Barrier (during second field test)

Table 5.1. Gestosa tests

	Test 1	Test 2
Ambient temperature [ºC]	17.9	21.3
Relative humidity [%]	52	45
Fuel bed area [m^2]	400	400
Fuel moisture content [%]	38.97	24.91
Average fuel bed height [cm]	50	50
Wind speed [m/s]	7.9	8.9
Propagation speed [cm/s]	-	3.33
Maximum temperature reached [ºC]	-	794.0
Flame height at the fence [m]	-	3

5.3. Discussion

From these tests two conclusions can be immediately withdrawn.

From the first test, in which it was intended to study only the fence, using water sprinkling on the ground, the flames did not approach the fence, burning only the dry vegetation leaving an unburnt perimeter of about 3m long (even though the wind was in the opposite direction to combustion).

From the second test, in which it was intended to study the resistance of the barrier, water spraying on the ground was not performed, as a result the fire front reached the barrier with a height of about 3m (flame heights almost three times higher than those obtained in laboratory), yet the barrier resisted well, without suffering visible damage and mitigating the passage of fire.

6. CONCLUSION

6.1. Achievements

As it has been mentioned throughout this work, the final solution that is intended to be developed is of extreme importance and necessity. It is also a solution to be used in a WUI (regardless of terrain type) or in the direct protection of infrastructures.

The solution is based on the principle of suppression and combating flames, when it is no longer possible to prevent its beginning but when it is essential to prevent its progression. This solution offers advantages over the other options, since it makes use not only of fire resistant fabrics but also of a water sprinkling system.

Even though a market ready solution was not fully developed, important steps were taken in this direction.

Throughout this work five barriers were studied, of different manufactures that are differentiated by their composition, thickness, density, service temperature and coating. In order to study these barriers several tests were carried out, in the first phase these were tested in the scale simulation of a real wildfire from which pre-selection of Tela2 and Tela4, one with aluminum coating and another without coating, resulted. In later stages these barriers continued to be tested in order to obtain their maximum resistance without and with an active water cooling system. These results led to the dimensioning of the entire water supply circuit for an example installation with a 200m perimeter. In the end, the results revealed that Tela4 would be the best barrier and would show the best performance when cooled with a flow rate of 2.6l/minute per linear meter.

In addition to the selection of the barrier it was still possible with these tests to determine its height so that it is able to combat a wildfire characteristic of a WUI.

Finally, in the phase of the field tests, which allowed to overcome the difficulties of scale, it was proven separately that both the fence and the barrier are able to withstand a real scale fire, with a vegetation height of approximately 0.5m, proving that together the results will be very positive.

However during these tests some problems were encountered, namely temperature measurement problems with thermocouples, which kept frequently falling from their fixing points in the barrier or failed to work. Even with regard to temperature measurement, IR cameras also showed some problems, not being calibrated, having been calibrated at a later stage. Also in the field trials some difficulties were found, the logistics involved and the terrain topography made it impossible to obtain some important data, such as, the fuel mass or the maximum heat flow reached.

6.2. Future work

Once the main conclusions of this work are exposed, some recommendations for future work are presented.

Regarding heat transfer modeling it is advisable to study the barriers in such a way that it is possible to predict their performance for different temperatures, operating times and water flows.

With regard to heat flow calculation it is recommended to carry out the study already indicated, in order to obtain the heat flows that will have to be counterbalanced to guarantee a barrier temperature that must be previously established.

As it was possible to verify the water sprinkling system used was not able to meet the needs of the barrier, so it is recommended to adopt a new system and with it a new calculation of the necessary flows and pressures.

Finally, during the calculation of the flows, it is also recommended to obtain the amount of evaporated water, which plays an important role in the cooling of the barriers.

To conclude, this is a solution that if developed according to the given recommendations, could be put on the market in a short time and could play a central role in avoiding the tragedies inherent in a WF.

BIBLIOGRAPHY

1. Relatório Final. Available at: http://www.parlamento.pt/sites/COM/XIILeg/GTARAPIF/Paginas/RelatorioFinal.aspx. (Accessed: 29th August 2018)
2. Instituto Português do Mar e da Atmosfera. Available at: http://www.ipma.pt/pt/publicacoes/boletins.jsp?cmbDep=cli&cmbTema=pcl&cmbAno=2017&idDep=cli&idTema=pcl&curAno=2017. (Accessed: 29th August 2018)
3. Estudo Geral - Percorrer o repositório. Available at: https://estudogeral.sib.uc.pt/handle/10316/112/browse?type=author&order=ASC&rpp=20&authority=rp59333. (Accessed: 29th August 2018)
4. Wildfire protection system. (2000). Available at: https://patents.google.com/patent/US6360968B1/en. (Accessed: 29th August 2018)
5. Fireproof building panels. (1987). Available at: https://patents.google.com/patent/US4744186A/en. (Accessed: 29th August 2018)
6. Multilayered fire-barrier canvases. (2007). Available at: https://patents.google.com/patent/US20090194297A1/en. (Accessed: 29th August 2018)
7. Laboratório de Estruturas e Resistência ao Fogo. Available at: http://lerf.web.ua.pt/. (Accessed: 29th August 2018)
8. BS EN 1363-1:2012 - Fire resistance tests. General requirements. Available at: https://shop.bsigroup.com/ProductDetail/?pid=000000000030251439. (Accessed: 20th April 2018)
9. EN 13501-2 / EN 1634-1. Available at: http://www.serc-europe.com/serc/portugues/ppci/SERC%20DOC.010.R1-Euroclasses%20de%20Resistencia%20ao%20Fogo.pdf. (Accessed: 20th April 2018)
10. BS EN 13381-2:2014 - Test methods for determining the contribution to the fire resistance of structural members. Vertical protective membranes. Available at: https://shop.bsigroup.com/ProductDetail?pid=000000000030259158. (Accessed: 17th December 2017)

11. Figueiredo, A. R. & Costa, J. J. Experimental analysis of the use of wet porous media for thermal protection against high intensity heat fluxes. (2004). https://www.sciencedirect.com/science/article/pii/S0017931003004137. (Accessed: 29th August 2018)
12. Empatec - Empatec. Available at: http://empatec.pt/product-item/tecidos-tratados/. (Accessed: 20th April 2018)
13. Fiberglass Mesh Can be Used for Fireproof Window Screen. Available at: http://www.security-screens.org/securityscreens/fiberglass-mesh.html. (Accessed: 20th April 2018)
14. Screening Material | Flame Retardant Polythene | Protecta Screen Ltd. Available at: http://www.protectascreen.com/Catalogue/temporary-screening/screening-materials/screening-material-flame-retardant. (Accessed: 20th April 2018)
15. archiproducts. Available at: http://www.archiproducts.com/en/products/studio-t/sound-absorbing-felt-workstation-screen-desktop-partition-aida-workstation-screen-desktop-partition_322130. (Accessed: 20th April 2018)
16. Tvc129. Available at: http://www.lizmontagens.com/media/profiles_media/flipbooks/pdf/Thermal_2013_POR.pdf. (Accessed: 20th April 2018)
17. Fibras AES – Alkaline Earth Silicates (Fibras BioSolúveis). Available at: http://www.lizmontagens.com/media/profiles_media/flipbooks/pdf/Thermal_2013_POR.pdf. (Accessed: 20th April 2018)

ANNEX A

TVL 126

FORTAGLAS™ ALUMINIZADO – TVL 126

ESPECÍFICAÇÕES TÉCNICAS

PROPRIEDADES BÁSICAS	VALORES E UNIDADES
Composição	Filamento de fibra de vidro aluminizado
Acabamento	Folha de alumínio numa das faces
Diâmetro das fibras	6 – 9 µ
Peso	520 g / M^2
Espessura	0.5 mm
Estrutura	Satin
Total de fios 10cm: - teia - trama	 166 130
Resistência à tensão: - teia - trama	 3550 N / 50 mm 2300 N / 50 mm
Reacção ao fogo	M0 Incombustível
Temperatura de serviço: - Períodos curtos de tempo - Em contínuo	 600 ºc 150 ºc
Análise Química Al_2O_2 $Si\ O_2$ $Ca\ O_2$ $B_2\ O_3$ Mg O F	 14 – 15.5 % 53 – 55 % 16.5 – 17 % 6.5 – 8.5 % 4 – 5.5 % 0.2 – 0.6 %

APLICAÇÕES :

× Telas e cortinas de protecção contra fontes de calor radiante, para proteger da queda de líquidos corrosivos, compensadores de dilatação, protecção de tubos de escape, etc.

× Fundições, industria naval e automóvel.

Formato : Rolos com 1 metro de largura e 50 metros de comprimento.

Os tecidos Fortaglas ® satisfazem os requisitos das Normas Britânicas, Europeias e Internacionais mais restritas, incluindo: **BS476 partes 4, 6 e 7 / BS5438** .

Dados fornecidos pelo fabricante

TSI 291

TSI – 291

ESPECÍFICAÇÕES TÉCNICAS

PROPRIEDADES BÁSICAS	VALORES E UNIDADES
Composição	Fios de silício puro - FORTASIL™
Acabamento	Vermiculita
Peso	650 g / M^2
Espessura	0.7 mm
Estrutura	Satin
Total de fios 10cm: - teia - trama	 210 130
Reacção ao fogo	M0 Incombustivel
Temperatura de serviço	950 ºc
Temperatura de fusão	1600 ºc
Análise Química Al_2O_2 $Si\ O_2$ $Ca\ O_2$ $B_2\ O_3$ Mg O F	 0.48 % 98.9 % 0.14 % 0.01 % 0.01 % 0.46 %

APLICAÇÕES :

Filtragem de metal fundido; filtragem de pó em gases a alta temperatura; protecção contra soldadura e fogo (fabrico de roupa de protecção, cortinas, etc... .); na indústria aeroespacial na fabricação de foguetes e mísseis, fabrico de calorífugados, compensadores têxteis de dilatação e em todas as aplicações que requeiram um tecido resistente ao choque térmico.

Formato : Rolos com 0,92 metros de largura e 50 metros de comprimento

Dados fornecidos pelo fabricante

ANNEX B

Satellite view (Coentral Area)

Plot layouts

1st Test

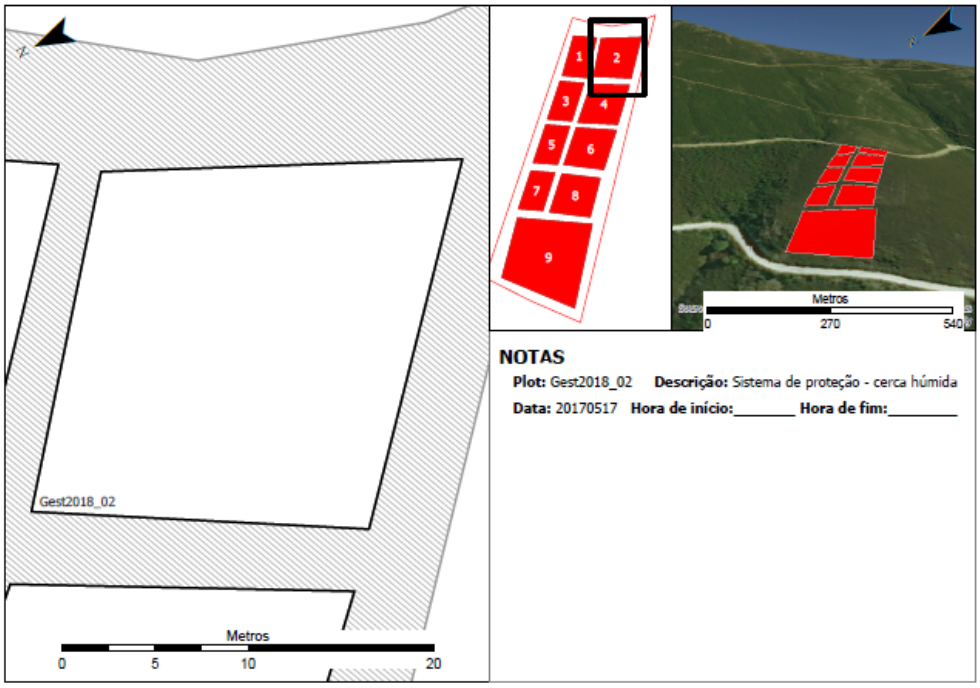

2nd Test

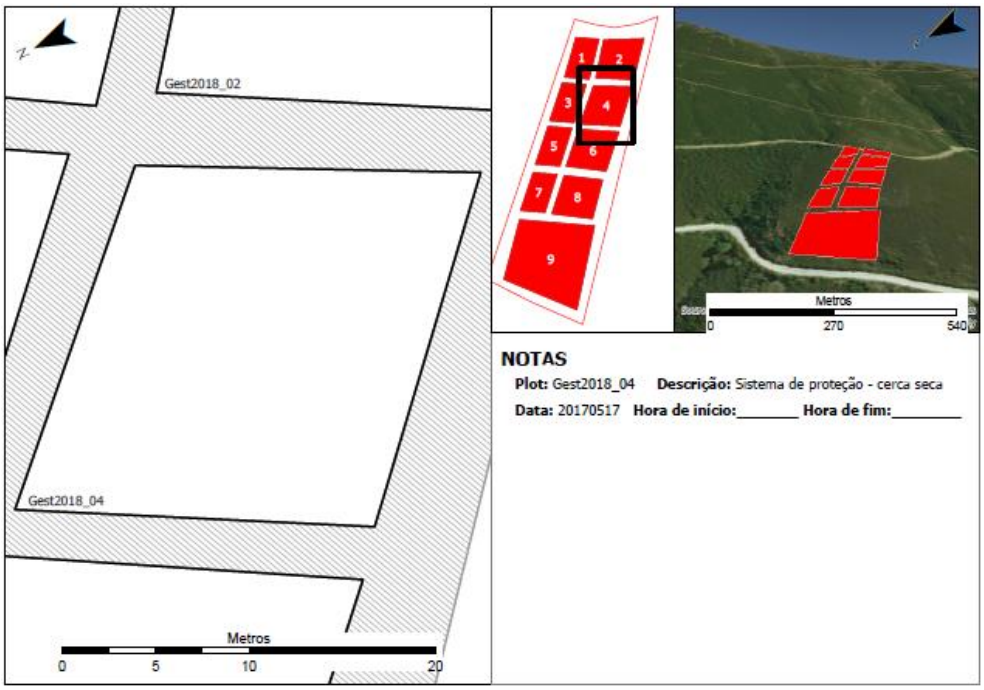

APPENDIX A

1st Phase's experimental procedure

Experimental procedure applied to 1st phase tests:

- Record of air temperature and relative humidity;
    - These properties were obtained using a simple analyzer;
- Setting of the fuel load by determining fuel moisture content and fuel's mass and fixing the area of the fuel bed;
    - The fuel load must be chosen in order to provide an one meter high flame (about 1.0 kg/m^2, similar to the fuel load present in the plots of the experimental field of Gestosa). In order to ensure reproducibility of the tests, the fuel bed preparation was done using a fuel load value on dry basis, thus ensuring the same fuel conditions in all tests. For this, in each test the moisture content was previously measured with a sample of approximately 2g of fuel. This moisture content was determined on a moisture analyzer, where the sample was subjected to 105°C for fifteen minutes. Subsequently, through the fuel bed area and fuel load, the dry mass of fuel to be used in the fuel bed was obtained. The mass of the fuel was weighed on a scale and then evenly distributed to form the fuel bed;
- Measurement of fuel bed height:
    - In order to be able to remove the average height of the fuel bed four measurements are made (each one near the corners of the fuel bed);
- Set the wind speed (0, 1 or 2m/s);
    - These speeds are selected by means of a frequency variator, which constitutes the combustion tunnel;
- Start the thermocouples:
    - On each face of the fabric are installed 3 K type thermocouples (K PTFE twin twist fine thermocouple wire), arranged
      in its vertical axis, at three different heights, 0.15m, 0.50m and 0.85m, in order to obtain a vertical profile of temperatures in the faces of the

fabric. The thermocouples are still responsible for obtaining the maximum temperature.

- Start the IR camera:
    - The infrared camera (Flir Systems, ThermaCAM S Series) is installed behind the fabric to obtain its temperature distribution;
- Start the flowmeter:
    - The water-cooled flowmeter (Vatell Corp, Thermogage 9000-9) is installed above the fabric to obtain both the radioactive and total heat flow;
- Set the pin rulers, wool yarn and stopwatch:
    - Combined to obtain the propagation velocity of the flame front, several wires were placed in the fuel bed at each 20cm and the cut times were recorded to access the fire propagation speed;
- Start the video cameras:
    - One of the video cameras is installed laterally near the barrier to obtain the flame height. Above this, and suspended from a platform, the second video camera must be installed, in order to obtain a top view of the test;
- Start combustion:
    - A linear ignition was chosen, because it allows to represent a front of flames and to determine its speed of propagation;
- Complete the data acquisition systems:
    - These systems must be stopped when the fuel is consumed or when the fabric is destroyed;

3rd Phase's experimental procedure (1st stage)

Experimental procedure applied to 3rd phase tests:

- Connect the data acquisition systems (video camera, IR camera, chronometer);
    - In order to respectively document the test, record the temperatures registered, as well as their distribution in the

fabric and record the times of interest, namely the time of beginning of the data acquisition, the time of the ignition, and the time of fabric disruption;

- Turn on the campingaz;
- Turn of the data acquisition systems:
    - These systems must be stopped as soon as the fabric breaks;

3rd Phase's experimental procedure (2nd stage)

Experimental procedure applied to 3rd phase (2nd stage) tests:

- Need to mount the sprinkler system (Figure 4.4), namely the 4mm micro-tube (10cm long) and the water tank;
- Need to weigh the water tank before and after the data was acquired, to obtain the mass of water used and consequently its volume and volume flow;
- Need to start the water sprinkler system (simultaneously with the start of the camping gas).

Micro-tube load losses experimental procedure

Experimental procedure applied to micro-tube load losses tests:

- Measure the length of each set of jars (section)(so that it is possible to see later how far this method can be used);
- Weight the sections at the beginning and at the end of each test in order to obtain the water mass in each one and consequently its volume and volume flow;
- Start the test at the same time as the stopwatch;
- Stop the test when the stopwatch marks 1 minute.

Field tests experimental procedure

Experimental procedure applied to field tests:

- Determine relative humidity, air temperature and wind speed;
- Mount the barrier to test;
- Beginning of the recording of the test in the infrared range. Capture of photographic images throughout the test;
- Combustion of fuel bed made with fire-breathing and linear ignition;
- Observation of the behavior of the Barrier with the approach of the flame front.

APPENDIX B

1st Phase's Results

In order to make the graphics of these tests less confusing, some abbreviations have been used in the graphics that can be found in this appendix, in Thermocouple temperatures vs time graphics, TFC, TTC, TTB, TTM, TFM, TFB, respectively represent thermocouple front up, thermocouple back up, thermocouple back low, thermocouple back middle, thermocouple front middle and thermocouple front low. In the graphs, Heat flow vs. time, RADIATIVE represents the radiative flow read by the flowmeter (when the flame front is away from it), while TOTAL represents the total flow read by the flowmeter, radiative and convective (especially when the flame is in contact with the flowmeter).

Table 0.1. Tela1

	Tela1_U0	Tela1_U1	Tela1_U2
Room temperature [ºC]	12.2	14.3	15.1
Relative humidity [%]	60	65	65
Fuel load [kg/m^2]	1	1	1
Fuel bed area [m^2]	5.40	5.40	5.40
Fuel moisture content [%]	14.3	16.3	14.3
Fuel mass [kg]	6.17	6.28	6.17
Average fuel bed height [cm]	11.75	13.75	12.25
Propagation speed [cm/s]	0.81	2.92	6.65
Maximum temperature reached [ºC]	451.7	459.5	632.6
Maximum heat flow reached [kW/m^2]	21.6	26.2	45.9
Fire line intensity [kW/m]	182.6	656.6	1495.5
Average Flame height [m]	0.98	1.20	1.05

Maximum temperature reached at the rear of the barrier- 169.4ºC.

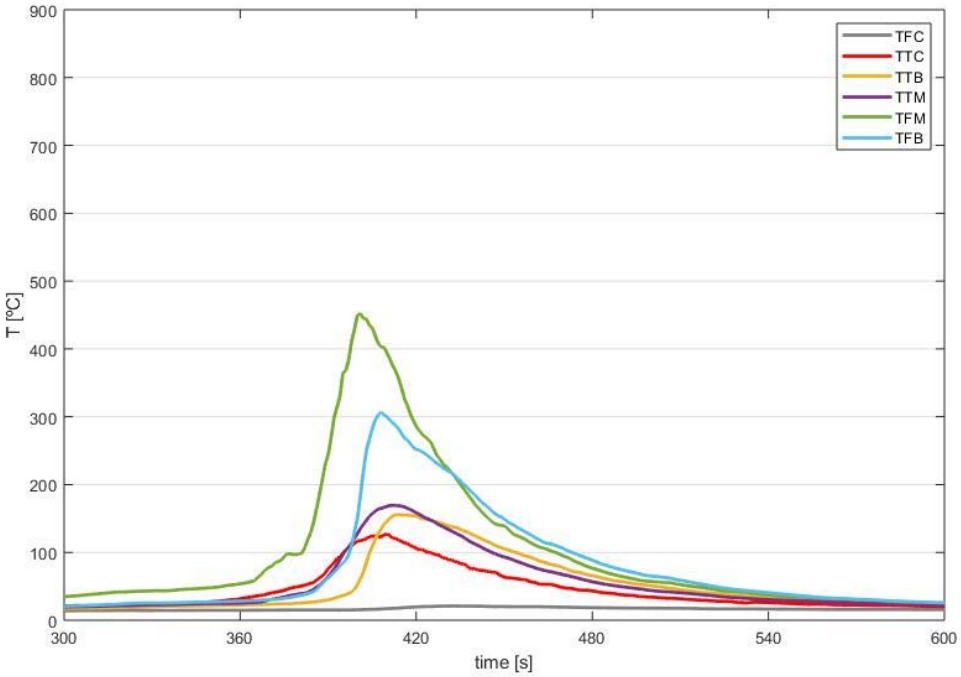

Figure 0.1. Thermocouple temperatures vs time (U=0 m/s)

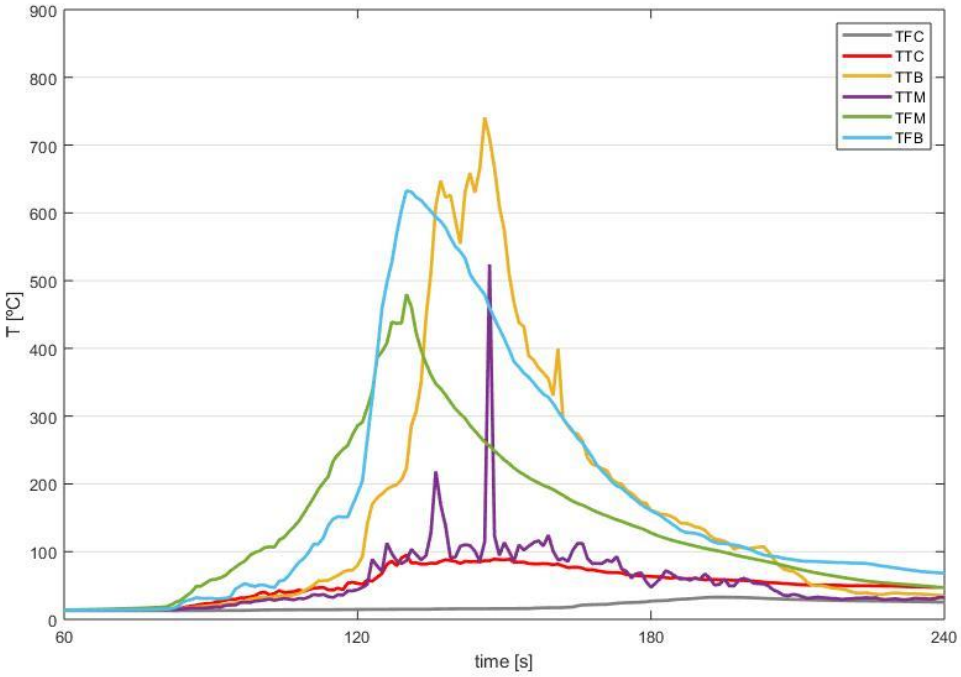

Figure 0.2. Thermocouple temperatures vs time (U=2 m/s)

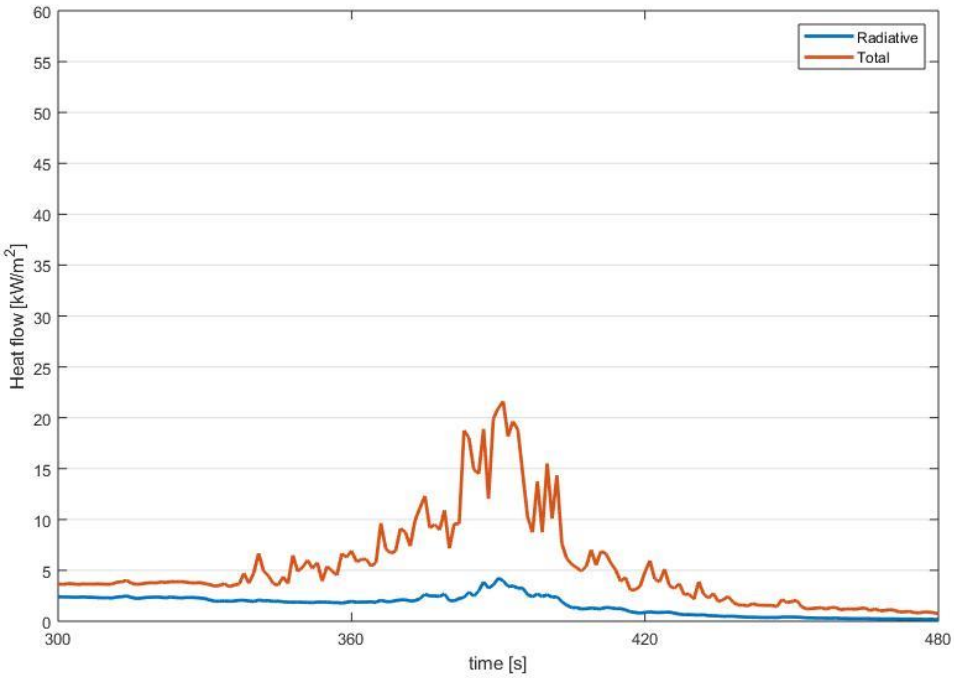

Figure 0.3. Heat flow vs time (U=0 m/s)

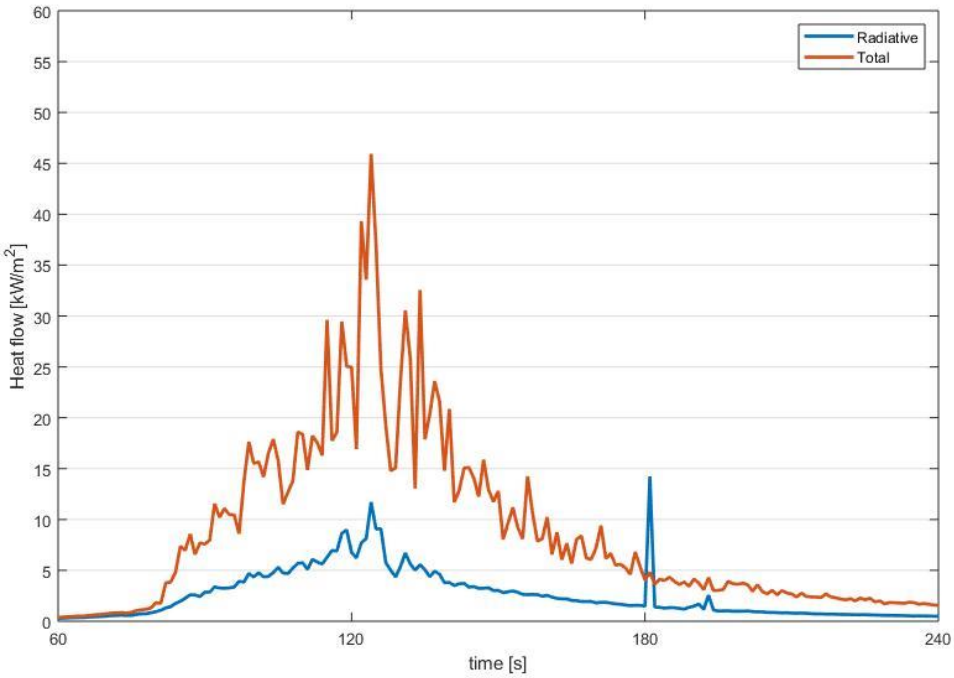

Figure 0.4. Heat flow vs time (U=2 m/s)

Figure 0.5. Tela1 at the end of the tests

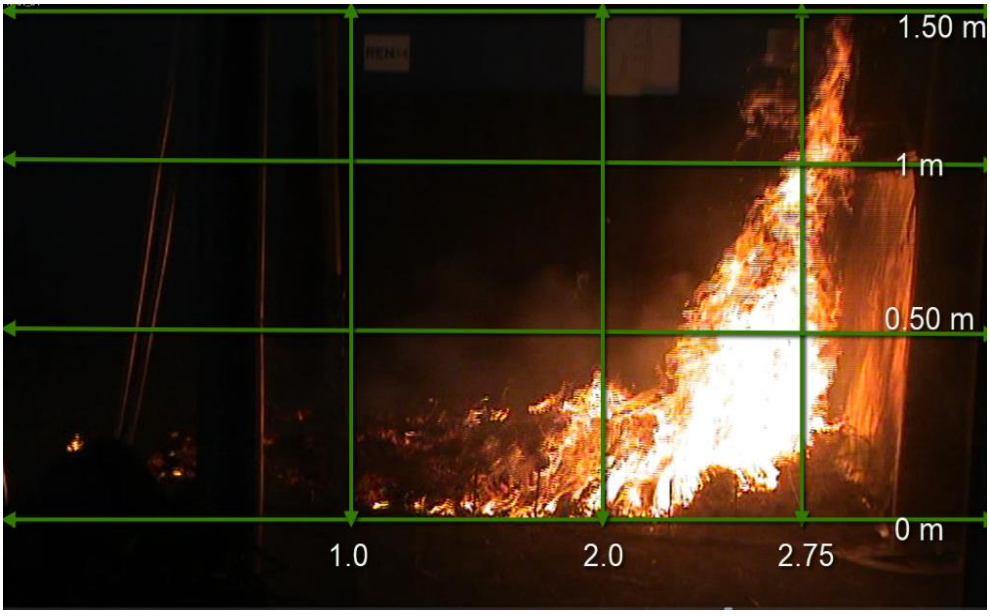

Figure 0.6. Flame height of Tela1 (U=1 m/s)

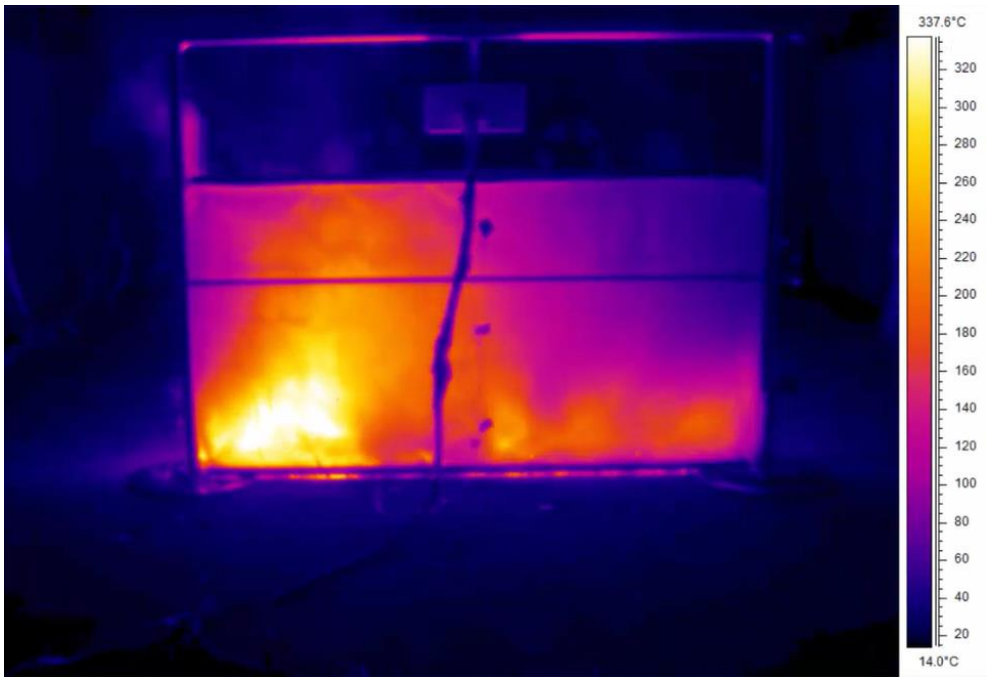

Figure 0.7. Maximum temperature recorded by the IR camera for wind speed U=2 m/s

Table 0.2. Tela2

	Tela2_U0	Tela2_U1	Tela2_U2
Room temperature [ºC]	10.4	14.4	16.3
Relative humidity [%]	52	44	51
Fuel load [kg/m^2]	1	1	1
Fuel bed area [m^2]	5.40	5.40	5.40
Fuel moisture content [%]	15.9	15.9	10.6
Fuel mass [kg]	6.26	6.26	5.98
Average fuel bed height [cm]	12.25	12.25	13.00
Propagation speed [cm/s]	1.0	3.0	6.0
Maximum temperature reached [ºC]	477.4	459.9	394.8
Maximum heat flow reached [kW/m^2]	17.5	37.7	44.4
Fire line intensity [kW/m]	268.3	752.2	1237.8
Average Flame height [m]	0.88	1.28	1.20

Maximum temperature reached at the rear of the barrier- 261.3ºC.

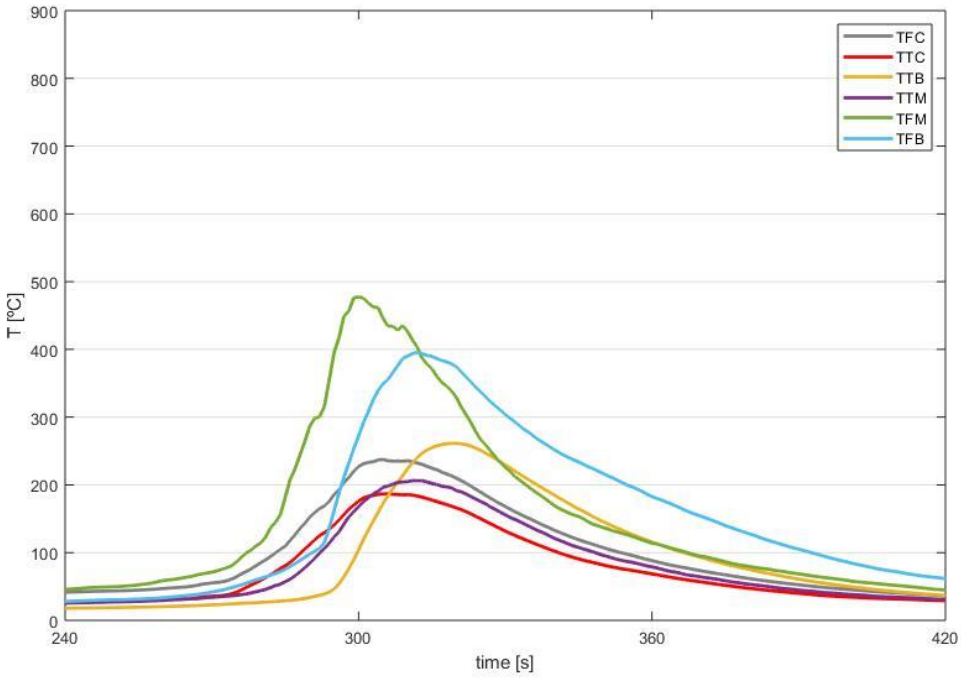

Figure 0.8. Thermocouple temperatures vs time (U=0 m/s)

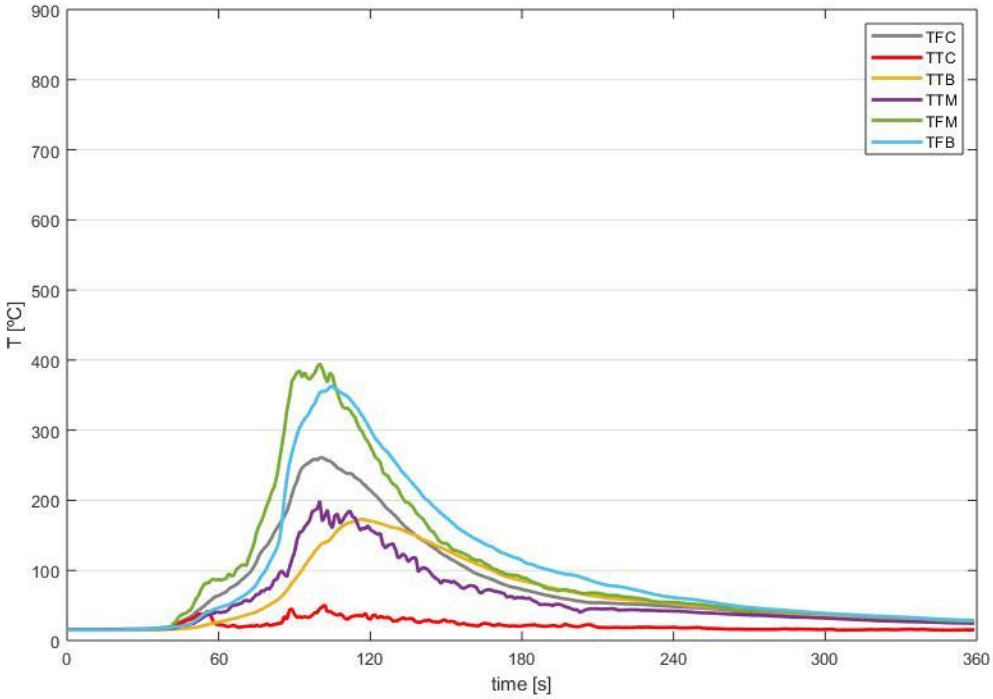

Figure 0.9. Thermocouple temperatures vs time (U=2 m/s)

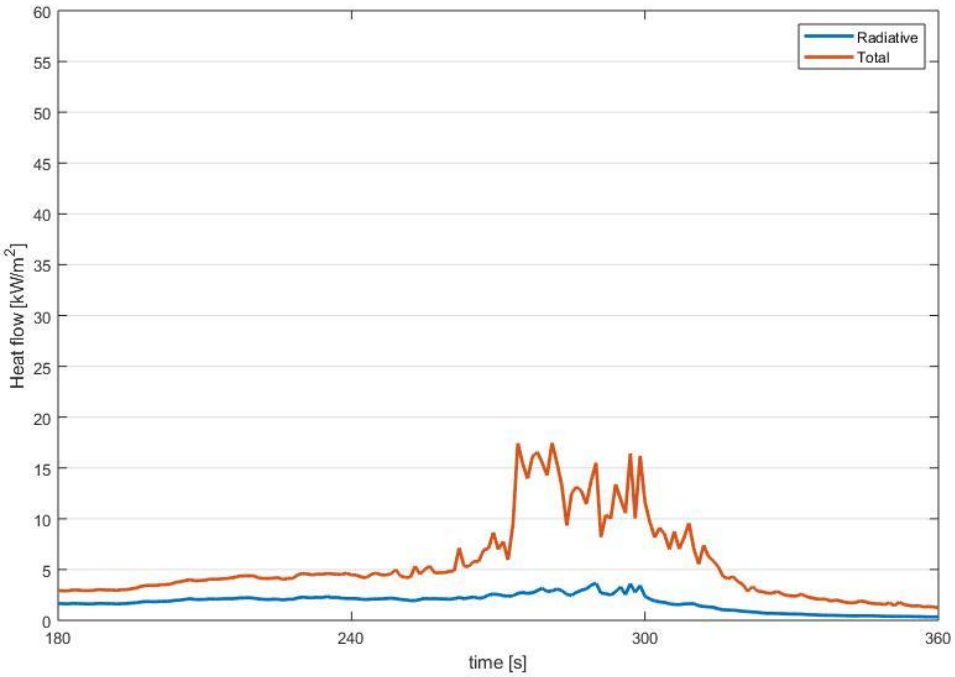

Figure 0.10. Heat flow vs time (U=0 m/s)

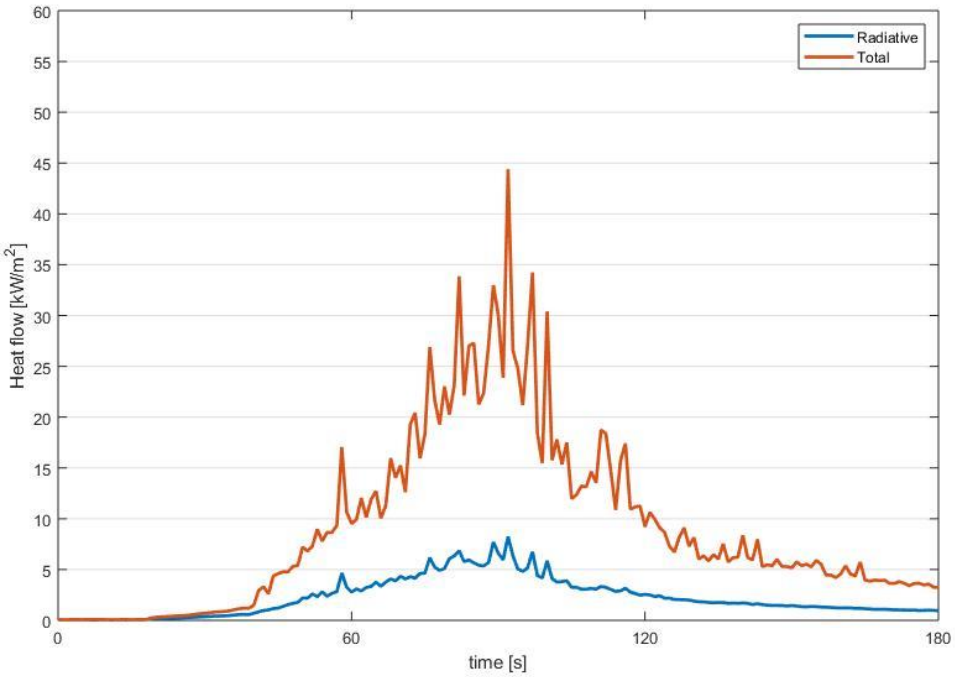

Figure 0.11. Heat flow vs time (U=2 m/s)

Figure 0.12. Tela2 at the end of the tests

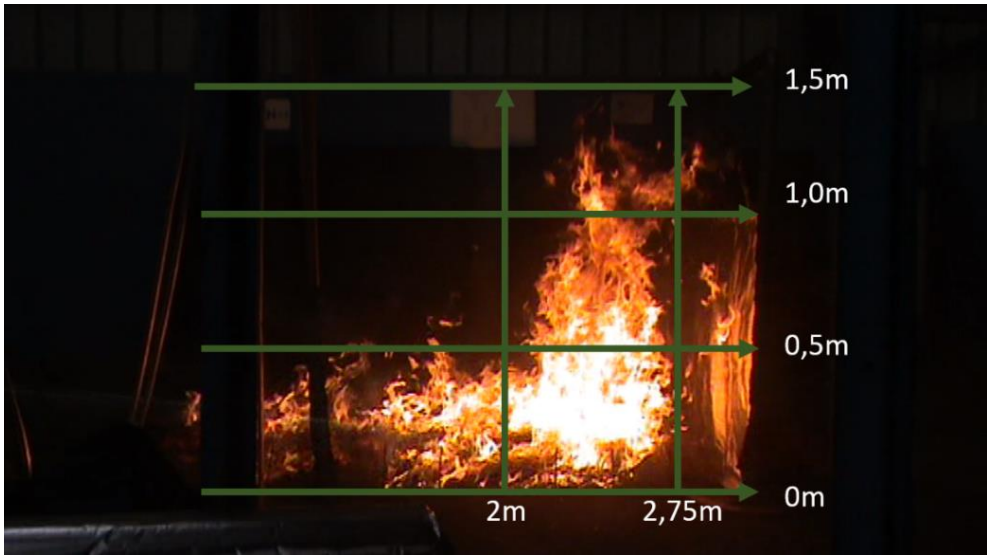

Figure 0.13. Flame height of Tela2 (U=1 m/s)

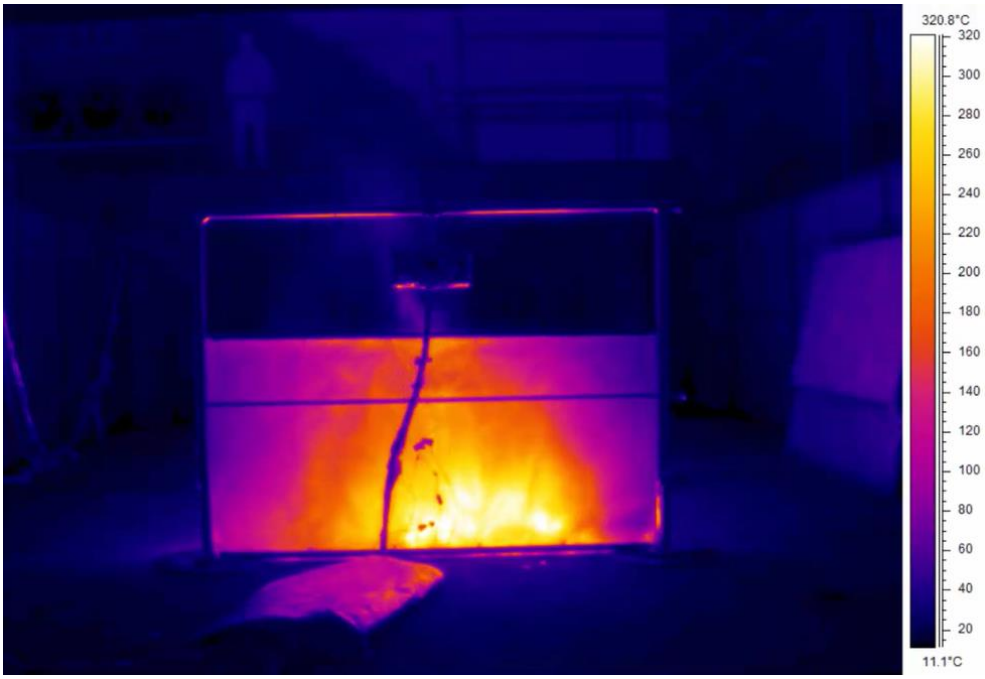

Figure 0.14. Maximum temperature recorded by the IR camera for wind speed U=2 m/s

Table 0.3. Tela3

	Tela3_U0	Tela3_U1	Tela3_U2
Room temperature [ºC]	7	10.4	12.3
Relative humidity [%]	50	50	50
Fuel load [kg/m^2]	1	1	1
Fuel bed area [m^2]	5.40	5.40	5.40
Fuel moisture content [%]	15.9	15.9	15.9
Fuel mass [kg]	6.26	6.26	6.26
Average fuel bed height [cm]	12.75	12.50	12.75
Propagation speed [cm/s]	1.0	3.0	6.0
Maximum temperature reached [ºC]	272.2	580.2	627.4
Maximum heat flow reached [kW/m^2]	26.3	38.7	49.6
Fire line intensity [kW/m]	312.0	678.4	1372.7
Average Flame height [m]	0.88	1.30	1.20

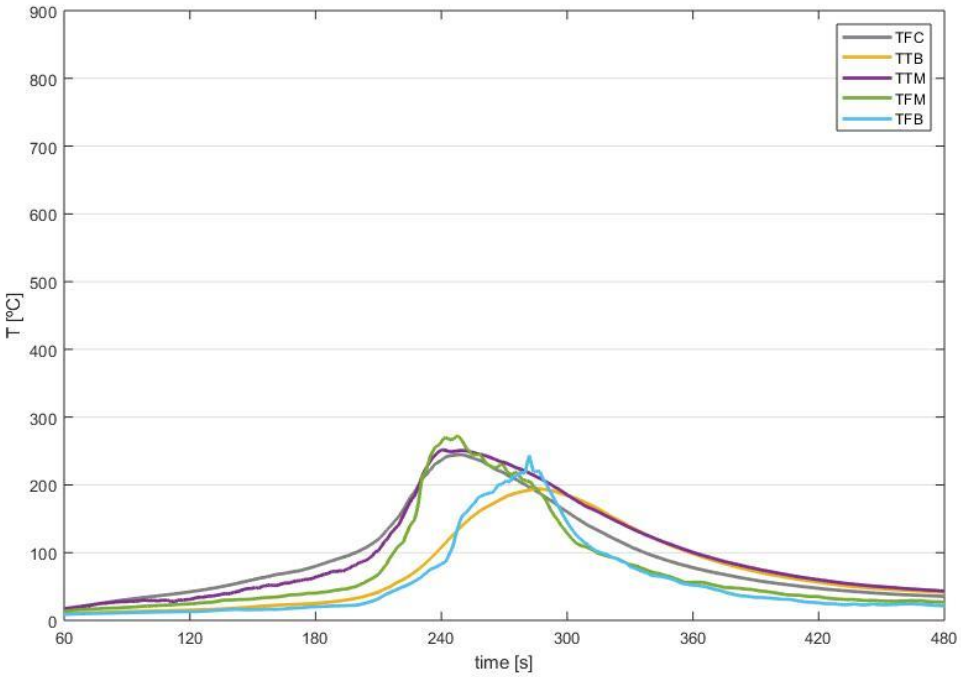

Figure 0.15. Thermocouple temperatures vs time (U=0 m/s)

Maximum temperature reached at the rear of the barrier- 395.4ºC.

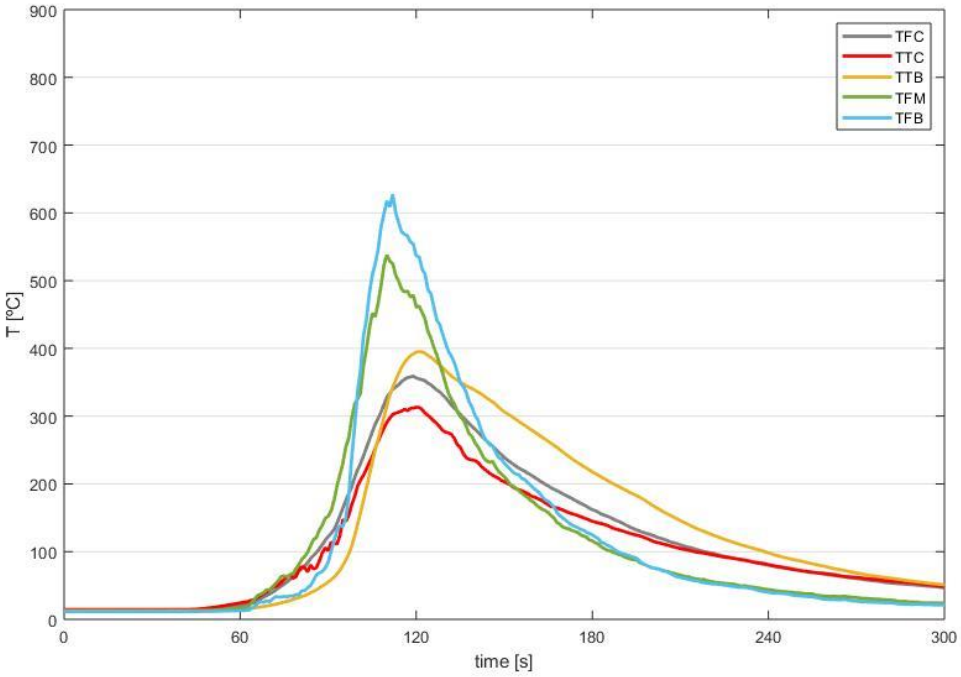

Figure 0.16. Thermocouple temperatures vs time (U=2 m/s)

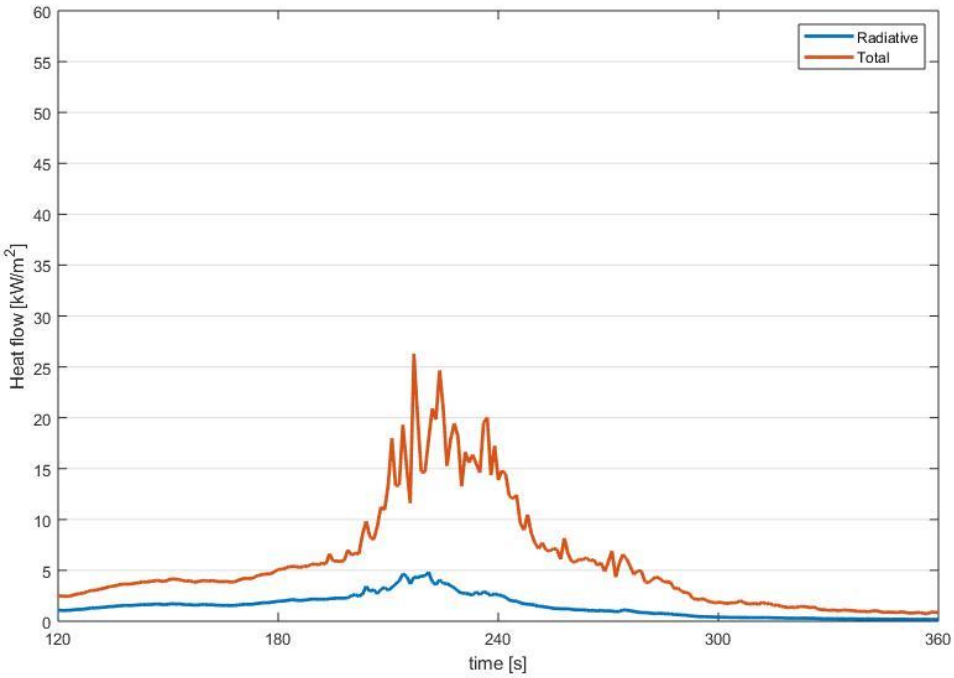

Figure 0.17. Heat flow vs time (U=0 m/s)

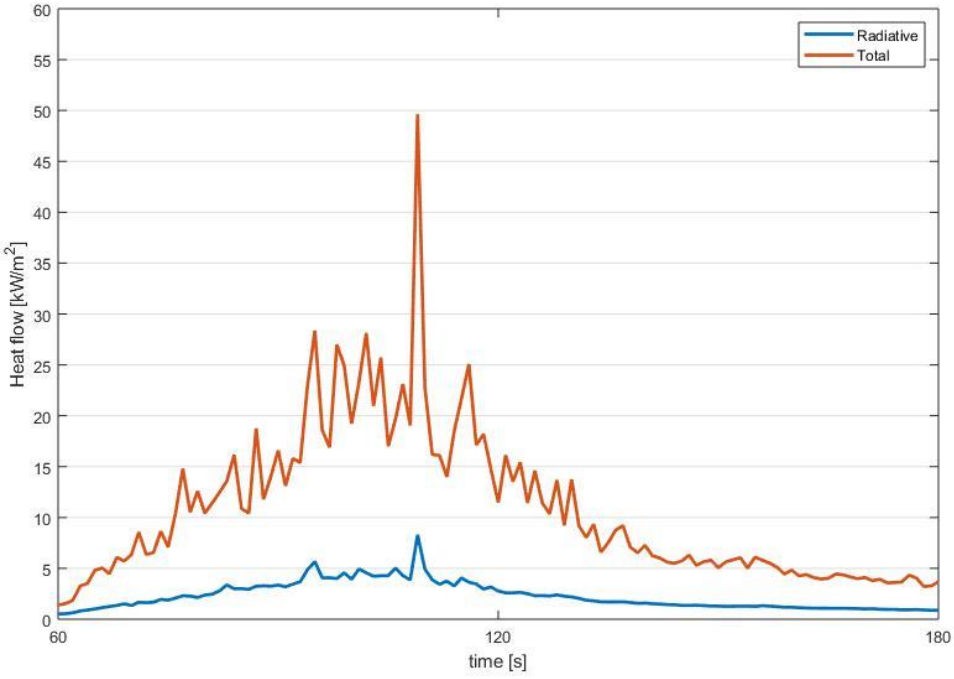

Figure 0.18. Heat flow vs time (U=2 m/s)

Figure 0.19. Tela3 at the end of the tests

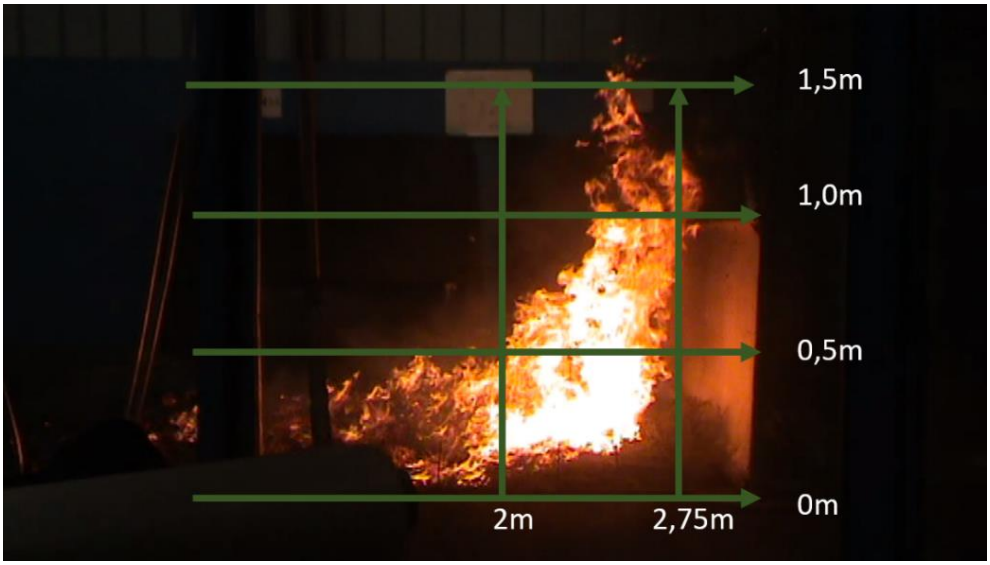

Figure 0.20. Flame height of Tela3 (U=1 m/s)

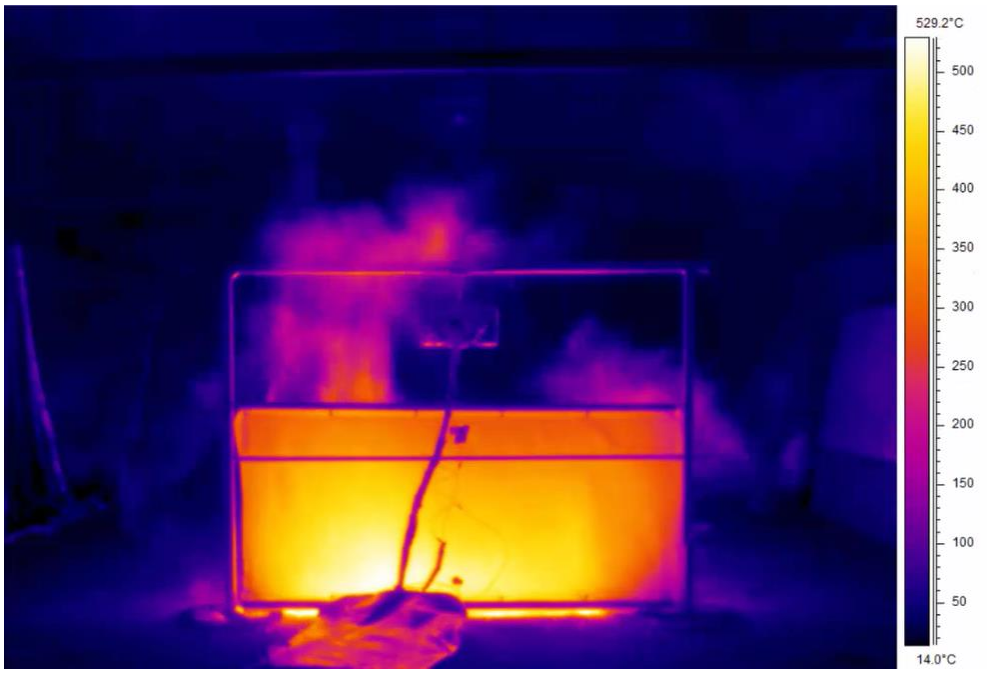

Figure 0.21. Maximum temperature recorded by the IR camera for wind speed U=2 m/s

Table 0.4. Tela4

	Tela4_U0	Tela4_U1	Tela4_U2
Room temperature [ºC]	13.6	21.2	20.2
Relative humidity [%]	60	62	60
Fuel load [kg/m^2]	1	1	1
Fuel bed area [m^2]	5.40	5.40	5.40
Fuel moisture content [%]	12.30	12.30	12.30
Fuel mass [kg]	6.16	6.16	6.16
Average fuel bed height [cm]	12.75	13.5	14
Propagation speed [cm/s]	1.0	4.0	7.0
Maximum temperature reached [ºC]	572.2	404.8	565.5
Maximum heat flow reached [kW/m^2]	38.8	44.7	56.3
Fire line intensity [kW/m]	263.1	902.0	1607.0
Average Flame height [m]	0.95	1.28	1.23

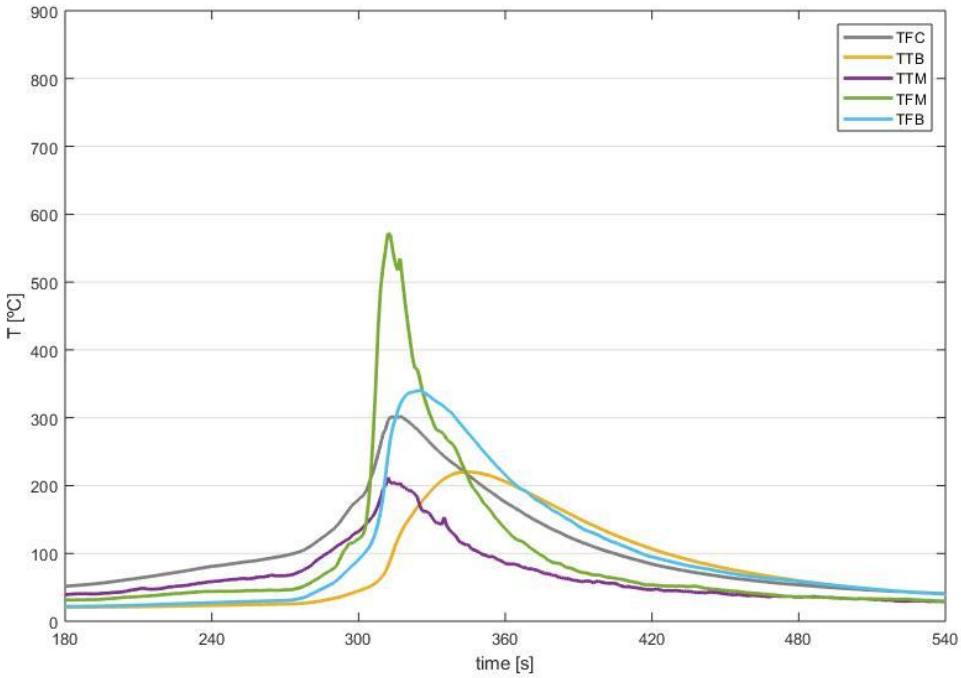

Figure 0.22. Thermocouple temperatures vs time (U=0 m/s)

Maximum temperature reached at the rear of the barrier- 308.0ºC.

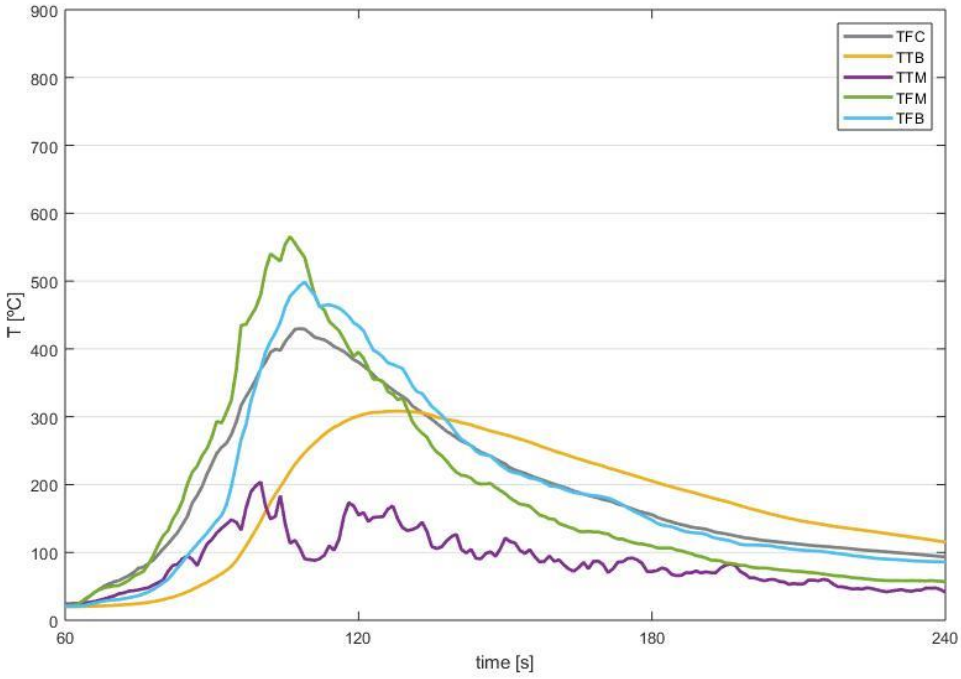

Figure 0.23. Thermocouple temperatures vs time (U=2 m/s)

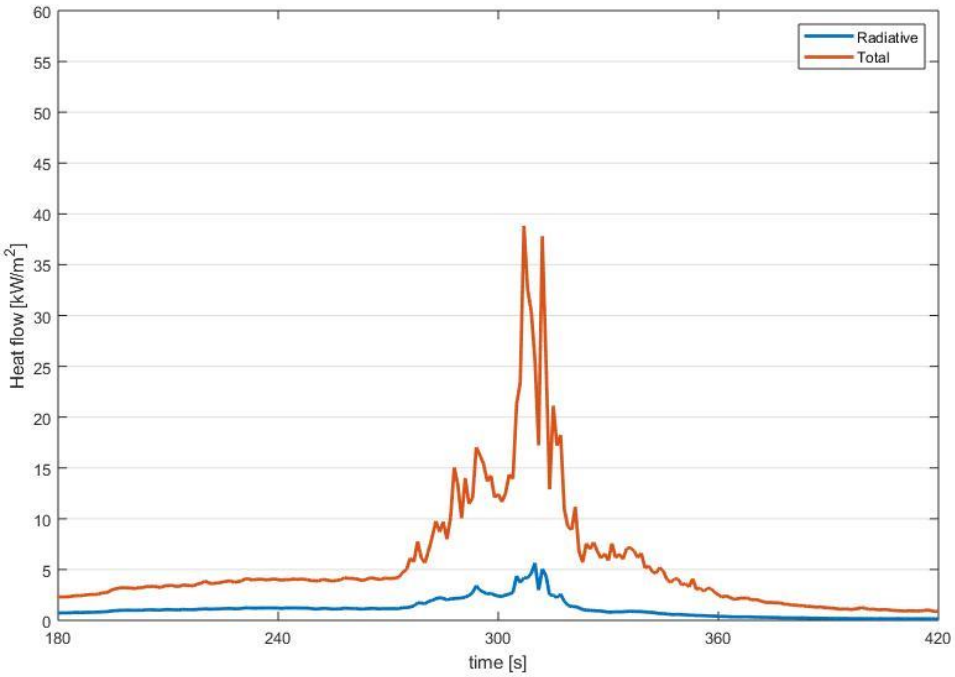

Figure 0.24. Heat flow vs time (U=0 m/s)

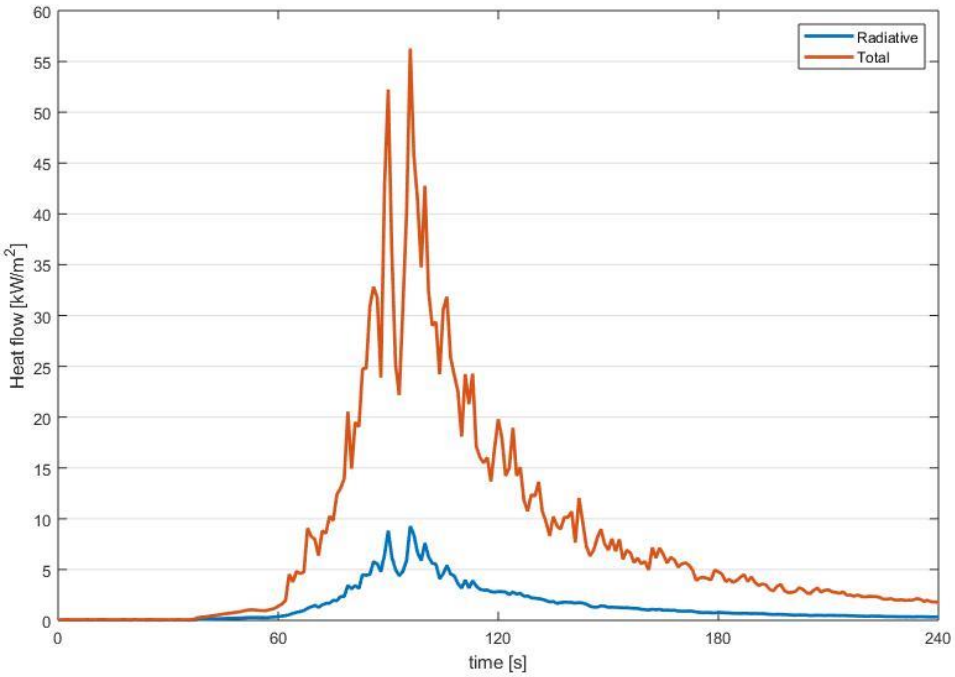

Figure 0.25. Heat flow vs time (U=2 m/s)

Figure 0.26. Tela4 at the end of the tests

Figure 0.27. Flame height of Tela4 (U=1 m/s)

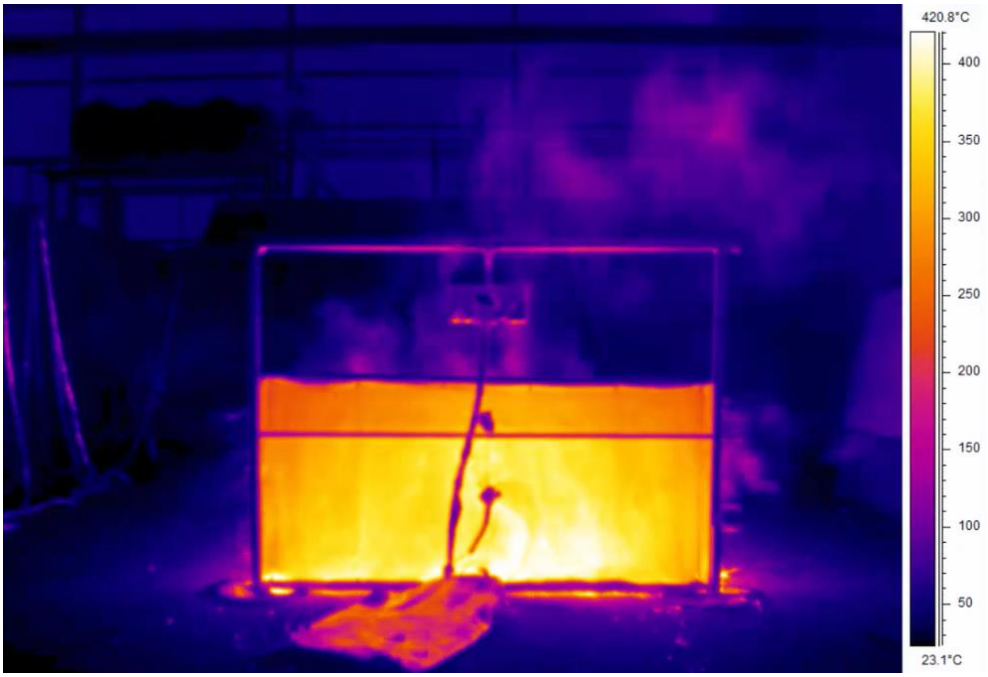

Figure 0.28. Maximum temperature recorded by the IR camera for wind speed (U=2 m/s)

Table 0.5. Tela5

	Tela5_U0	Tela5_U1	Tela5_U2
Room temperature [ºC]	18.0	18.0	19.9
Relative humidity [%]	55	55	45
Fuel load [kg/m^2]	1	1	1
Fuel bed area [m^2]	5.40	5.40	5.40
Fuel moisture content [%]	16.41	16.41	16.41
Fuel mass [kg]	6.29	6.29	6.29
Average fuel bed height [cm]	16.5	17.8	15.5
Propagation speed [cm/s]	1.41	3.24	6.42
Maximum temperature reached [ºC]	594.7	400.2	478.00
Maximum heat flow reached [kW/m^2]	44.6	46.8	42.9
Fire line intensity [kW/m]	317.8	729.8	1445.2
Average Flame height [m]	0.85	1.15	0.95

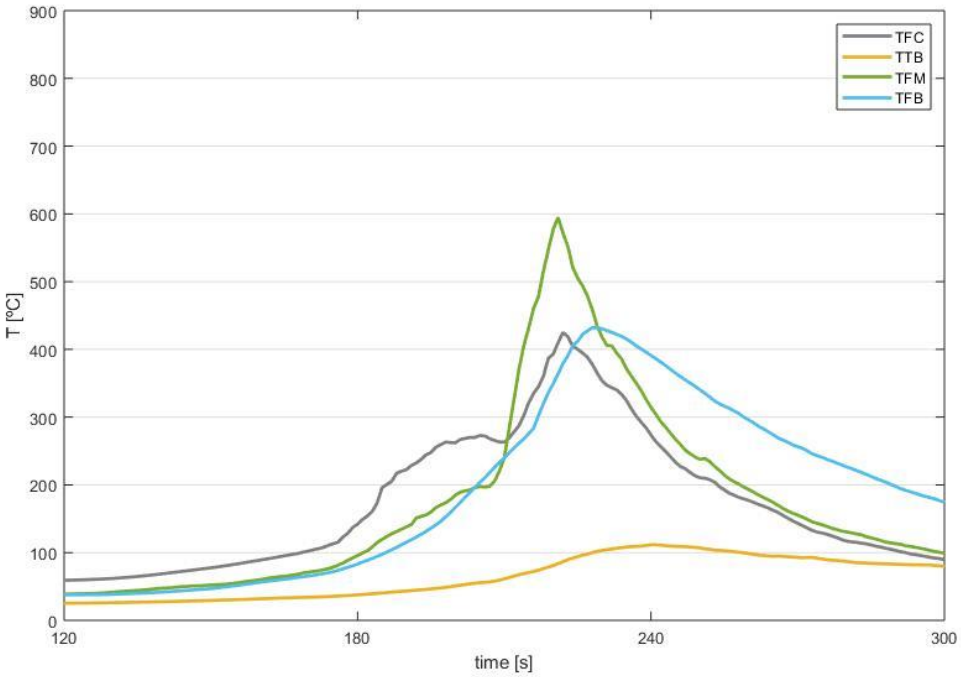

Figure 0.29. Thermocouple temperatures vs time (U=0 m/s)

Maximum temperature reached at the rear of the barrier- 329.6ºC.

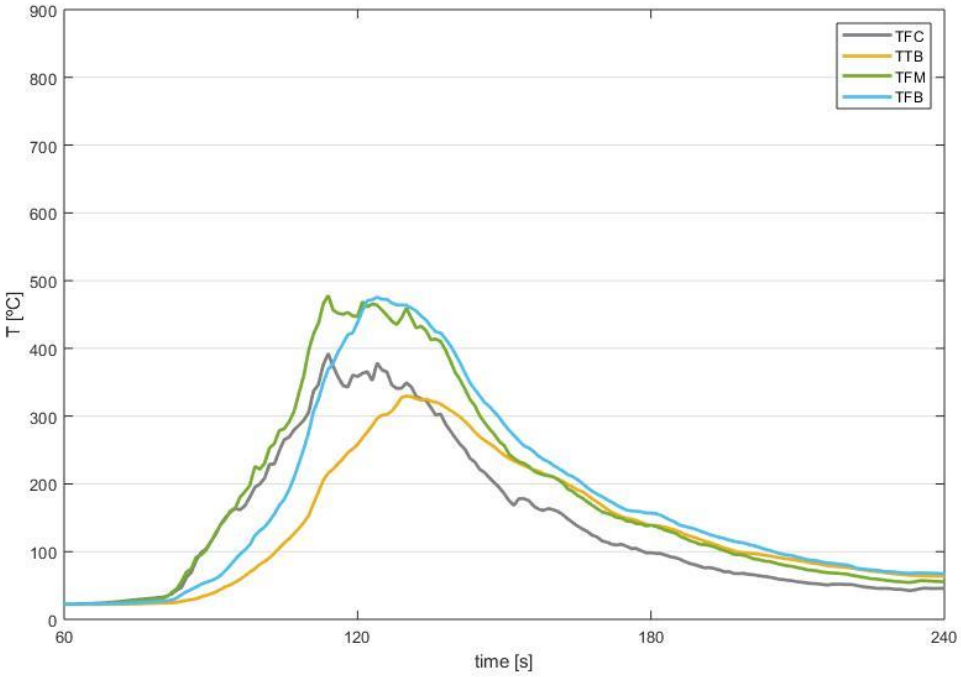

Figure 0.30. Thermocouple temperatures vs time (U=2 m/s)

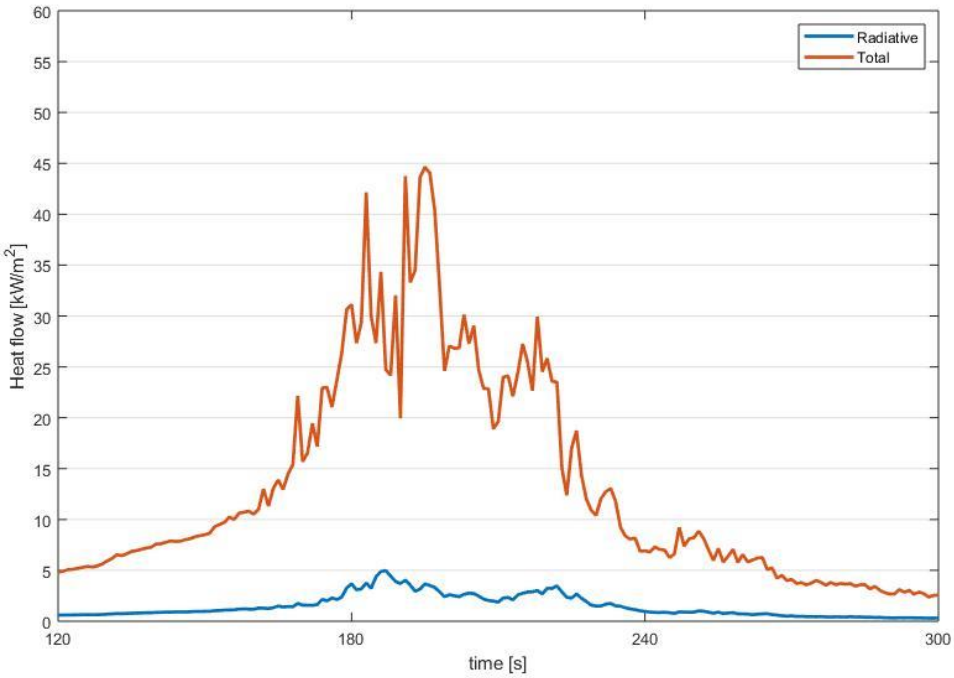

Figure 0.31. Heat flow vs time (U=0 m/s)

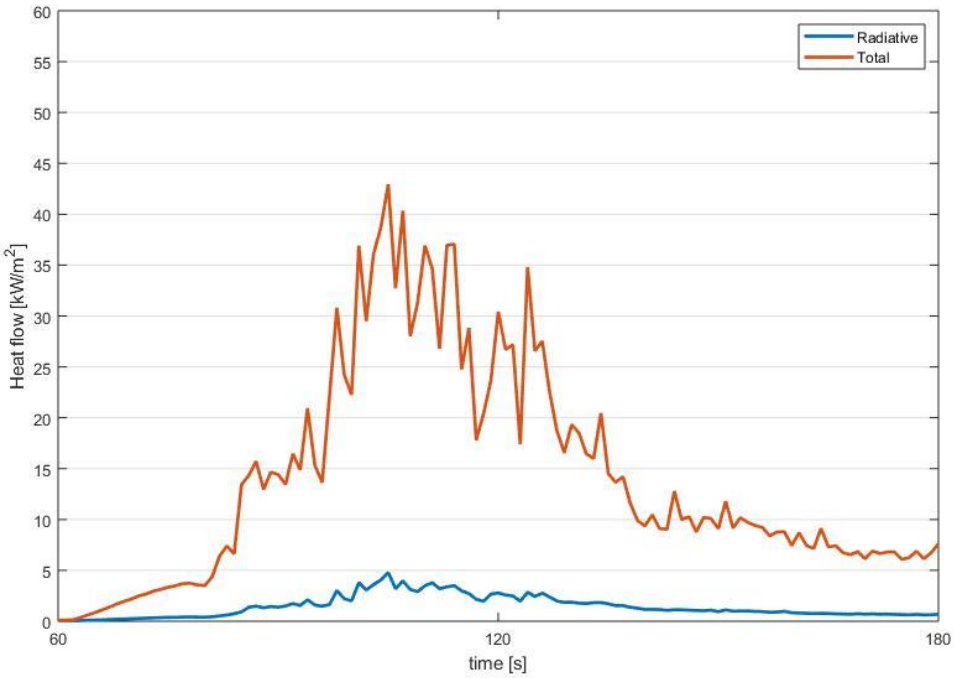

Figure 0.32. Heat flow vs time (U=2 m/s)

Figure 0.33. Tela5 at the end of the tests

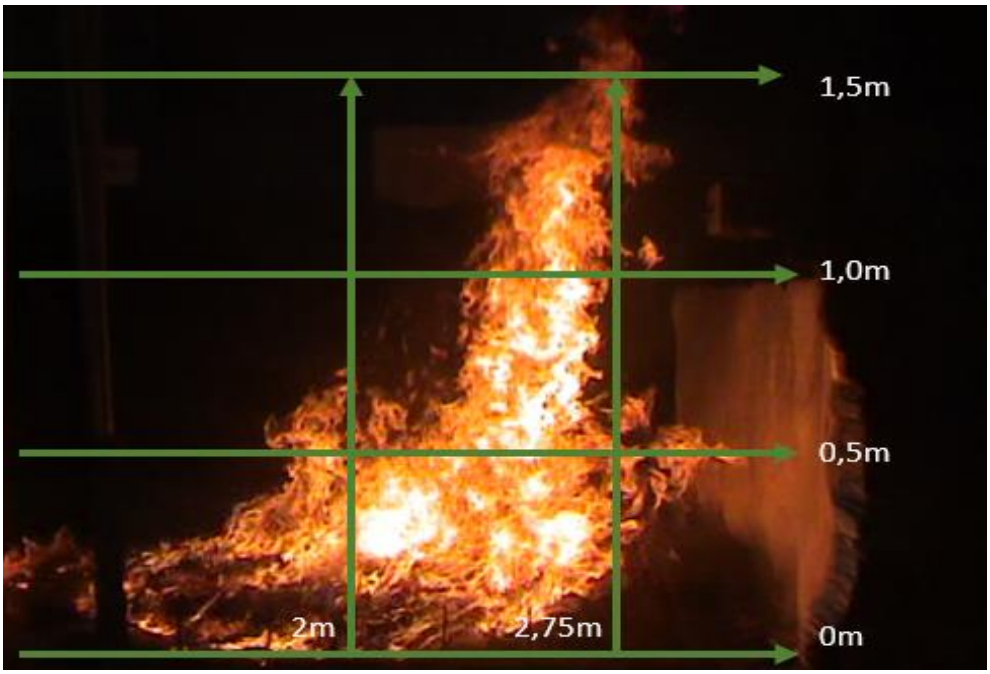

Figure 0.34. Flame height of Tela5 (U=1 m/s)

2nd Phase's Results

Tela2d_U3_2.5

Maximum temperature reached at the rear of the barrier- 383.1ºC

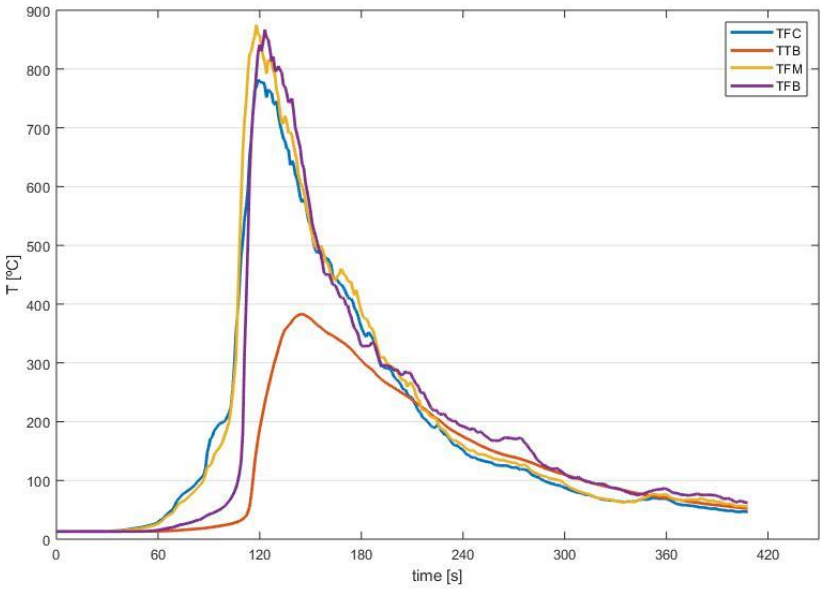

Figure 0.35. Thermocouple temperatures vs time (U=3 m/s; Fuel mass=2.5 kg/m²)

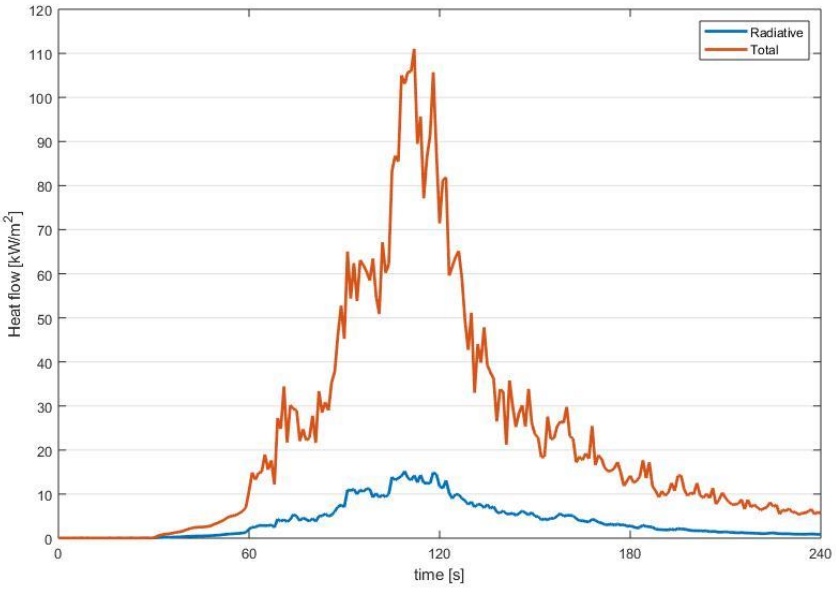

Figure 0.36. Heat flow vs time (U=3m/s; Fuel mass=2.5 kg/m²)

Figure 0.37. Flame height of Tela2 (wind speed, 3m/s; Fuel mass, 2.5 kg/m^2)

Figure 0.38. Tela2 at the end of the tests (wind speed, 3m/s; Fuel mass, 2.5 kg/m^2)

Tela2d_U3_3.5

Maximum temperature reached at the rear of the barrier- 490.6ºC

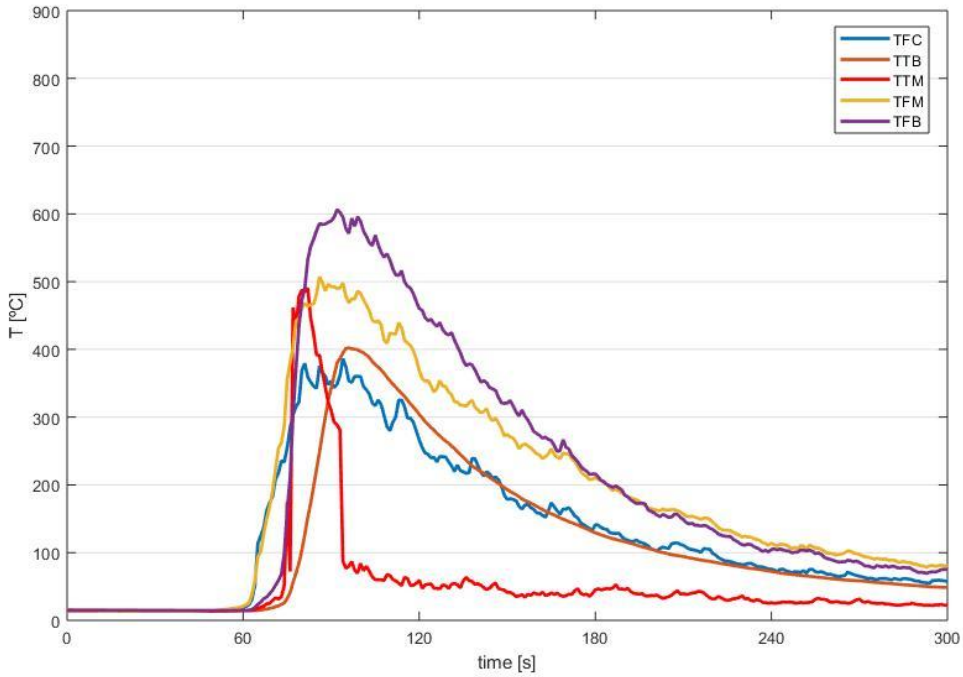

Figure 0.39. Thermocouple temperatures vs time (U=3 m/s; Fuel mass=3.5 kg/m²)

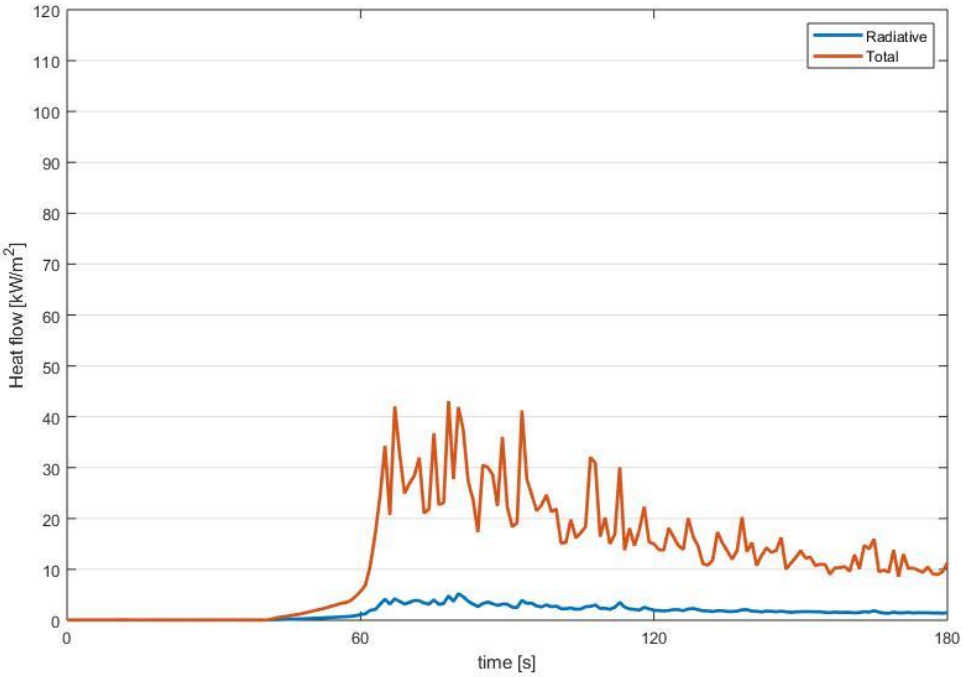

Figure 0.40. Heat flow vs time (U=3m/s; Fuel mass=3.5 kg/m²)

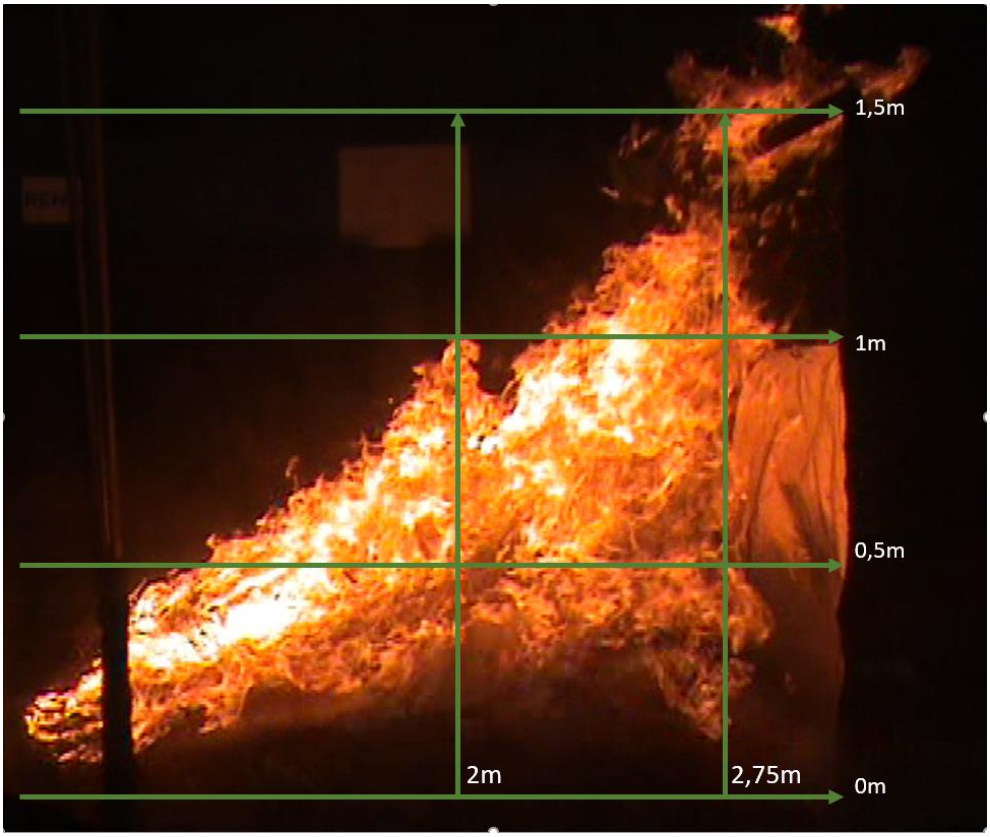

Figure 0.41. Flame height of Tela2 (wind speed, 3m/s; Fuel mass, 3.5 kg/m^2)

Figure 0.42. Tela2 at the end of the tests (wind speed, 3m/s; Fuel mass, 3.5 kg/m^2)

Tela2d_U1_3.5

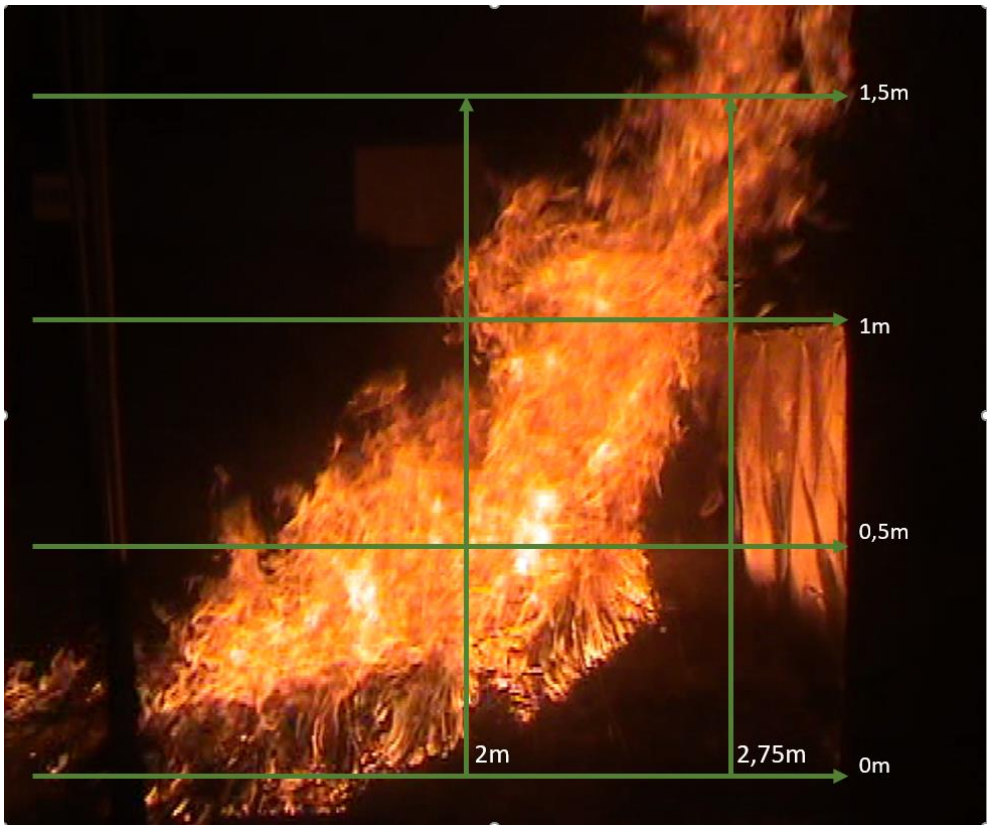

Figure 0.43. Flame height of Tela2 (wind speed, 1m/s; Fuel mass, 3.5 kg/m^2)

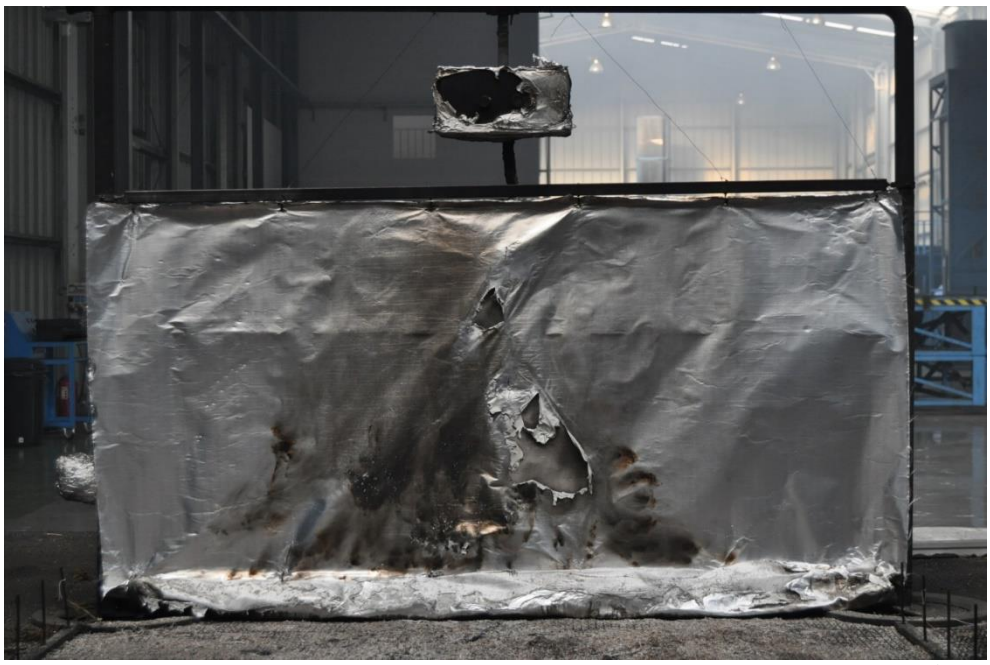

Figure 0.44. Tela2 at the end of the tests (wind speed, 1m/s; Fuel mass, 3.5 kg/m^2)

3rd Phase's Results (1st stage)

Tela2 (TVL-126)

Table 0.6. Times at the time of the rupture of the fabrics

Tela2	Time [1st test] [s]	Time [2nd test] [s]	Time [3rd test] [s]	Time [4th test] [s]	Time [5th test] [s]
Distance [10cm]	9.89	62.90	12.09	9.70	7.80
Distance [12.5cm]	14.50	95.02	18.09	32.19	17.80

Table 0.7. Temperatures at the time of the rupture of the fabrics

Tela2	Temperature [1st test] [°C]	Temperature [2nd test] [°C]	Temperature [3rd test] [°C]	Temperature [4th test] [°C]	Temperature [5th test] [°C]
Distance [10cm]	937.3	930.3	902.4	934.3	934.9
Distance [12.5cm]	933.5	837.1	898.2	883.9	888.6

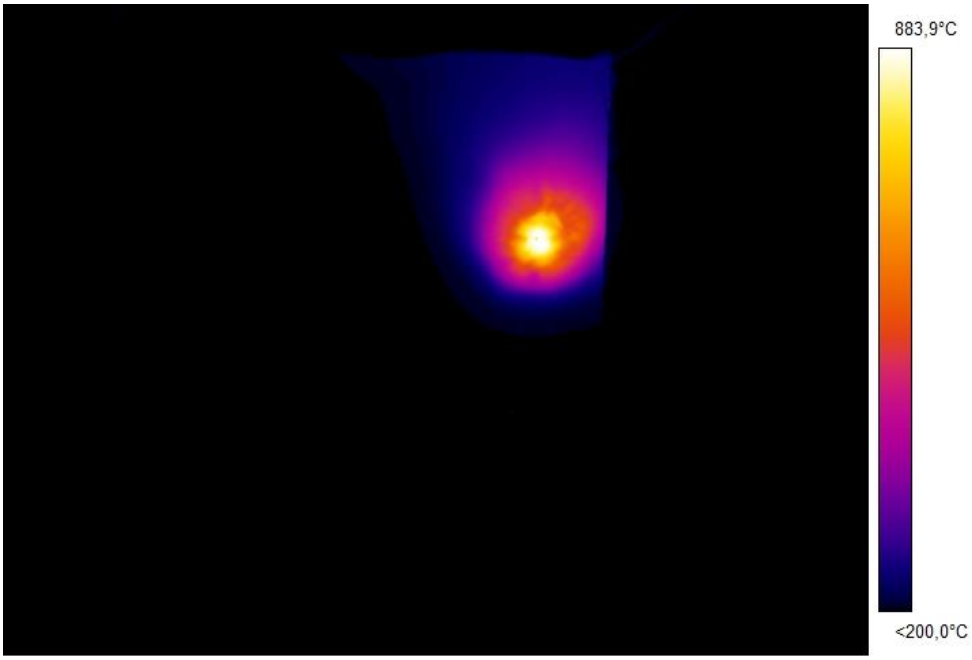

Figure 0.45. Tela2 (TVL-126) ; 4th test ; D=12.5cm

Tela4 (Liztherm 500)

Table 0.8. Times at the time of the rupture of the fabrics

Tela4	Time [1st test] [s]	Time [2nd test] [s]	Time [3rd test] [s]	Time [4th test] [s]	Time [5th test] [s]
Distance [10cm]	7.71	7.40	8.03	9.19	7.43
Distance [12.5cm]	11.53	8.3	10.07	11.80	13.73

Table 0.9. Temperatures at the time of the rupture of the fabrics

Tela4	Temperature [1st test] [°C]	Temperature [2nd test] [°C]	Temperature [3rd test] [°C]	Temperature [4th test] [°C]	Temperature [5th test] [°C]
Distance [10cm]	914.4	921.6	921.5	924.6	934.4
Distance [12.5cm]	878.5	893.3	897.6	889.8	884.3

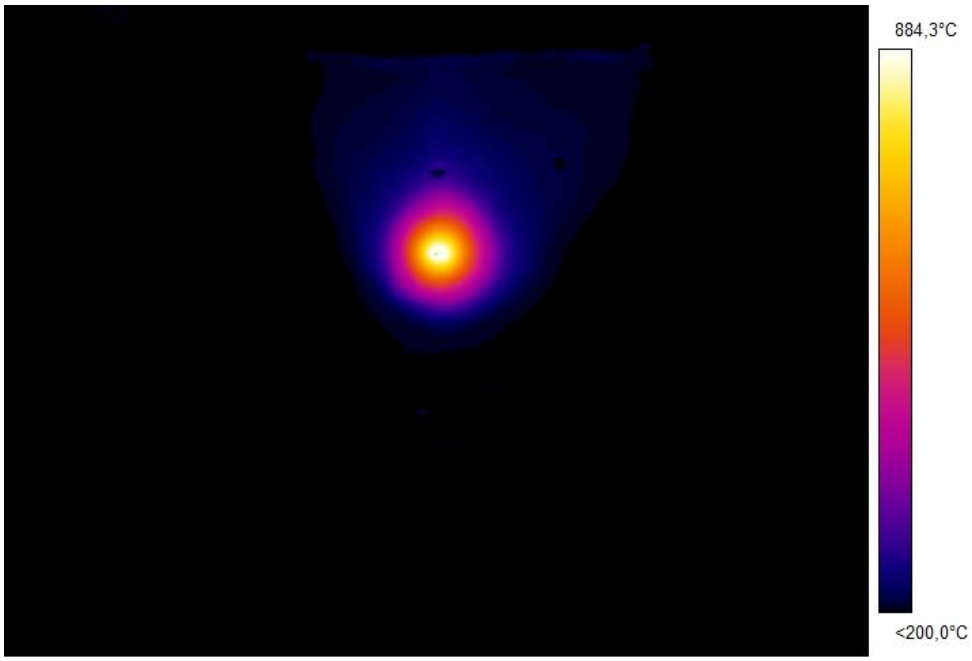

Figure 0.46. Tela4 (Liztherm 500) ; 5th test ; D=12.5cm

Tela5 (Type E)

Table 0.10. Times at the time of the rupture of the fabrics

Tela5	Time [1st test] [s]	Time [2nd test] [s]	Time [3rd test] [s]	Time [4th test] [s]	Time [5th test] [s]
Distance [10cm]	2.52	2.48	2.10	2.82	2.42
Distance [12.5cm]	2.80	3.18	3.78	3.05	3.24

Table 0.11. Temperatures at the time of the rupture of the fabrics

Tela5	Temperature [1st test] [°C]	Temperature [2nd test] [°C]	Temperature [3rd test] [°C]	Temperature [4th test] [°C]	Temperature [5th test] [°C]
Distance [10cm]	940.6	942.5	916.0	914.1	929.9
Distance [12.5cm]	884.2	896.2	908.6	917.2	906.3

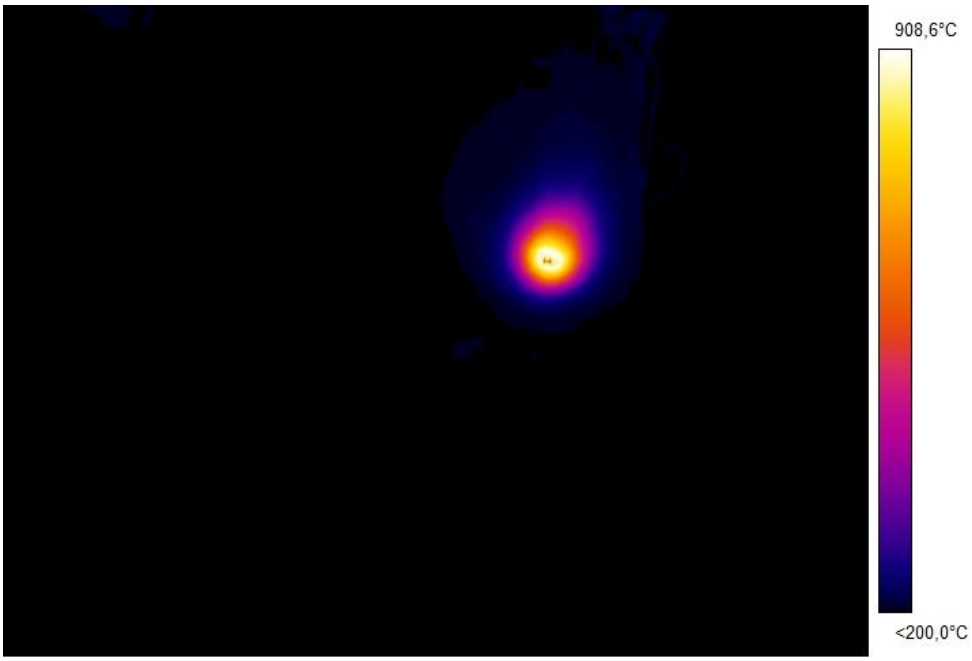

Figure 0.47. Tela5 (Type E) ; 3rd test ; D=12.5cm

3rd Phase's Results (2nd stage)

Tela2 (TVL-126)

Table 0.12. Times at the time of the rupture of the fabrics

Tela2	Time [1st test] [s]	Time [2nd test] [s]	Time [3rd test] [s]	Time [4th test] [s]	Time [5th test] [s]
Distance [10cm]	120.89	120.05	124.40	121.80	44.23

Table 0.13. Average time at the time of the rupture of the fabrics

Tela2	Average times [s]
Distance [10cm]	84.32

Table 0.14. Temperatures at the time of the rupture of the fabrics

Tela2	Temperature [1st test] [°C]	Temperature [2nd test] [°C]	Temperature [3rd test] [°C]	Temperature [4th test] [°C]	Temperature [5th test] [°C]
Distance [10cm]	690.9	434.2	862.7	802.3	904.0

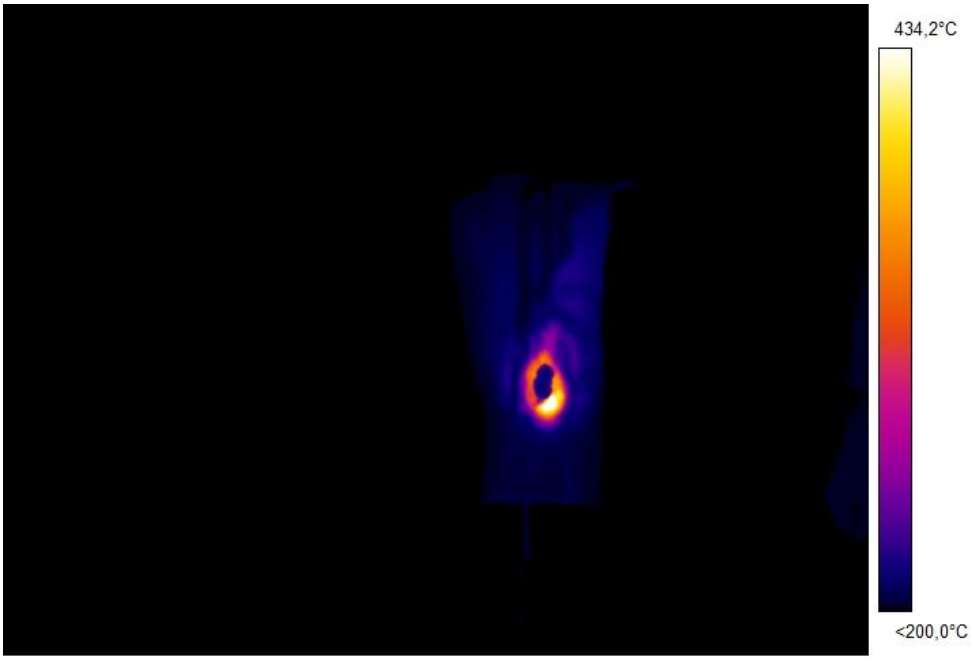

Figure 0.48. Tela2 (TVL-126) ; 2nd test ; D=10cm

Table 0.15. Average temperature at the time of the rupture of the fabrics

Tela2	Average temperatures [°C]
Distance [10cm]	738.8

The following calculated flow rates were obtained taking into account a water density of 0.9991 kg/l for an average water temperature of 15°C.

Table 0.16. Water flows at the time of the rupture of the fabrics

Tela2	Water flow [1st test]	Water flow [2nd test]	Water flow [3rd test]	Water flow [4th test]	Water flow [5th test]
Distance [10cm]	1.91 l	0.25 l	0.41 l	0.71 l	0.035 l
Distance [10cm]	0.96 l/min	0.125 l/min	0.21 l/min	0.36 l/min	0.048 l/min

Table 0.17. Average water flows at the time of the rupture of the fabrics

Tela2	Average water flows
Distance [10cm]	0.66 l
Distance [10cm]	0.34 l/min

However, this fabric ruptured twice, for the third and fifth tests, in which the respective times and water flows were already reported. Thus, it is not correct to calculate the water flows considering these tests. Thus in **Erro! A origem da referência não foi encontrada.** the average flow rates of water required for non-disruption of the fabrics were recalculated.

Table 0.18. Average water flows at the time of the rupture of the fabrics (recalculated)

Tela2	Average water flows
Distance [10cm]	0.96 l
Distance [10cm]	0.48 l/min

Tela4 (Liztherm 500)

Table 0. 19. Times at the time of the rupture of the fabrics

Tela4	Time [1st test] [s]	Time [2nd test] [s]	Time [3rd test] [s]	Time [4th test] [s]	Time [5th test] [s]
Distance [10cm]	90.88	36.86	90.00	90.00	92.70

Table 0. 20. Average time at the time of the rupture of the fabrics

Tela4	Average times [s]
Distance [10cm]	36.86

Table 0. 21. Temperatures at the time of the rupture of the fabrics

Tela4	Temperature [1st test] [°C]	Temperature [2nd test] [°C]	Temperature [3rd test] [°C]	Temperature [4th test] [°C]	Temperature [5th test] [°C]
Distance [10cm]	< 200	856.7	483.2	243.5	< 200

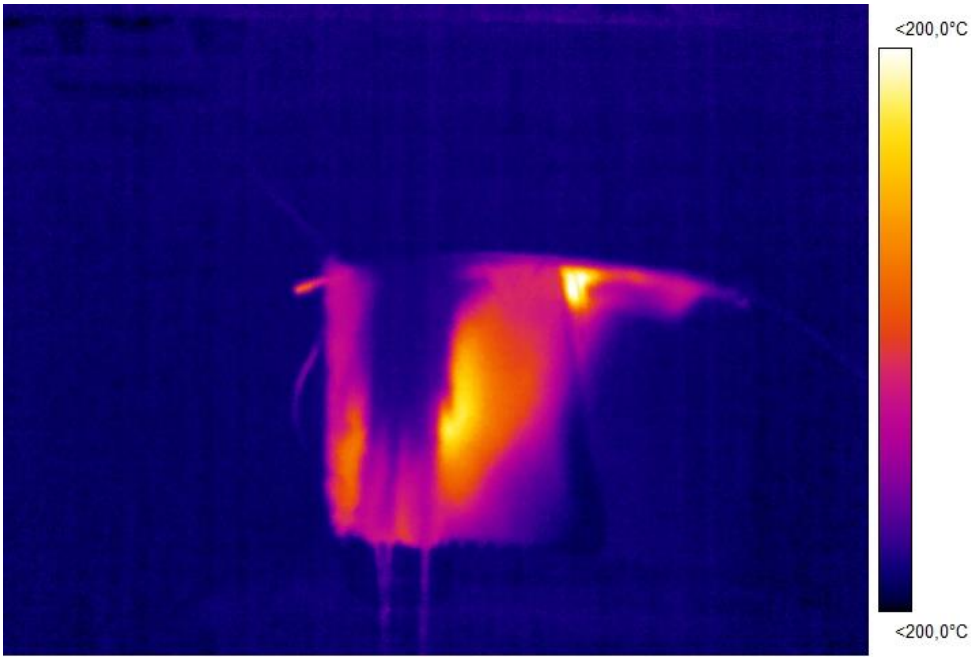

Figure 0.49. Tela4 (Liztherm 500) ; 1st test ; D=10cm

Table 0. 22. Average temperature at the time of the rupture of the fabrics

Tela4	Average temperatures [°C]
Distance [10cm]	527.8

Table 0. 23. Water flows at the time of the rupture of the fabrics

Tela4	Water flow [1st test]	Water flow [2nd test]	Water flow [3rd test]	Water flow [4th test]	Water flow [5th test]
Distance [10cm]	0.81 l	0.0062 l	0.15 l	0.41 l	0.19 l
Distance [10cm]	0.54 l/min	0.01 l/min	0.1 l/min	0.27 l/min	0.13 l/min

Table 0. 24. Average water flows at the time of the rupture of the fabrics

Tela4	Average water flows
Distance [10cm]	0.31 l
Distance [10cm]	0.21 l/min

However, this fabric ruptured once, for the second test, in which the respective time and water flow were already reported. Thus, it is not correct to calculate the water flows considering this test. Thus in Table 0. 25 the average flow rates of water required for non-disruption of the fabrics were recalculated.

Table 0. 25. Average water flows at the time of the rupture of the fabrics (recalculated)

Tela4	Average water flows
Distance [10cm]	0.39 l
Distance [10cm]	0.26 l/min

Tela5 (Type E)

For there to be more than one satisfactory result in order to draw conclusions for this fabric, it was necessary to perform one more test than for the others.

Table 0. 26. Times at the time of the rupture of the fabrics

Tela5	Time [1st test] [s]	Time [2nd test] [s]	Time [3rd test] [s]	Time [4th test] [s]	Time [5th test] [s]	Time [6th test] [s]
Distance [10cm]	37.03	19.80	6.67	97.68	64.93	98.02

Table 0. 27. Average time at the time of the rupture of the fabrics

Tela5	Average times [s]
Distance [10cm]	35.56

Table 0. 28. Temperatures at the time of the rupture of the fabrics

Tela5	Temperature [1st test] [°C]	Temperature [2nd test] [°C]	Temperature [3rd test] [°C]	Temperature [4th test] [°C]	Temperature [5th test] [°C]	Temperature [6th test] [°C]
Distance [10cm]	831.2	839.8	877.5	727.0	832.9	669.4

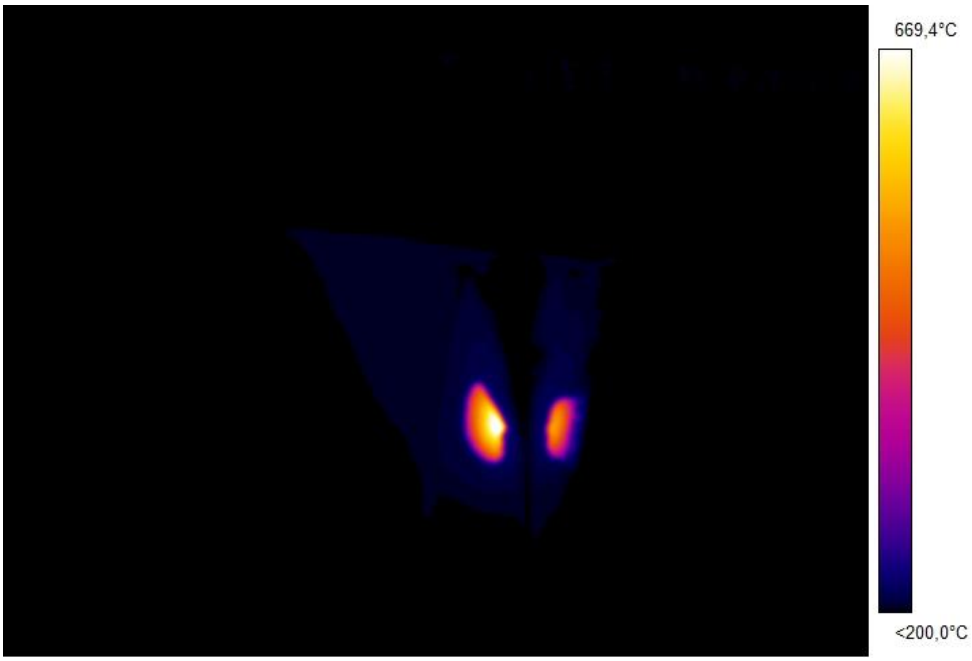

Figure 0.50. Tela5 (Type E) ; 6th test ; D=10cm

Table 0. 29. Average temperature at the time of the rupture of the fabrics

Tela5	Average temperatures [°C]
Distance [10cm]	796.3

Table 0. 30. Water flows at the time of the rupture of the fabrics

Tela5	Water flow [1st test]	Water flow [2nd test]	Water flow [3rd test]	Water flow [4th test]	Water flow [5th test]	Water flow [6th test]
Distance [10cm]	0.043 l	0.054 l	0.021 l	0.91 l	0.27 l	0.79 l
Distance [10cm]	0.070 l/min	0.16 l/min	0.19 l/min	0.56 l/min	0.25 l/min	0.48 l/min

Table 0. 31. Average water flows at the time of the rupture of the fabrics

Tela5	Average water flows
Distance [10cm]	0.35 l
Distance [10cm]	1.71 l/min

However, this fabric ruptured four times, for the first, second, third and fifth tests, in which the respective times and water flows were already reported. Thus, it is not correct to calculate the water flows considering these tests. Thus in Table 0. 32 the average flow rates of water required for non-disruption of the fabrics were recalculated.

Table 0. 32. Average water flows at the time of the rupture of the fabrics (recalculated)

Tela5	Average water flows
Distance [10cm]	0.85 l
Distance [10cm]	0.52 l/min

Micro-tube load losses Results

Table 0.33. 1st Test

Section	Initial mass [g]	Final mass [g]	Mass wins [g]	Volume wins [l]	Length [cm]	Cumulated length [m]
1	151.3	2346.5	2195.2	2.20	70	0.7
2	151.5	1350.6	1199.1	1.20	75	1.45
3	151.3	612.3	461	0.46	75	2.20
4	151.7	173.9	22.2	0.022	74	2.94
5	152.1	170.3	18.2	0.018	74	3.68
6	151.0	-	-	-	73	4.41
7	153.1	-	-	-	75	5.16
8	148.8	-	-	-	74	5.90
9	153.1	-	-	-	71	6.61
10	151.1	-	-	-	73	7.34
11	158.9	-	-	-	72	8.06
12	153.1	-	-	-	70	8.76
13	160.2	-	-	-	73	9.49
14	162.4	-	-	-	74	10.23

Table 0.34. 2nd Test

Section	Initial mass [g]	Final mass [g]	Mass wins [g]	Volume wins [l]	Length [cm]	Cumulated length [m]
1	162.6	3053.6	2891	2.89	70	0.7
2	159.3	2298.8	2139.5	2.14	75	1.45
3	156.9	1256.6	1099.7	1.10	75	2.20
4	153.7	328.8	175.1	0.18	74	2.94
5	153.2	321.3	168.1	0.17	74	3.68
6	151.0	-	-	-	73	4.41
7	153.1	-	-	-	75	5.16
8	148.8	-	-	-	74	5.90
9	153.1	-	-	-	71	6.61
10	151.1	-	-	-	73	7.34
11	158.9	-	-	-	72	8.06
12	153.1	-	-	-	70	8.76
13	160.2	-	-	-	73	9.49
14	162.4	-	-	-	74	10.23

IR camera calibration

Tela2

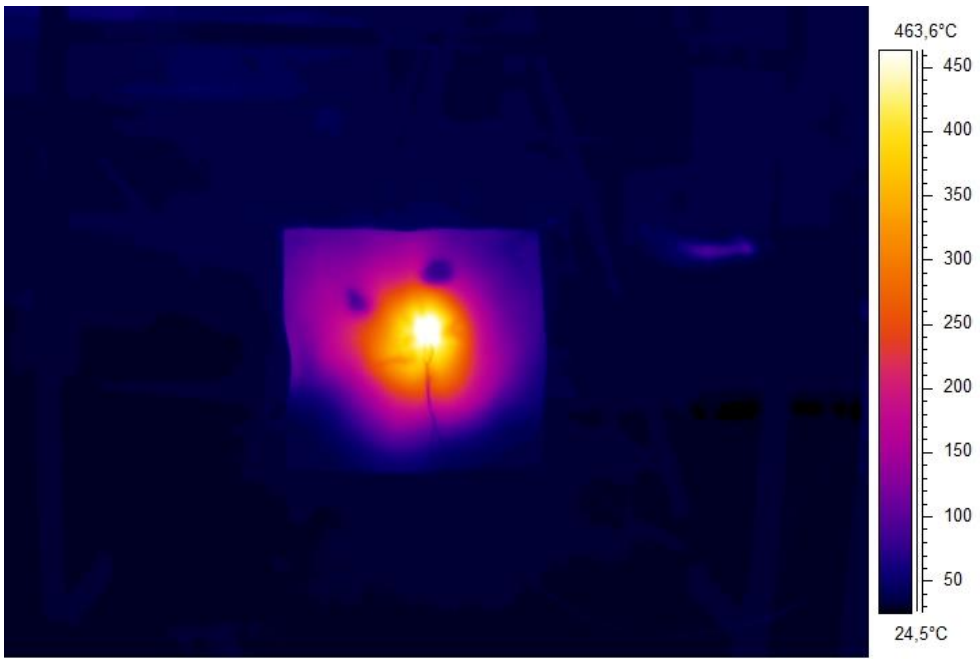

Figure 0.51. Maximum temperature recorded in the IR camera (Tela2)

Tela3

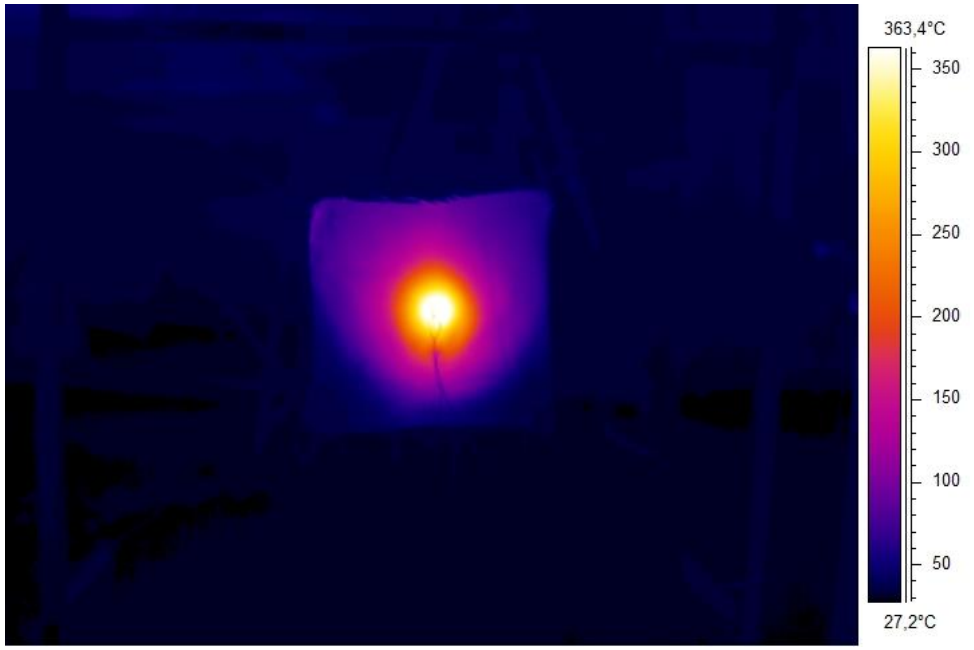

Figure 0.52. Maximum temperature recorded in the IR camera (Tela3)

Tela4

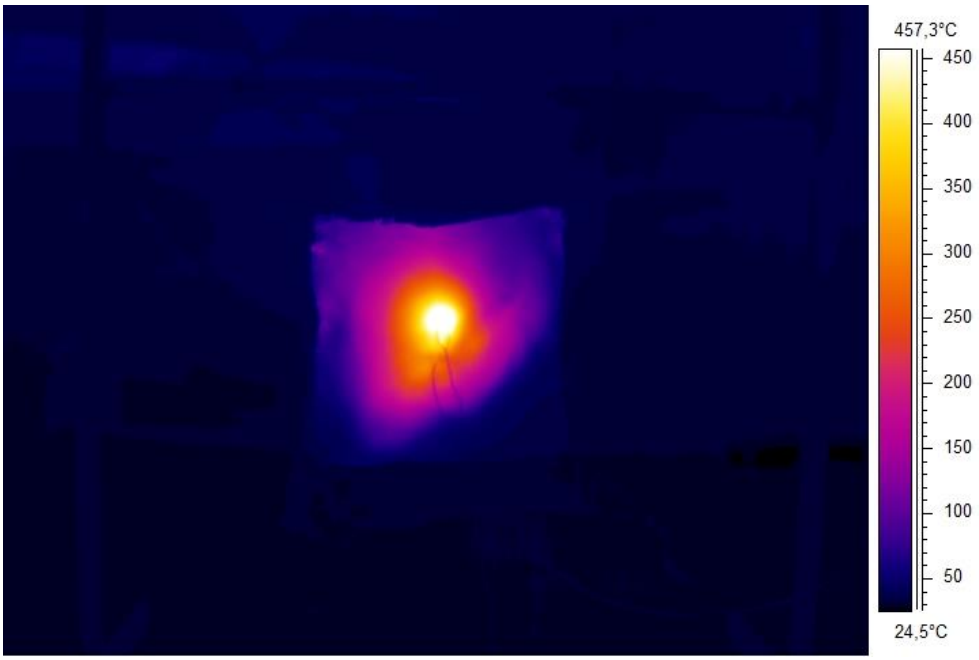

Figure 0.53. Maximum temperature recorded in the IR camera (Tela4)

Tela5

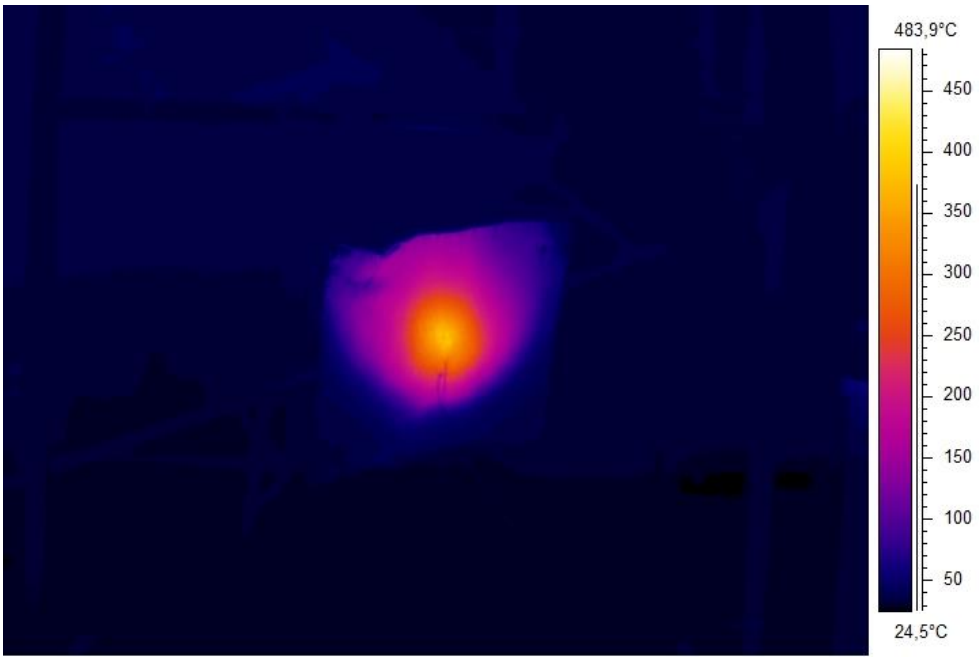

Figure 0.54. Maximum temperature recorded in the IR camera (Tela5)